

**Water requirements and distribution of
Ammophila arenaria and *Scaevola plumieri*
on South African coastal dunes**

Thesis

Submitted in fulfilment of the
requirements for the degree of
Master of Science
of Rhodes University

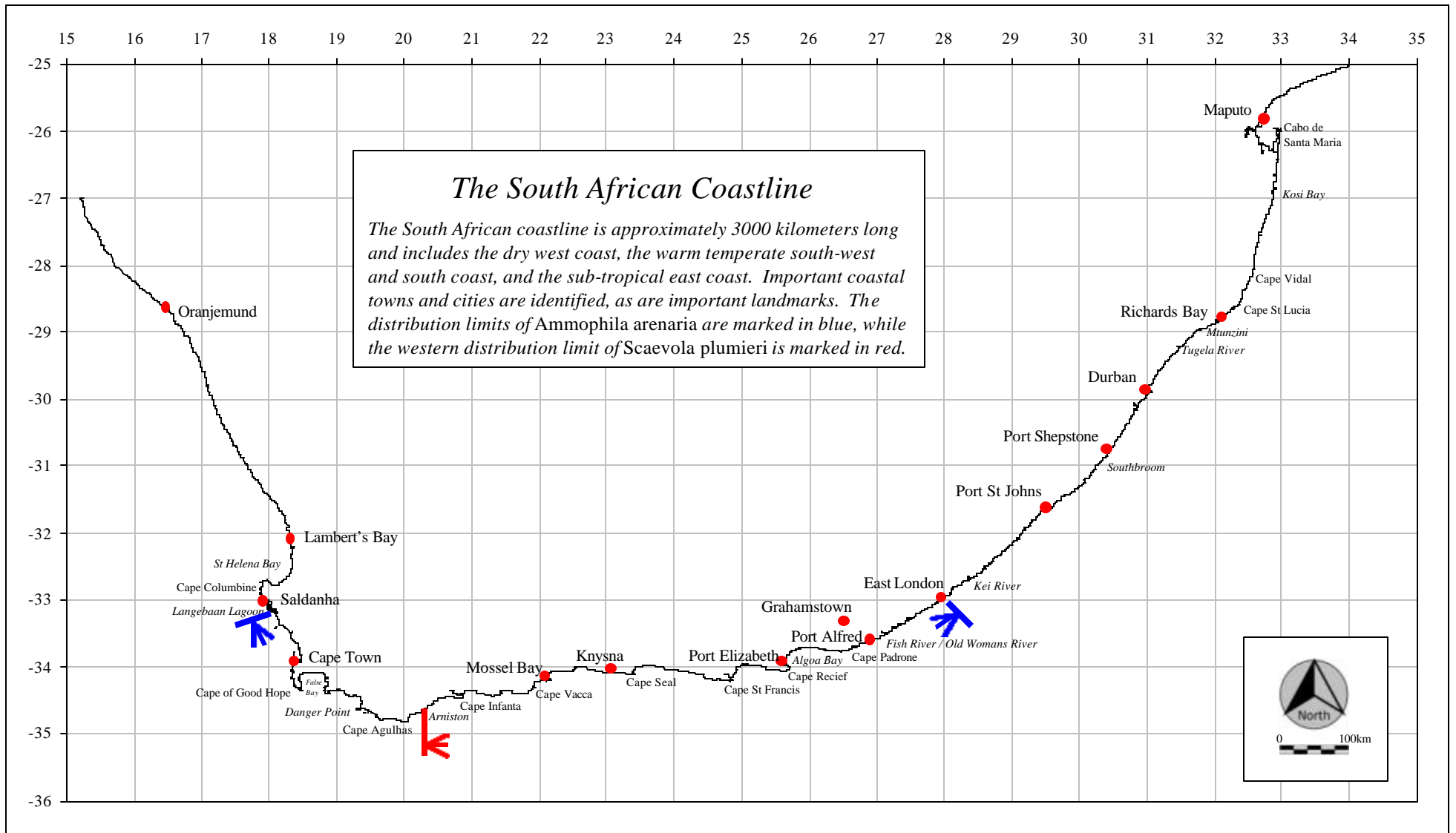
by

CRAIG INGRAM PETER

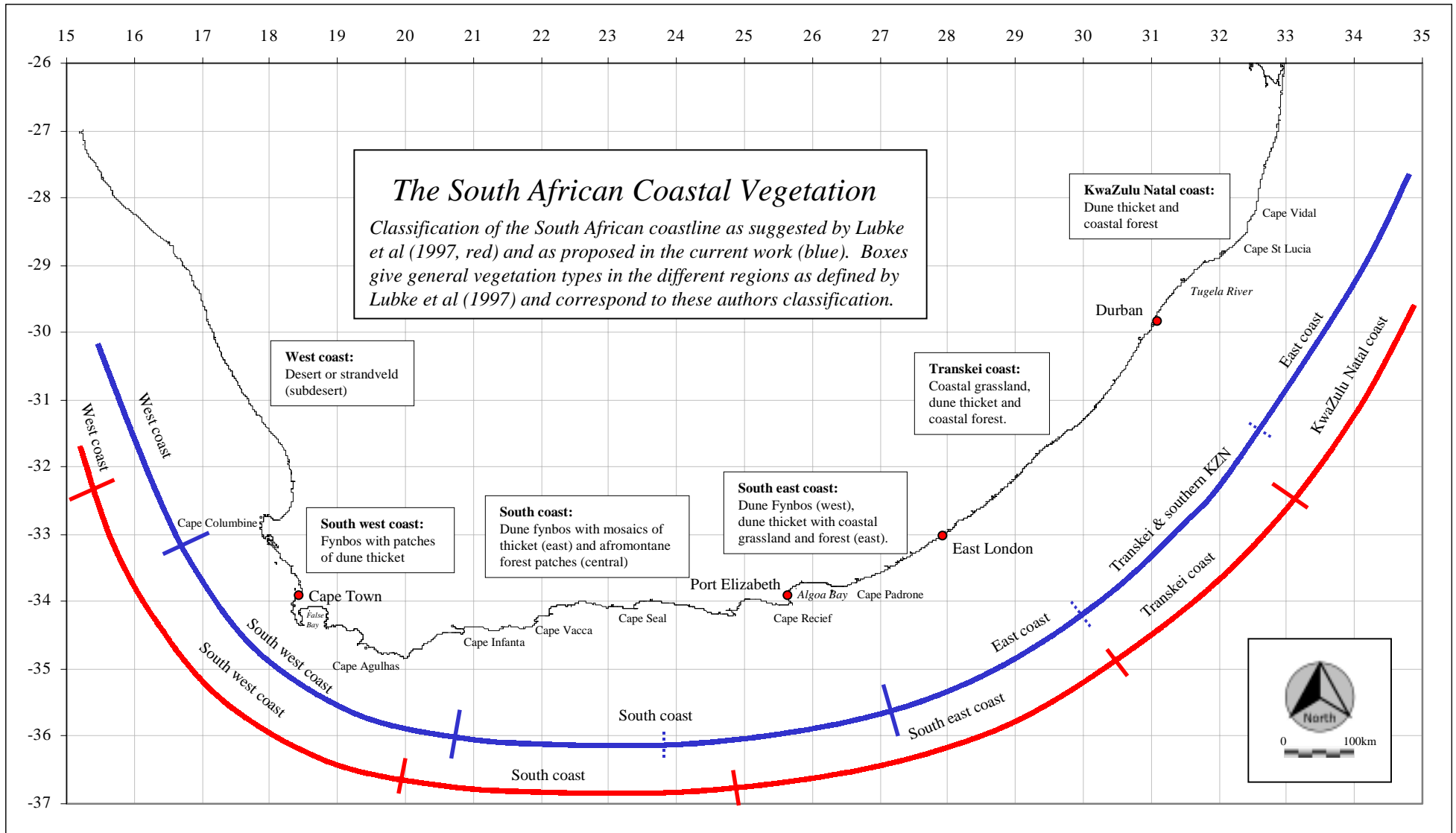
Department of Botany
Rhodes University

February 2000

Map 1



Map 2



“There is something fascinating about science. One gets such wholesale returns of conjecture out of such a trifling investment of fact”

Mark Twain

Abstract

Phenomenological models are presented which predicts transpiration rates (E) of individual leaves of *Scaevola plumieri*, an indigenous dune pioneer, and *Ammophila arenaria*, an exotic grass species introduced to stabilise mobile sand. In both cases E is predictably related to atmospheric vapour pressure deficit (VPD). VPD is calculated from measurements of ambient temperature and humidity, hence, where these two environmental variables are known, E can be calculated. Possible physiological reasons for the relationships of E to VPD in both species are discussed. Scaling from measurements of E at the leaf level to the canopy level is achieved by summing the leaf area of the canopy in question. E is predicted for the entire canopy leaf area by extrapolation to this larger leaf area. Predicted transpiration rates of individual shoot within the canopy were tested gravimetrically and shown to be accurate in the case of *S. plumieri*, but less so in the case of *A. arenaria*. Using this model, the amount of water used by a known area of sand dune is shown to be less than the rainfall input in the case of *S. plumieri* in wet and dry years. The water use of *A. arenaria* exceeds rainfall in the low-rainfall year of 1995, while in 1998 rainfall input is slightly higher than water extraction by the plants.

Using a geographic information system (GIS), regional maps (surfaces) of transpiration were calculated from surfaces of mean monthly temperature and mean monthly relative humidity. Monthly surfaces of transpiration were subtracted from the monthly median rainfall to produce a surface of mean monthly water deficit. Areas of water surpluses along the coast correspond with the recorded distribution of both species in the seasons that the plants are most actively growing and reproducing. This suggests that unfavourable water availability during these two species growth periods limit their distributions along the coast. In addition to unfavourable water deficits, additional climatic variables that may be important in limiting the distribution of these two species were investigated using a discriminant function analysis.

Table of Contents

ABSTRACT.....	III
TABLE OF CONTENTS.....	IV
LIST OF FIGURES	VI
LIST OF TABLES	X
ACKNOWLEDGEMENTS	XI
CHAPTER 1: INTRODUCTION.....	12
RATIONALE	12
THE INVASS PROGRAMME.....	15
AIMS AND QUESTIONS.....	17
AN INTRODUCTION TO THE SPECIES: <i>SCAEVOLA PLUMIERI</i> AND <i>AMMOPHILA ARENARIA</i>	18
<i>Scaevola plumieri</i>	19
Nomenclature	19
Ecology and distribution.....	20
Physiology	20
<i>Ammophila arenaria</i>	22
Nomenclature	22
Ecology and distribution.....	22
Physiology	24
SAND DUNES AND CLIMATE OF THE SOUTH AFRICAN COAST	25
<i>An overview of South African coastal climate.....</i>	26
<i>The distribution of sandy beaches along the South African coastline.</i>	28
<i>Dune vegetation in South Africa.....</i>	28
<i>The coastal sand dunes environment.....</i>	31
CHAPTER 2: ESTIMATING TRANSPIRATION RATES OF <i>SCAEVOLA PLUMIERI</i> AND <i>AMMOPHILA ARENARIA</i> LEAVES.....	33
INTRODUCTION.....	35
<i>Transpiration.....</i>	35
<i>The control of transpiration by stomata.....</i>	39
<i>Modelling transpiration.....</i>	41
STUDY SITES.....	44
MATERIALS AND METHODS.....	45
<i>Calibration and configuration of the IRGA.....</i>	45
<i>Field measurements.....</i>	47
<i>Weight loss experiment</i>	49
<i>Water potential.....</i>	50
<i>Integrated light data.....</i>	51
<i>CO₂ Experiment.....</i>	51
RESULTS.....	53
<i>Transpiration in relation to vapour pressure deficit.....</i>	53
<i>Physiological explanations for the relationship of E to VPD in S. plumieri.....</i>	56
<i>Elevated CO₂ experiment results.....</i>	62
<i>Physiological explanations for the relationship of E to VPD in A. arenaria.....</i>	65
DISCUSSION	68

CHAPTER 3: SCALING FROM LEAF TO CANOPY AND INVESTIGATIONS INTO THE INTERACTION BETWEEN PLANT WATER USE AND SAND WATER AVAILABILITY	71
INTRODUCTION.....	77
<i>Scaling up</i>	77
<i>Water relations of fore-dune vegetation</i>	80
STUDY SITES.....	82
MATERIALS AND METHODS.....	82
<i>Leaf area calculations</i>	83
<i>Shoot area determinations</i>	84
<i>Leaf Area Index</i>	84
<i>Scaling from leaf to shoot</i>	85
<i>Sand water</i>	86
<i>Changing sand water concentration</i>	86
RESULTS.....	88
<i>Leaf and shoot areas</i>	88
<i>Scaling from leaf to canopy</i>	90
<i>Sand water profiles</i>	92
<i>Compound sand water content</i>	93
DISCUSSION	96
<i>Scaling from leaf to canopy</i>	96
<i>Compound sand water</i>	99
CHAPTER 4: GIS INVESTIGATION OF FACTORS WHICH MAY LIMIT THE DISTRIBUTION OF SCAEVOLA PLUMIERI AND AMMOPHILA ARENARIA	93
INTRODUCTION.....	102
<i>Distribution of vegetation and species</i>	102
<i>Modelling the distribution of organisms</i>	105
<i>Geographic Information Systems</i>	108
MATERIALS AND METHODS.....	110
<i>Distribution data</i>	111
<i>Importing point data</i>	114
<i>Climatic surfaces</i>	116
<i>Calculations</i>	118
<i>GIS processing</i>	120
<i>Extraction of data from deficit surfaces</i>	123
<i>Discriminant Function Analysis</i>	125
RESULTS.....	128
<i>Potential water deficits in relation to distribution</i>	140
Regional water deficits of <i>S. plumieri</i>	141
Regional water deficits of <i>A. arenaria</i>	142
<i>Discriminant Function Analysis</i>	143
DISCUSSION	147
CHAPTER 5: CONCLUSION AND FURTHER STUDIES	141
CLASSIFICATION OF THE SOUTHERN AFRICAN COASTLINE	162
FURTHER STUDIES.....	163
APPENDICES	166
APPENDIX 1: ABBREVIATIONS AND UNITS.....	166
APPENDIX 2: COASTAL SAND DUNE SPECIES DISTRIBUTIONS.....	167
APPENDIX 3: MACRO FOR CALCULATING WATER DEFICIT SURFACES	170
APPENDIX 4: MACRO FOR EXTRACTING SURFACE DATA.....	173
APPENDIX 5: COMPONENT LOADING OF DIFFERENT PRINCIPLE COMPONENTS.....	174
REFERENCES	175

List of Figures

- Figure 1-1: *Scaevola plumieri* plants growing on the sand dunes to the west of the Old Woman's River, in Waterloo Bay. Note the extensive fore-dunes formed by this species and the open sparse canopy of this species.-----18
- Figure 1-2: *Ammophila arenaria* plants growing on sand dunes to the west of Old Woman's River, looking west towards Waterloo Bay. Note the varying densities of culms making up the different clumps. Some culms are flowering.-----21
- Figure 1-3: Distribution of *A. arenaria* in the Northern Hemisphere. The native distribution of this species includes most of the Mediterranean coast as well as the west and north-west coast of Europe. The plant has been introduced to the west coast of North America, Australia, New Zealand, Chile and South Africa. In a number of these countries, notably the first three listed, this species has become invasive (web-site 2, see also Huiskes 1979, Tutin *et al.* 1980). -----22
- Figure 2-1: Position of various study sites (blue) along the south-east coast of South Africa, in relation to major centres (red). Altitude increases with darker shades of grey. Inset shows the position of these sites in relation to the entire country. -----41
- Figure 2-2: The LCA2 portable IRGA was set up in an open configuration. The Mass Flow controller (MFC) was positioned upwind from where measurements were being made, to avoid CO₂ contamination from the user. The MFC provided a constant stream of dry air at known flow rate to the Parkinson leaf chamber (PLC) where it is passed over the leaf. The PLC measures photosynthetically active radiation in the same orientation as the leaf. The PLC also measures the ambient air temperature and the relative humidity of the air after passing over the leaf. After passing over the leaf, the air is returned to the Leaf chamber analyser (LCA2) where CO₂ concentrations are compared to ambient air (also provided by the MFC). Data was logged using a DL-2 data logger connected to the LCA-2. All instruments from the Analytical Development Company, Hoddeson, UK. -----43
- Figure 2-3: Rigging scheme for piping air with elevated CO₂ to individual *S. plumieri* leaves. Air from a cylinder made up to the desired CO₂ concentration is blown through a buffer tank which contains water to humidify the air. The humidified air then exits via six separate pipes to individual leaves, blowing air over both surfaces of the leaf. All outlet pipes are the same lengths. Clamps were used to set the flow rate at the mouth of the pipes. Changing the temperature of the water in the buffer tank altered the humidity of the outflowing air.-----48
- Figure 2-4A: Transpiration rates of individual excised *S. plumieri* leaves calculated by weight loss compared to transpiration rates measured with the LCA2 IRGA (n = 43, r²=0.93, p=0.0000).-----50
- Figure 2-4B: Transpiration rates of individual excised *A. arenaria* leaves calculated by weight loss compared to transpiration rates measured with the LCA2 IRGA (n = 46, r²=0.61, p=0.0000).-----50
- Figure 2-5: Transpiration of *S. plumieri* as determined from gaseous exchange data (corrected according to the relationship in Figure 2-4A) related to VPD calculated from weather data collected at Old Woman's River (○) on various dates from 1997 to 1999 and Southbroom (●) on 21-06-98. Data were collected at approximately hourly intervals from dawn until sunset on the days indicated in the text (n=226, r²=0.88, p=0.0000). The equation refers to the mean regression line (solid black). Dotted lines are the 95% confidence limits for the regression line.-----51
- Figure 2-6: Transpiration of *A. arenaria* as determined from gaseous exchange data (corrected according to the relationship in Figure 2-4B) related to VPD calculated from weather data collected at Old Woman's River on various dates in 1998 & 1999. Data was collected at approximately hourly intervals from dawn until sunset on the days indicated in the text (n=145, r²=0.71, p=0.000). The equation refers to the mean regression line (solid black). Dotted lines are the 95% confidence limits for the regression line.-----51
- Figure 2-7: *S. plumieri* leaf conductance to water vapour related to VPD calculated from weather data collected at Old Woman's River on various dates from 1997 to 1999 as well as at Southbroom on 21-06-98 (n=226, r²=0.61 p = 0.0000). The equation refers to the mean regression line (solid black). Dotted lines are the 95% confidence limits for the regression line.-----52

- Figure 2-8: Atmospheric vapour pressure deficit, calculated according to Equation 2-3, is correlated to solar radiation. Solar radiation integrated over an hour was measured at the South African Weather Bureau Port Elizabeth station. Variability in the data may be a result of variable relative humidity near the sea (n=187, $r^2=0.76$, $p=0.0000$). The equation refers to the mean regression line (solid black). Dotted lines are the 95% confidence limits for the regression line.-----54
- Figure 2-9: *S. plumieri* assimilation rates, measured concurrently to the collection of transpiration data and related to photosynthetically active radiation measured in the same orientation as the leaf by the PLC, collected at Old Woman's River and Southbroom (n=226, $r^2=0.64$, $p=0.0000$). The equation refers to the mean regression line (solid black). Dotted lines are the 95% confidence limits for the regression line.-----55
- Figure 2-10: Intercellular CO₂ concentration of *S. plumieri* leaves calculated from gaseous exchange data in relation to photosynthetically active radiation measured in the same orientation as the leaf by the PLC. The data was collected at both Old Woman's River and Southbroom (n=226, $r^2=0.66$, $p=0.0000$). The equation refers to the mean regression line (solid black). Dotted lines are the 95% confidence limits for the regression line.-----55
- Figure 2-11: *S. plumieri* leaf conductance to water vapour in relation to solar radiation integrated over an hour as measured at the South African Weather Bureau Port Elizabeth station (n=187, $r^2=0.39$, $p=0.0000$). The equation refers to the mean regression line (solid black). Dotted lines are the 95% confidence limits for the regression line.-----57
- Figure 2-12: *S. plumieri* transpiration rates in relation to solar radiation integrated over an hour, as measured at the South African Weather Bureau Port Elizabeth station (n=187, $r^2=0.68$, $p=0.0000$). The equation refers to the mean regression line (solid black). Dotted lines are the 95% confidence limits for the regression line.-----57
- Figure 2-13: Leaf conductance to water vapour related to atmospheric VPD of *S. plumieri* leaves exposed to (○) ambient CO₂ (n=226, $r^2=0.61$, $p=0.0000$) and (●) elevated CO₂ ($r^2=0.54$, n=49, $p=0.0000$).-----59
- Figure 2-14: Transpiration rates related to atmospheric VPD of *S. plumieri* leaves at (○) ambient (n=226, $r^2=0.88$, $p=0.0000$) and elevated (●) CO₂ ($r^2=0.80$, n=49, $p=0.0000$).-----60
- Figure 2-15: *A. arenaria* leaf conductance to water vapour related to VPD calculated from weather data collected at Old Woman's River on various dates in 1998 and 1999 (n=145, $r^2=0.53$, $p=0.0000$). The equation refers to the mean regression line (solid black). Dotted lines are the 95% confidence limits for the regression line.-----61
- Figure 2-16: *A. arenaria* assimilation rates related to photosynthetically active radiation measured in the same orientation as the leaf by the PLC (n=145, $r^2=0.60$, $p=0.0000$). The equation refers to the mean regression line (solid black). Dotted lines are the 95% confidence limits for the regression line.---62
- Figure 2-17: Intercellular CO₂ concentration of *A. arenaria* leaves calculated from gaseous exchange data in relation to photosynthetically active radiation measured in the same orientation as the leaf by the PLC (n=145, $r^2=0.52$, $p=0.0000$). The equation refers to the mean regression line (solid black). Dotted lines are the 95% confidence limits for the regression line.-----62
- Figure 2-18: Leaf water potential (●) and transpiration rates (○) for *S. plumieri* (A) and *A. arenaria* (B) in relation to VPD. Each point for *S. plumieri* water potential represents the mean of five measurements. Water potentials for *A. arenaria* represent individual measurements.-----63
- Figure 3-1: Allometric relationship of leaf area to length and breadth in *S. plumieri*. (n=110, $r^2=0.99$, $p=0.0000$). The equation refers to the mean regression line (solid black). Dotted lines are the 95% confidence limits for the regression line.-----81
- Figure 3-2: Allometric relationship of leaf area to length and breadth in *A. arenaria*. (n=15, $r^2=0.97$, $p=0.0000$). The equation refers to the mean regression line (solid black). Dotted lines are the 95% confidence limits for the regression line.-----82
- Figure 3-3: Transpiration rates of individual *S. plumieri* shoots calculated by weight loss, compared to transpiration rates calculated from measurements of ambient temperature, using the equation of the regression line in Figure 2-5 (n=42, $r^2=0.63$, $p=0.0000$). The equation refers to the mean regression line (solid black). Dotted lines are the 95% confidence limits.-----83
- Figure 3-4: Transpiration rates of individual *A. arenaria* culms calculated by weight loss, compared to transpiration rates calculated from measurements of ambient temperature, using the equation of the regression line in Figure 2-6 (n= 31, $r^2=0.25$, $p=0.0043$). The equation refers to the mean regression line (solid black). Dotted lines are the 95% confidence limits for the regression line.-----84

Figure 3-5: Percent sand water content at increasing depths in the sand column, from the surface down to the free aquifer water. Data collected at Old Woman's River (OWR), Port Alfred and Bushman's River mouth on the dates indicated.-----	85
Figure 3-6: The regression equation of E to VPD for leaves of <i>S. plumieri</i> , modified to have a zero y intercept so as to avoid predicting negative transpiration values at low VPDs.-----	85
Figure 3-7: The regression equation of E to VPD for leaves of <i>A. arenaria</i> was modified to have a zero y intercept so as to avoid predicting negative transpiration values at low VPDs.-----	85
Figure 3-8: Compound sand water for one square metre of vegetated sand dune, with a sand column three metres deep, assuming that the dune aquifer is at this depth. The values presented are estimates calculated from climatic data for each day of the year. Inputs of hourly temperature and relative humidity were used to calculate mean daily values from which daily transpiration rates were calculated. From a starting value of 156 litres of water in this sand column (4% sand water from Figure 3-5 and a sand density of 1.3 kg l ⁻¹ after Pammenter 1983), water transpired by the canopy was subtracted, while rain falling on the one square metre of vegetated sand dune was added. The green line gives the volume of sand water assuming 4% sand water. A) Compound sand water in 1995 when 571.8 mm of rain fell and B) in 1998 with 733.6 mm of rain falling on the square metre of sand dune.-----	87
Figure 4-1: Routes surveyed along KwaZulu-Natal (A) and Eastern Cape (B) coasts. These stretches of the coasts were surveyed from a vehicle for continuous presence or absence distribution data of <i>S. plumieri</i> as well as <i>A. arenaria</i> in parts of the Eastern Cape. See text for definitions of numbered routes.-----	102
Figure 4-2: The climatic surfaces as produced by Schulze <i>et al.</i> (1997) end short of the coastline. Because of this, distribution points were assigned to the nearest raster pixel and the adjusted distribution data set was used to extract values from the surfaces.-----	105
Figure 4-3: Comparison of data points collected with a Magellan GPS 315 and points inferred from 1:50 000 topographic sheets. Both points represent the same 'target point' on the ground as measured by the two methods. While accurate latitude and longitude data can be calculated from 1:50 000 topographic sheets, this relies on the accurate marking of the point in question on the map.-----	106
Figure 4-4: Transpiration rates of <i>S. plumieri</i> in relation to VPD as determined in Chapter 2 and modified to have a zero y intercept in Chapter 3 (Figure 3-6). Equations of the regression line (solid) and upper and lower 95% prediction limits (dotted) are listed in Table 4-2.-----	109
Figure 4-5: Transpiration rates of <i>A. arenaria</i> in relation to VPD as determined in Chapter 2 and modified to have a zero y intercept in Chapter 3 (Figure 3-7). Equations of the regression line (solid) and upper and lower 95% prediction limits (dotted) are listed in Table 4-2.-----	110
Figure 4-6: Schematic representation of the calculation of deficit surfaces. Input surfaces are given in 'lime green', intermediate surfaces in 'pale blue', operations in 'rose' and the output deficit surface in 'gold'. This is necessarily simplified and each step shown here may entail more than one calculation. Text and Appendix 3 gives additional details as to how the various surfaces were calculated. See text for explanation of abbreviations.-----	111
Figure 4-7A: Distribution of <i>S. plumieri</i> in South Africa. Altitude increases with darker shades of grey.	118
Figure 4-7B: Distribution of <i>A. arenaria</i> in South Africa. Altitude increases with darker shades of grey.	118
Figure 4-8: A) January monthly deficit for <i>S. plumieri</i> calculated from the mean regression of E to VPD (see Table 4-1). Inputs of temperature and relative humidity were used to calculate E from this regression. E was subtracted from rainfall to give the water deficit on a 'litres per square metre of vegetated sand dune' basis. Data was then extracted from coastal pixels in Figure 4-8A, to show water surpluses and deficits graphically along the coast, x-axis: latitude, y-axis: longitude, z-axis: water balance (litres). Perspectives from the south-east (B) and from the north (C). Corresponding distribution of <i>S. plumieri</i> is plotted in blue.-----	119
Figure 4-9: A) June monthly deficit for <i>S. plumieri</i> calculated from the mean regression of E to VPD (see Table 4-1). Inputs of temperature and relative humidity were used to calculate E from this regression. E was subtracted from rainfall to give the water deficit on a 'litres per square metre of vegetated sand dune' basis. Data was then extracted from coastal pixels in Figure 4-8A, to show water surpluses and deficits graphically along the coast, x-axis: latitude, y-axis: longitude, z-axis: water balance (litres). Perspectives from the south-east (B) and from the north (C). Corresponding distribution of <i>S. plumieri</i> is plotted in blue.-----	120

- Figure 4-10: A) Annual average deficit for *S. plumieri* calculated from the mean regression of E to VPD (see Table 4-1). Inputs of temperature and relative humidity were used to calculate E from this regression. E was subtracted from rainfall to give the water deficit on a 'litres per square metre of vegetated sand dune' basis. Data was then extracted from coastal pixels in Figure 4-8A, to show water surpluses and deficits graphically along the coast, x-axis: latitude, y-axis: longitude, z-axis: water balance (litres). Perspectives from the south-east (B) and from the north (C). Corresponding distribution of *S. plumieri* is plotted in blue.----- 121
- Figure 4-11: Data extracted from monthly deficit surfaces (calculated using mean and 95% prediction limits - see Table 4-1) at a number of locations around the coast. Because of space limitations, data from some points have been omitted. The x-axis represents the month of the year and the y-axis represents the water balance. The red line is the mean water balance while the two gray lines represent the positive and negative 95% prediction limits. The dotted line separates data where *S. plumieri* is present (red) from data where it is absent (blue).----- 122
- Figure 4-12: A) January monthly deficit for *A. arenaria* calculated from the mean regression of E to VPD (see Table 4-1). Inputs of temperature and relative humidity were used to calculate E from this regression. E was subtracted from rainfall to give the water deficit on a 'litres per square metre of vegetated sand dune' basis. Data was then extracted from coastal pixels in Figure 4-8A, to show water surpluses and deficits graphically along the coast, x-axis: latitude, y-axis: longitude, z-axis: water balance (litres). Perspectives from the south-west (B) and from the north (C). Corresponding distribution of *A. arenaria* is plotted in blue.----- 123
- Figure 4-13: A) June monthly deficit for *A. arenaria* calculated from the mean regression of E to VPD (see Table 4-1). Inputs of temperature, and relative humidity were used to calculate E from this regression. E was subtracted from rainfall to give the water deficit on a 'litres per square metre of vegetated sand dune' basis. Data was then extracted from coastal pixels in Figure 4-8A, to show water surpluses and deficits graphically along the coast, x-axis: latitude, y-axis: longitude, z-axis: water balance (litres). Perspectives from the south-west (B) and from the north (C). Corresponding distribution of *A. arenaria* is plotted in blue.----- 124
- Figure 4-14: A) Annual average deficit for *A. arenaria* calculated from the mean regression of E to VPD (see Table 4-1). Inputs of temperature, and relative humidity were used to calculate E from this regression. E was subtracted from rainfall to give the water deficit on a 'litres per square metre of vegetated sand dune' basis. Data was then extracted from coastal pixels in Figure 4-8A, to show water surpluses and deficits graphically along the coast, x-axis: latitude, y-axis: longitude, z-axis: water balance (litres). Perspectives from the south-west (B) and from the north (C). Corresponding distribution of *A. arenaria* is plotted in blue.----- 125
- Figure 4-15: Data extracted from monthly deficit surfaces (calculated using mean and 95% prediction limits - see Table 4-1) at a number of locations around the coast. Because of space limitations, data from some points have been omitted. The x-axis represents the month of the year and the y-axis represents the water balance. The red line is the mean water balance while the two gray lines represent the positive and negative 95% prediction limits. The dotted line separates data where *A. arenaria* is present (red) from data where it is absent (blue).----- 126
- Figure 4-16: Discriminant function analysis of sites where *S. plumieri* is present along the southern coast as well as sites on the south-west and west coasts where this plant is absent. Coefficients defining root one and root two are listed in Table 4-3. Sites from the extreme west of the distribution of *S. plumieri* (at Arniston & Witsands), indicated with an asterisks, mark sites where the species is found but where climatic variables are intermediate to those of the south east coast and those of the south west coast.----- 131
- Figure 4-17: Discriminant function analysis of sites where *A. arenaria* is present along the southern coast as well as sites on the east and west coasts where this plant is absent. Coefficients defining roots one and two are listed in Table 4-4.----- 132
- Figure 4-18: Monthly leaf production rates compared to monthly water deficits as determined at three separate sites along the east coast of South Africa. Monthly leaf production rates determined by Pammenter (1983) for plants growing at Mtunzini, by Steinke & Lambert (1983) for plants growing near Durban, and Ripley (unpublished data) for plants growing at Old Woman's River (n=36, $r^2=0.62$, $p=0.0000$)----- 139

List of Tables

Table 2-1: Co-ordinates of the study sites where this work was conducted.-----	41
Table 3-1: Characteristics of <i>S. plumieri</i> and <i>A. arenaria</i> canopies. -----	82
Table 4-1: Equations used in calculations of the mean regression lines and 95 % prediction limits. ----	109
Table 4-2: Components surfaces used in the discriminant function analysis. C1 and C2 refer to components one and two respectively.-----	115
Table 4-3: Standardized coefficients defining roots one and two in Figure 4-16 discriminating between presence and absence (on both the east and west coast) of <i>S. plumieri</i> . See Table 4-2 for an explanation of the abbreviations used. The component surfaces are ordered in terms of their coefficients from most positive to most negative. The most positive coefficients discriminate in a positive direction while highly negative coefficients discriminate in a negative direction for a particular root.-----	131
Table 4-4: Standardized coefficients defining roots one and two in Figure 4-17 discriminating between presence and absence (on both the east and west coast) of <i>A. arenaria</i> . See Table 4-2 for an explanation of the abbreviations used. The component surfaces are ordered in terms of their coefficients from most positive to most negative. The most positive coefficients discriminate in a positive direction while highly negative coefficients discriminate in a negative direction for a particular root.-----	132
Table A-2A: List of species found in the pioneer strand zone (Zone 1 of Tinley 1985) around the South African coast as compiled by Tinley (1985). Names have been checked and modified according to Arnold & de Wet (1993). Distributions are those given by Tinley (1985): M = south Mozambique, T = Tongaland, N = Natal (and north Transkei), E = former east Cape (and southern Transkei), S = south coast, C = south west coast, W = west coast. Asterisks mark the most important pioneer species in the strand zone. -----	151
Table A-2B: List of species found in the shrub zone (Zone 2 of Tinley 1985) around the South African coast as compiled by Tinley (1985). Names have been checked and modified according to Arnold & de Wet (1993). Distributions are those given by Tinley (1985): M = south Mozambique, T = Tongaland, N = Natal (and north Transkei), E = former east Cape (and southern Transkei), S = south coast, C = south west coast, W = west coast.-----	152
Table A-3: Section of the macro used to produce monthly water deficit for the two species (<i>S. plumieri</i> in this case). Only one month is included here. In the full macro this set of lines is repeated twelve times to produce twelve deficit surfaces for each species.-----	154
Table A-4: Section of a macro written to extract the values of a pixel which corresponds with a point.--	157
Table A-5: Contribution of monthly surfaces to the loading of specific components used in the discriminant function analysis (DFA), see table 4-2. -----	158

Acknowledgements

- Brad Ripley is thanked for excellent supervision at all stages of this project. Brad has put up with many 'silly questions' and his constant advice, guidance and encouragement is gratefully acknowledged.
- Mark Robertson taught me all I know about GIS and set aside many afternoons to talk me through the intricacies of IDRISI. He (and a number of others) also set aside valuable time to help demolish fine red wine which inevitably lead to many, previously tricky, problems being solved. Brian, Leigh and Barney in particular contributed with regard to the latter although the wine was not always as fine!
- Martin Villet is thanked for the valuable advice he gave me about many aspects of modelling distributions using GIS, and particularly for his help with the discriminant function analysis and other statistical problems. Sarah Radlof and Lindsey Bangay also provided valuable assistance with statistical problems.
- Thank you to Irma Knevel for assistance in the field, for efficient organisation of numerous field trips and many thoughts on the biology of many dune pioneer species. Freyni Killer is also thanked for her help on a number of field trips.
- Roy Lubke, the INVASS project leader, is thanked for many helpful comments and his wealth of 'coastal' knowledge.
- Norman Pammenter contributed many suggestions to all sections of this project. His comments and expertise with regard to *S. plumieri* and ecophysiology generally are greatly appreciated.
- Urshula Hertling provided many suggestions about the biology of *A. arenaria* and made her distribution data available for the present study, saving a considerable amount of surveying work.
- Tony Dold and the staff at the Schönland Herbarium Grahamstown (GRA) and Natal Herbarium (NU) are thanked for assistance in collecting distribution data from their specimens and general advice about collecting distribution data from different sources.
- The management of the Fish River Sun is acknowledged for providing stables for the use as a base camp and allowing the use of their property.
- My Family is thanked for their considerable support. From lending me their printer to lending me their vehicles
- Finally a special thank you to Kerry Theobald for being so positive and putting up with many thesis-induced bad moods. She also spent many windswept days in the field hanging onto scraps of paper. These bits of paper became this work which she read through more than once making numerous suggestions and corrections. Thank you.

Chapter 1

Introduction

Rationale

This study was prompted by observations made by B.S. Ripley while working on the ecophysiology of dune pioneer plants on the Eastern Cape coast South Africa. He noted that in the tropical dune pioneer, *Scaevola plumieri*, which is perhaps the most important dune pioneer along the east and south coasts of South Africa, there is a strong relationship of transpiration to ambient temperature (pers. com.). This suggests that it may be possible to model transpiration rates of *S. plumieri* from measured environmental variables. This study therefore investigates the relationship between transpiration rates and relevant factors such as leaf to air vapour pressure deficit (VPD). VPD describes the gradient of water vapour concentration from the leaf air spaces to the atmosphere and is thus important in driving transpiration in plants (Kramer 1983). Strong correlations of transpiration to factors such as ambient temperature or VPD (which is calculated from ambient temperature, relative humidity and leaf temperature) would make it possible to estimate transpiration rates of this species from readily available climatic data.

The second species, *Ammophila arenaria*, is an exotic grass introduced to stabilise shifting sand. There is some concern about the potential for this species to invade sand dunes along the South African coast as has occurred elsewhere and this species forms the focus of the INVASS programme which is introduced below. Because of the overlap of distributions of *S. plumieri* and *A. arenaria* along the south-east and south coasts, *S. plumieri* might be threatened along these sections of the coast should *A. arenaria* become invasive. It is therefore appropriate to compare the biology, specifically the physiology and distribution of these two species.

An unpublished report by researchers at the University of Port Elizabeth estimated water use of *Ipomea pes-capre* based on maximal transpiration measurements. Their findings suggest that water is not limiting in the Alexandria dune field. It was hoped, based on

more realistic and accurate measurement of transpiration rates, that more precise estimates of the water requirements for *S. plumieri* and *A. arenaria* could be determined. This would have application in resolving what limits the distribution of these two species in the south west of the country, as well as revealing more about the water relations of coastal plants in general, of which little is known (Campbell *et al.* 1992).

Urshula Hertling (1997) has made a preliminary investigation of *A. arenaria* (a European dune grass) in this country. Her study was prompted by the concerns that this species has become invasive in a number of countries where it has been introduced for dune stabilisation purposes. She found that in South Africa, *A. arenaria* is not an aggressive invader and suggests that the climate in this country is possibly unsuitable for this species. Specifically, she speculates that there is an unsuitable combination of temperature and rainfall. On the west coast she notes that the temperature may be suitable but the rainfall too low. At the eastern extent of *A. arenaria* distribution in South Africa, it is considerably wetter, but the temperature is also considerably higher. She notes further that in-between these two extremes, on the Cape south coast, there is lower temperature and higher rainfall and this is where the healthiest populations of *A. arenaria* are found. Hertling & Lubke (1999) make the further suggestion that mean annual temperature is higher at the sites in South Africa where *A. arenaria* grows than in the species natural range.

This study therefore investigates whether the climate along the South African coast is adequate to support populations of *A. arenaria*, and whether the limited distribution of *A. arenaria* in South Africa can be explained in terms of the local climate, particularly at the extremities of its distribution. Knowledge of the plant's transpiration and water relations facilitates such investigations. Naturalised exotic species, which have been introduced by man, may not be in equilibrium with the environment (Beerling *et al.* 1995), complicating investigations as to what may control or limit the plant's distribution. Indigenous plants, on the other hand, may have reached their existing distribution naturally and so the role of climate in determining their distribution may be more evident.

S. plumieri is an indigenous species and it is therefore likely that this species has spread to its present distribution naturally. This allows useful comparison to be drawn between the introduced exotic *A. arenaria*, and the indigenous *S. plumieri*, with regard to the role climate plays in determining the distribution of these two different species. This study also hopes to identify climatic variables which may be important in limiting the distribution of *S. plumieri* in the extreme west of its range near Cape Agulhas.

A considerable amount of work has been conducted on temperate dune systems which are dominated by grass pioneers. *A. arenaria* is by far the most important pioneer on northern hemisphere temperate sand dunes. *Elymus* also contributes significantly to the vegetation cover in these regions (Doing 1985, van der Maarel & van der Maarel-Versluys 1996).

Distinct from these are more tropical dune systems, which are dominated by woody species (e.g. *Scaevola*) as well as low-creeping grasses, specifically the ubiquitous pan-tropical grass *Sporobolus virginicus* (Doing 1985). These tropical systems might therefore be subject to distinct processes.

For example, wind may be less intense in the tropics compared to more temperate sites, which in turn may result in less sand movement and so less extensive dune systems. The growing season is also significantly longer and often associated with high rainfall, which favours the growth of relatively dense, woody, salt-tolerant vegetation zones near the shoreline (Doing 1985). Hopefully this study will contribute to the understanding of tropical (or subtropical) dune systems through a better appreciation of the biology of *S. plumieri* which is an important plant on the sub-tropical South African sand dunes. In the pioneer zone of Eastern Cape sand dunes, this species scored an 80% importance value on the importance scale of Avis (1992). This species is also probably important on many tropical sand dunes throughout the Indo-Atlantic region (Doing 1985).

At present little is known about the water relations of plants growing on the sand dunes and sand dune systems in general. It is possible (or probable) that dune plants get some of their water from the dune aquifers. As this water is used extensively by coastal towns

in South Africa (Campbell *et al.* 1992) there is potential for conflict between human needs and that of the dune flora and ecosystems.

The new water law of South Africa (Act 36 of 1998) treats all water in the hydrological cycle in the same manner. In addition to the basic right of human access to a minimum quantity of fresh water, this act makes provision for the protection of an ecological reserve to protect ecosystem functioning, primarily in fresh water systems (Department of Water Affairs and Forestry 1997). However, in the spirit of this law, dune systems which may rely on ground water for their continued functioning should be protected from unrestricted tapping of the water they contain. Quotas need to be established based on rational studies aimed at further identifying the exact requirement of these systems. Water available over and above this 'ecosystem reserve' can then be tapped, but must be paid for in accordance with the new water law.

The INVASS programme

This project is a component of the EC-INCO-DC program, INVASS (contract ERBIC18CT970145), which is investigating "the impact of invasive grass species on the structure, functioning and sustainable use of coastal and inland dune ecosystems in Southern Africa". Broadly, the aims of this programme are:

1. To determine the natural behaviour of *A. arenaria* in South Africa and European dunes in different phases of its life history.
2. To investigate the current and likely future impact of *A. arenaria* on the dune systems of South Africa.
3. To compare the effect of soil-borne pathogens and arbuscular mycorrhizal fungi on vegetation succession in temperate European sand dunes with coastal and inland dunes in Southern Africa.
4. To provide management prescriptions for the wise use and, if appropriate, control of *A. arenaria* to maximise its beneficial properties for coast protection without concomitant threat to ecosystem function, biodiversity and wildlife.

This programme has additional aims but they are not relevant to this study as they relate to *Cenchrus bifloris*, an invasive grass of Kalahari sand dunes.

In addition and as a by-product of work on alien plants occurring on our sand dunes, the programme will afford better understanding of our local sand dune systems and the plants associated with them, hopefully identifying possible indigenous replacements for alien dune stabilisers.

As far as coastal sand dunes are concerned, INVASS is primarily investigating the status of *A. arenaria* in South Africa. This species is indigenous to the temperate coasts of Europe and the Mediterranean where it has been used for stabilising mobile sands for a number of centuries. In the last century *A. arenaria* has been imported to Chile, South Africa, New Zealand, Australia and the United States of America. Success as a sand stabiliser has been varied, but in the case of the latter three countries, particularly the USA, it has become invasive, displacing indigenous species, altering the topography of the sand dunes and fixing previously mobile sand (the original, perhaps misguided reason that the plants were introduced to these countries).

Hertling (1997) has extensively investigated the aspects of the first, second and fourth questions posed by INVASS (listed above). She concluded that *A. arenaria* is a useful dune stabiliser and, although it is visibly alien in South Africa, it is neither aggressively spreading and out-competing indigenous dune plants nor altering the topography of South African natural dunes. *A. arenaria* is 'succeeded' in most cases by indigenous species within forty or fifty years, and Hertling does not classify it as invasive or likely to become invasive.

The main aims of the INVASS programme attempt to answer questions as to why this species is not invasive in this country in terms of its genetic fitness and escape from natural predators for example. However, a more obvious question is "is the climate in this country adequate to support this species?" This study investigates the suitability of the climate in supporting this alien temperate grass and draws comparisons to the indigenous tropical dicotyledonous pioneer, *S. plumieri*.

Aims and Questions

The aims of this study therefore can be summarised to include the following:

- To investigate the relationship of transpiration to atmospheric variables, with the intention of identifying empirical relationships between transpiration rates and atmospheric vapour pressure deficit. The elucidation of such relationships allows the prediction of transpiration rates from readily available weather data.
- If predictions of transpiration rates can be made for individual leaves, to investigate the possibility of scaling these predictions to the level of the canopy which is a more functional unit for investigating the interactions between plants and the environment.
- To investigate water relations and water use at the level of individual sand dunes or stands of plants. How does water use of these plants relate to water availability in the form of rainfall, sand water or dune aquifer water?
- To investigate the role of climatic variables in physiologically limiting the distribution of these two species in South Africa. Is the South African climate adequate to support *A. arenaria*? Are there climatic explanations for the current limit in the east and west of the distribution of *A. arenaria*? Can knowledge of the physiology of *S. plumieri* explain the observed distribution limit in the south-west?

To address these aims, this study attempts to answer the following questions:

1. Is it possible to simply model transpiration rates of *A. arenaria* and *S. plumieri* from readily available climatic data? (Chapter 2)
2. Can transpiration rates be scaled up to whole dunes or larger areas? (Chapter 3)
3. Can budgets of water use and water availability be constructed? (Chapter 3)

4. Can budgets of water use and water availability be used to explain the observed distribution of these two species at a regional level? (Chapter 4)

An introduction to the species: *Scaevola plumieri* and *Ammophila arenaria*

This study investigates the water use and distribution of two quite different species. *S. plumieri* (Figure 1-1) is an indigenous sand dune pioneer from tropical areas. *A. arenaria* (Figure 1-2) is an alien temperate grass species which has been introduced for sand stabilisation on coastal dunes. Vegetatively, *S. plumieri* is quite different from the vertically growing clumps of *A. arenaria*, forming a large ‘under-ground trunkless tree’ with only the tips of the ‘branches’ emerging above the sand dune.



Figure 1-1: *Scaevola plumieri* plants growing on the sand dunes to the west of the Old Woman’s River, in Waterloo Bay. Note the extensive fore-dunes formed by this species and the open sparse canopy of this species.

Scaevola plumieri

Nomenclature

The genus *Scaevola* L., in the family Goodeniaceae, is centred in Australia and includes over 400 species (Dyer 1967). However, two species form an important and

conspicuous component of coastal vegetation, growing in the warmer parts of the world. These two species are similar but distinct. There is an Indo-Atlantic (western) species with inconspicuous calyx lobes, glabrous or slightly hairy leaf axils and black fruit; and an Indo-Pacific (eastern) species with well-marked calyx lobes, tufts of white woolly hairs in the leaf axils and white fruit. The Indo-Atlantic species has been known by a number of names (*Lobelia plumieri*, *Scaevola lobelia* and locally as *Scaevola thunbergii* Eckl. & Zeyh.), but *Scaevola plumieri* (L.) Vahl. is recognised as being the accepted name. The Indo-Pacific species has been known as, amongst other, *Lobelia taccada*, *Scaevola taccada* *Scaevola frutescens* and locally as *Scaevola koenigii*, but *Scaevola sericea* Vahl. is the valid name for this species (Jeffrey 1979).

Ecology and distribution

S. plumieri is found along many of the tropical sandy beaches in the Indo-Atlantic region. It is found along the east coast of the Americas, from north of Palm Bay in Florida (web site 1), south through the Caribbean Islands (Guppy 1917), the Gulf of Mexico and central America (Espejel 1987) to the coast of Brazil. In Brazil, *S. plumieri* is found around Cape de Sao Roque and the City of Natal (N. W. Pammenter pers. com.), at least as far south as Rio de Janeiro (Guppy 1917, Doing 1985). *S. plumieri* is found on the west coast of Africa from Angola (from the Kwanza River), north around the Gulf of Guinea (Tinnley 1985), at least as far north as the Senegal coast of north-west Africa (Doing 1985). In the Indian Ocean, *S. plumieri* is found as far east as Indian and Sri Lanka as well as the Islands of Mauritius and Madagascar (Ridley 1930). Along the east coast of Africa, *S. plumieri* is found from Mombassa in Kenya (Doing 1985, Tinnley 1985) on the African north-east coast (possibly further north), south to Arniston near Cape Agulhas (personal observations, Figure 4-7A). *Scaevola sericea* is found throughout the tropical and subtropical regions of the Indo-Pacific from Hawaii (Alpha *et al.* 1996) in the extreme east to the east coast of Africa in the west where it is found south to Kosi Bay in KwaZulu-Natal (Natal Herbarium (NU) records, Jeffrey 1979). Along the east coast of Africa its distribution overlaps with that of *S. plumieri*. The detailed distribution of *S. plumieri* in South Africa forms part of the results of this project and are given in Figure 4-7A.

Physiology

The physiology of *S. plumieri* has been investigated previously by N.W. Pammenter (1983, 1985 and an unpublished work with V.R. Smith), Harte & Pammenter (1983) and Steinke & Lambert (1985). Alpha *et al.* (1996) investigated the morphological and physiological response of *S. sericea* (the sister species of *S. plumieri*) seedlings to salinity.'

Pammenter (1983) made a preliminary investigation of a number of aspects of *S. plumieri* ecophysiology. He notes that this species shows moderate to high rates of transpiration but seldom seems to experience severe water stress. This author presents a preliminary water budget for a dune covered by *S. plumieri* and suggests that rainfall is sufficient to meet the plant's requirements (KwaZulu Natal coast). In addition this author presents data on the photosynthetic characteristics, internal nutrient cycling and phenology of this species. The phenological details given by Pammenter (1983) agree with that given by Steinke & Lambert (1985), who worked on aspects of the phenology of *S. plumieri* growing on dunes near Durban. They found that leaf production and abscission was higher in summer month than in winter, although in summer leaf production exceeds leaf abscission. During winter more leaves were shed than were produced. Reproduction is limited to the summer months, with flowering beginning in October and all fruit having fallen by March.

Pammenter (1985) examined aspects the photosynthesis and transpiration of *S. plumieri* grown in controlled environment. This work confirms the earlier work (1983) noting that this species is a C₃ species with maximum photosynthesis rates of around 12 $\mu\text{mol m}^{-2} \text{s}^{-1}$, broad temperature optimas (22 – 30 °C) and light saturated photosynthesis occurring at 1000 $\mu\text{mol m}^{-2} \text{s}^{-1}$.

Pammenter & Smith (unpublished manuscript) examine factors affecting the carbon assimilation of *S. plumieri* under field conditions. They note that the fleshy leaves of isobilateral and CO₂ assimilation is not saturated at full sunlight. As a result CO₂ assimilation is limited by intercepted irradiance even though stomatal limitation may be

high under high light conditions. These authors note that *S. plumieri* seldom realises its full photosynthetic capacity.

Harte & Pammenter (1983) examined the concentration of nutrients within leaves of *S. plumieri* in relation to leaf age. They note that *S. plumieri* has relatively low nutrient concentrations compared to a range of other herbaceous species. They also note that key nutrient concentrations decline with leaf age, which suggests that these scarce nutrients are exported from senescing leaves.



Figure 1-2: *Ammophila arenaria* plants growing on sand dunes to the west of Old Woman's River, looking west towards Waterloo Bay. Note the varying densities of culms making up the different clumps. Some culms are flowering.

Ammophila arenaria

Nomenclature

The genus *Ammophila* (Host: family Poaceae, subfamily Pooideae, tribe Aveneae; Gibbs-Russel *et al.* 1990) consists of two species, *A. breviligulata* Fren. and *A. arenaria* (L.) Link; the former only being recognised as distinct in 1920 (Maun & Baye 1989). *A. breviligulata* differs from *A. arenaria* in the structure of the ligule and the morphology of the abaxial surface of the leaf. More obvious is the fact that this species forms widely dispersed creeping tussocks with broader, typically flat leaves

compared to the more clumped tussocks with narrow (3 to 6 mm) involute (rolled) leaves of *A. arenaria* (Maun & Baye 1989).

Ecology and distribution

A. arenaria is native to the European and north-African coasts (Figure 1-3, Tutin *et al.* 1980). Subspecies *A. a. arundinacea* is found on sandy beaches of the Mediterranean and Black Seas, from the coast of Romania to the north of Portugal, extending south to about 32° north (N). Subspecies *A. a. arenaria* is found on the north and west coasts of Europe from north-west Spain, north to about 63° north on the Scandinavian coast (Huiskes 1979), including many of the islands and much of the British Isles. Knowledge of the natural distribution of this species may help identify general climatic tolerance of this species and is discussed further in Chapter 4. *A. breviligulata* is the ‘sister species’ of *A. arenaria* and is found on the American north-east coast, between 46° and 52° north and around the great Lakes (Maun & Baye 1989).

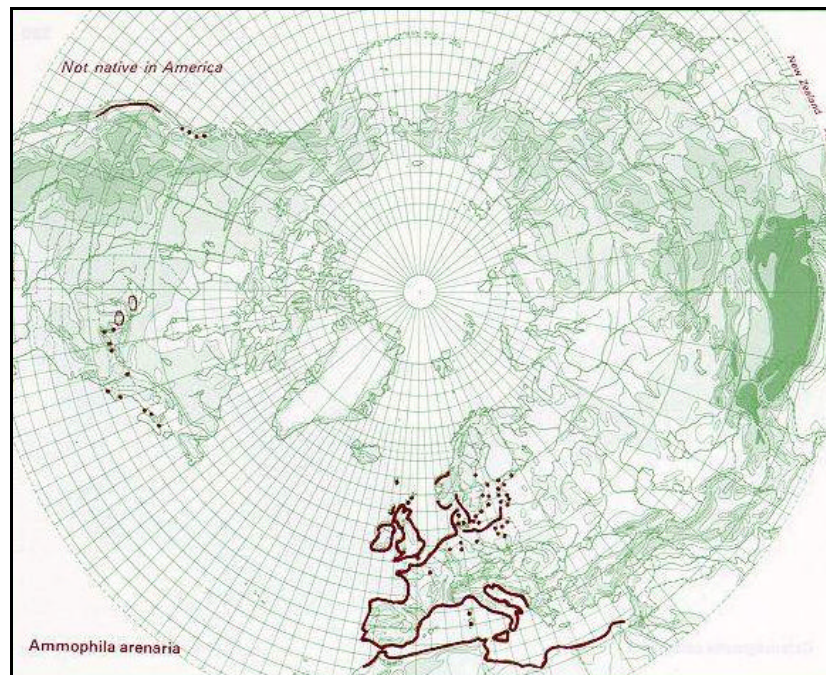


Figure 1-3: Distribution of *A. arenaria* in the Northern Hemisphere. The native distribution of this species includes most of the Mediterranean coast as well as the west and north-west coast of Europe. The plant has been introduced to the west coast of North America, Australia, New Zealand, Chile and South Africa. In a number of these countries, notably the first three listed, this species has become invasive (web-site 2, see also Huiskes 1979, Tutin *et al.* 1980).

As mentioned above, *A. arenaria* is one of the main species being investigated by the INVASS programme. It is a temperate sand dune pioneer which has been used for dune stabilisation along the European coast since about 1423 in the Netherlands (van der Putten 1989, cited in Hertling 1997), but probably earlier (van der Meulen & van der Maarel 1989). In the last hundred years or so it has been introduced to a number of countries around the world as a sand dune stabiliser, often without first investigating the suitability of native species for this purpose (Hertling 1997). These countries include North America (Wiedemann & Pickart 1996), Australia (Heyligers 1985), New Zealand (Gadgil & Ede 1998), Chile and South Africa. This species was introduced to South Africa as a dune stabilisation species in 1870 (Hertling 1997), and is now found from Langebaan on the semi-arid west coast to Nahoon Point, East London on the subtropical east coast (pers. obs.). As in the case of *S. plumieri*, the detailed distribution of *A. arenaria* in South Africa forms part of the results of this project and is given in Figure 4-7B.

In South Africa, it appears that this species is not spreading naturally and relies on being transplanted and maintained artificially in the areas where it has been planted. Hertling (1997) suggests that a major hazard for the growth of *A. arenaria* in South Africa is the lack of rainfall as many stabilisation sites are irrigated – suggesting in turn that rainfall in this country may not be sufficient to support this species naturally.

Physiology

To date the majority of the recent physiological work conducted on *A. arenaria* has been undertaken by Bruce Pavlik (1983a, 1983b, 1983c, 1984, & 1985), comparing this species with *Elymus mollis*, an indigenous North American dune species. He has investigated the gas exchange characteristics, primarily photosynthesis, of the two species as influenced by nitrogen supply. While *E. mollis* had higher photosynthetic rates in the field, *A. arenaria* had higher nitrogen use efficiency (Pavlik 1983a). Pavlik (1983b & 1983c) further investigated the role of nitrogen in nutrient partitioning and growth form. Similarly, Willis (1965) has investigated the role of nutrients on growth form. This author records the natural density of plants on sand dunes in the United Kingdom, as well as the impact of fertilisers on the growth and tillering of this species

in the field. Huiskes (1979) describes all aspects of the biology of this species around the British Isles and discusses some aspects of the ecophysiology and physiology of this species and notes that this species has relatively low transpiration rates. Huiskes (1980) has investigated the effect of habitat perturbations on the growth of *A. arenaria* and notes the decline in density of *A. arenaria* on stabilised dunes.

More relevant to this study, Pavlik (1984 & 1985) investigated the water relations of these two species. He found that midday water potentials did not drop below -2.0 MPa and suggests that these plants are rooted in a salt-free water table. Both species were, however, observed to show partial stomatal closure in response to low midday water potentials. He suggests that these responses were imposed by atmospheric factors or the plants themselves, as opposed to factors associated with the substrate. Comparatively, *A. arenaria* maintained higher rates of stomatal conductance and transpiration than *E. mollis*.

Sand dunes and climate of the South African coast

South Africa has roughly 3000 kilometres of coastline, fifty (Lubke *et al.* 1997) to eighty percent (Tinley 1985) of which is estimated to be composed of sandy beaches with associated mobile and vegetated sand dunes. The Frontispiece Map 1 gives the location of key coastal landmarks mentioned here. Various criteria have been used to classify the coast into regions, however, in this study the regions will be defined according to Lubke *et al.* (1997), viz. West, South-west, South, South-east, Transkei and KwaZulu-Natal coasts. The suitability of this classification is discussed in Chapter 5. See Frontispiece Map 2 for representations of these two classifications.

A brief description of the climate of the coastal areas of South Africa is given here. This is discussed in relation to the distribution of *S. plumieri* and *A. arenaria* in Chapter 4 and gives background information as to what conditions the plants are exposed to.

A. arenaria and *S. plumieri* are plants which inhabit sandy coasts, requiring some degree of beach sand movement. The distribution of suitable sandy beaches is therefore an important variable influencing the distribution of both species. At present there are no high-resolution maps showing the nature of the coastline (sandy versus rocky) along the South African coast. The most readily available maps are those of Tinley (1985), and while these are relatively low resolution, they do give the general distribution of sandy beaches and dune fields along the South African coast.

An overview of South African coastal climate

The climate of South Africa is complex. It is driven primarily by the sun and involves complex interactions between the land, the ocean and the atmosphere (Stone *et al.* 1998). Solar radiation is highest in the north and west, exceeding $30 \text{ MJ m}^{-2} \text{ day}^{-1}$, while in the east and south radiation is under $20 \text{ MJ m}^{-2} \text{ day}^{-1}$ (Schulze *et al.* 1997). In addition, the weather of coastal areas, and to an extent the country as a whole, is strongly influenced by the two main ocean currents (Stone *et al.* 1998).

The fast-flowing Agulhas current is one of the strongest in the world, attaining a velocity of 13 km hr^{-1} . Along the KwaZulu-Natal and Transkei coasts, the continental shelf slopes steeply, allowing the Agulhas current to bring very warm water inshore. Along the south-east and south coasts the continental shelf widens, forcing the Agulhas current further offshore, allowing smaller eddies and counter currents to come inshore, bringing either warm, tropical water or cool, deep-sea water. As a result the waters along these stretches of the coast are somewhat variable in temperature. The cold, nutrient-rich, slow-moving Benguela current flows up the west coast bringing much cooler water inshore along this coast. In summer along this coast strong offshore winds cause upwelling of very cold water (as low as 9°C) near the shore (Shillington 1986).

Long term data for coastal and inland stations show that oceans play an important role in moderating temperatures of these areas. Briefly, this may entail the dampening of high temperatures in summer, or the elevation of low temperatures winter (Tinley 1985, Stone *et al.* 1998). For both minimum and maximum temperatures, Schulze *et al.* (1997) show that summer temperatures are lower at the coast compared to inland areas.

In winter the coastal areas have higher temperatures than inland stations. These researchers also show that the range of temperature (minimum temperature subtracted from maximum temperature) is under 11°C although there is a slightly wider range of temperature along the west coast. Inland the range of temperature exceeds 19°C in some places.

Schulze *et al.* (1997) shows a similar trend in the case of relative humidity. Along the east and southern coasts, the proximity to warm oceanic water results in high relative humidity along these coasts. Tinley (1985) notes that relative humidity of most coastal stations is more than 70%. Inland, the relative humidity measurements are considerably lower. On the west coast the sea temperatures are low (Shillington 1986) and, as a result, the relative humidity along this coast is lower. More importantly, there is a steep decreasing gradient from the coast to inland areas where the relative humidity may be less than 30%.

Potential evaporation is lowest along the east and southern coasts where solar radiation (which provides the energy for evaporation) is low, temperatures are moderate and humidity is high. Inland and westwards, solar radiation increases, as does temperature, while humidity decreases resulting in very high evaporation rates in these areas (Schulze *et al.* 1997).

Rainfall occurs predominantly during the summer along the east coast and during the winter along the west and south-west coasts. On the south coast (from about Mossel Bay to the Kei River mouth) the rainfall is considered to be year round (Schulze *et al.* 1997).

Along the coast, rainfall exceeds 1000 mm on the east coast, south to East London; on the south coast, along the garden route from Cape St Francis to George and in the south-west Cape, around the Peninsula and Cape Hanglip. Regions of higher rainfall along this section of the coast generally correspond with regions of high relief (Tinley 1985). The other stretches of the south coast receive rainfall as low as about 500 mm. Along the west coast rainfall is generally less than 200 mm (Schulze *et al.* 1997).

The warm and wet tropical conditions along the eastern parts of the country, which are probably a result of the proximity to the warm tropical Agulhas current, result in the tropical and subtropical flora extending down the eastern coast of the country. This pattern is evident even in course examination of the vegetation such as those of Box (1981).

The distribution of sandy beaches along the South African coastline.

Tinley (1985) has surveyed the coastal dunes of South Africa and this author gives the distribution of all types of dunes in this country. As far as vegetated dunes are concerned, the south-west, south and south-east coasts are dominated by uni-directional nested parabolic dunes, particularly on the windward south-west facing stretches of the coast. On the south-east coast between the Bushman's River and the Kei River, as well as on the KwaZulu-Natal coast, north of the Tugela river, the coasts are dominated by bi-directional parabolic dunes. Along the Transkei and southern KwaZulu-Natal coasts, the sandy beaches are dominated by small dunes confined to bayheads and river mouths. Sandy beaches on this section of coasts are often very steep and generally comprised of coarse-grained beach sands (pers. obs.). On these beaches, littoral plants are confined to only a few metres above the high water mark and below the coastal bush or coastal forest.

Dune vegetation in South Africa

The coastline of Southern Africa forms a discontinuous U-shaped line of sandy beaches and sand dunes extending nearly 12° of latitude south of the Tropic of Capricorn. As a result the coastline traverses a number climatic regions as it curves around from the moist, tropical east coast through the warm, temperate regions of the southern coast to the hyper-arid tropical west coast (Tinley 1985).

The coastline in different parts of Southern Africa is colonised by various assemblages of vegetation. These assemblages are strongly influenced by the vegetation types of the adjacent hinterland and cannot be isolated from them (Lubke & van Wijk 1998).

The east coast is strongly influenced by the Tongoland-Pondoland flora as well as the Afromontane flora (Lubke & van Wijk 1998), and to an extent the Madagascan flora (Tinley 1985). The vegetation of the southern coast is dominated by elements of the Cape fynbos flora, and to a lesser extent the Karoo-Namib flora. All the floras listed above interact in a complex manner along the south-east coast of the Eastern Cape (Lubke & van Wijk 1998). The west coast of Southern Africa, north of Cape Columbine, is dominated by the Karoo-Namib flora with elements of the Cape flora (Tinley 1985, Lubke & van Wijk 1998). The general vegetation types found along the different sections of the coast are given in Frontispiece Map 2. This map is based on the work of Lubke *et al.* (1997).

Along many sandy coasts, strong successional gradients are evident from pioneer communities near the high water mark to some form of climax or mature community on stabilised sands inland. Doing (1985 and earlier works) has proposed a series of habitat zones which, in his own words, “have proved to be widely applicable.” Whether or not this is so remains to be seen, and the species listed by Doing (1985) in various zones for this coast from the literature are not wholly accurate. However, this work does provide a framework and common terminology for further studies. Lubke *et al.* (1997) and Tinley (1985) give a more detailed account of vegetation zonation and succession along different sections of the coast of South Africa. A general successional scheme may include elements of the following on moist parts of the coastline:

Closest to the sea is the youngest pioneer community, which includes low-creeping grasses and rhizomatous or stoloniferous succulent herbs. These plants colonise the mobile sands to form the first partly stable embryonic and primary sand dunes. *S. plumieri* and *A. arenaria* are most often associated with these primary sand dunes, but persist into the second zone. This secondary zone, behind the primary dunes, is dominated by a shrub community with an open, short cover of clumped bushes with an understorey of herbs and climbers. The important species occurring in the first two zones are given in Appendix 2 along with the species rough distribution around the South African coast. This is followed by a closed, more diverse “clipped hedge” canopy of scrub-thicket community and finally the oldest, mature community of tall thicket or

forest furthest from the sea (Tinley 1985). These more mature communities are made up of numerous species which are not listed in Appendix 2, but Frontispiece Map 2 gives some indication of the vegetation types found on the different sections of the coast.

On the drier west coast the succession sequence is truncated and there is only a sparse community of low pioneers. Inland, the coastal vegetation gives way to the desert vegetation of ancient desert sand dunes. Further south on the west coast, climax vegetation includes that dominated by strandveld, while on the south-west and southern coasts the climax vegetation is coastal fynbos (Lubke *et al.* 1997, Hertling 1997).

Because much of the South African coast is eroding, there are often incomplete sequences of succession as described above (Tinley 1985). The above sequence may be compressed into only a few metres between the high water mark and the climax coastal forest as occurs along parts of the KwaZulu-Natal south coast. In such cases some zones may be absent or poorly represented (pers. obs.).

Along the east coast between the Mlalazi and Tugela river mouths, the coast is prograding and there is a distinct set of successively older sand dunes which are in different stages of the succession sequence described above. Moll (1972) and Weisser *et al.* (1982) have described the vegetation along this section of the coast in some detail. For example, Weisser *et al.* (1982) show from successive aerial photographs that the coast has advanced by about 95 metres between 1937 and 1977 (a rate of 2.4 metres per year). *S. plumieri* dominated fore dunes are found closest to the sea with ages from 0 to 30 years, behind which is the 30 to 60 year-old open dune scrub dominated by *Passerina rigida*, then 60 to 90 year-old closed dune scrub and finally dune forest beginning at about 90 years.

There is evidence that these observed zonation patterns which are recorded in many parts of the world (Doing 1985) are a result of increased salt tolerance of the pioneers species closest to the sea (Barbour 1978, Donnelly & Pammenter 1983, Fink & Zedler 1990). Doing (1985) provides indirect evidence for the importance of salt in determining these zonation patterns. He suggests that along tropical coasts more

diverse woody communities are found close to the sea as a result of higher rainfall in these regions. Apart from providing water for these plants, high rainfall contributes to leaching salt out of the coastal sands these plants grow in, allowing less salt-tolerant species to grow closer to the shore.

The coastal sand dunes environment

The classic environmental factors associated with beach and fore dune environments include: salt spray; intense solar radiation (incident and reflected); highly mobile, abrasive substrate; coarse, well-drained substrate; high wind speeds; large temperature fluctuations; high air and substrate temperatures; low concentration of macro-nutrients; and low water retaining ability of the substrate (Hesp 1991, Lubke *et al.* 1997). Many authors consider dunes as xeric environments, aridity being considered an important synthetic stress as it is a product of several of the independent stresses mentioned above (Barbour 1992, Hesp 1991). Barbour *et al.* (1985) give a comprehensive review of the coastal sand dune environment as well as the ecophysiology of strand plants.

Salisbury (1952) has calculated that in the absence of precipitation the water stored in the root zone of dune plants would support them for about four or five days. Episodic increases in soil salinity can also contribute to the physiological desiccation of dune plants (Barbour & De Jong 1977, cited in Pavlik 1985). In addition, dune plants often possess xeromorphic attributes often observed in desert plants, which contribute to the perception that this is a xeric environment (Pavlik 1985). For example, leaf hairs (*Arctotheca populifolia*), succulence and waxy cuticles (*S. plumieri*), leaf rolling and sunken stomata (*A. arenaria*) are all traditionally associated with plants of dry environments.

As yet there is little consensus as to whether this is a xeric environment, and there is still little information as to whether dune plants experience water stress (water limited productivity) and acclimate to it. Many species have extensive root systems and probably utilise the dune aquifer water, which fluctuates in depth at an average of two to three metres (De Jong 1979, Pavlik 1985). Shallow-rooted plants may utilise water in

the superficial layers of sand which results from precipitation or evening dew. This dew may be a result of so-called internal dew formation; moist air from either the atmosphere (Salisbury 1952) or from deeper layers of sand condense on sand grains within the surface layers of the sand (Olsson-Seffer 1909b). Alternatively, dew may form on the surface of the sand and on the leaves of plants which drip onto the sand (Barbour *et al.* 1985).

The view that coastal dunes are inherently dry is disputed by a number of researchers. De Jong (1979) found that a number of dune pioneers on the American west coast had low xylem sap tensions compared to xerophytes. Pavlik (1983a, 1985) measured the water potential of *A. arenaria* and indigenous dune grasses of the American north-west coast. He found that these plants seldom have water potential more negative than -2.0 MPa and have predawn water potentials close to 0 MPa at dawn. Barbour *et al.* (1985) cite additional studies, all of which recorded midday water potentials which are less negative than -2.2 MPa.

Also important in these coastal systems are the high rates of sand movement and salt derived from sea spray and seawater. Because of the long, uninterrupted fetch over the sea, wind at the coast is often considerably higher than inland stations which results in high rates of sand movement. Vegetation has the effect of slowing wind speed, causing the deposition of sand. The vegetation needs to be able to outgrow high rates of sand accretion. Sand deposits of up to 90 cm per year can be tolerated by *A. arenaria*, while *Abronia maritima* can withstand burial for up to 4 months (Barbour *et al.* 1985). While a number of species may tolerate sand burial, many species may indeed be stimulated by high accretion rates (Martinez & Moreno-Casasola 1996) and species such as *A. arenaria* require high rates of sand deposition, possibly to escape soil pathogens (van der Putten *et al.* 1988). Maun (1998) has recently reviewed adaptations of coastal plants to sand burial.

As already mentioned, salt contributes to the physiological desiccation of plants growing on sand dunes. In a number of cases the decreasing salt concentration gradient from the fore-dune inland correlates with the observed zonation patterns at a number of

sites (Barbour 1978, Donnelly & Pammenter 1983). However, physiological mechanisms accounting for the observed zonation of different species in response to salinity however, are sketchy.

Alpha *et al.* (1996) investigated the impact of salt spray and substrate salinity on the morphology and physiology of *S. sericea* and concluded that these two variables contribute to limit the seaward expansion of this species. Salt as an environmental variable may also be closely linked to such factors as wind which moves salt spray landwards (Barbour *et al.* 1985), as well as tidal and storm surge movement of sea water which introduces salt water to the dune sands. While salt spray may limit the seaward spread of many taxa, Rozema *et al.* (1982) have noted that salt spray stimulates the growth of some dune species.

However, De Jong (1979) found that the salinity of the sand was not very high, particularly deeper in the sand where salt concentrations were constant. In the dune aquifer and groundwater, the salinity was always less than 3% sea water, and often less than 1% sea water. The water in dune slacks (where groundwater breaks the surface) is often fresh (pers. obs.). Near the surface, particularly on the seaward side of the dunes, De Jong (1979) recorded slightly higher and more variable salinity concentrations, a trend noted by other researchers (e.g. Barbour 1978, Donnelly & Pammenter 1983). Barbour *et al.* (1985) discuss the importance of salt (both salt spray and sand salinity) in influencing coastal vegetation in some detail.

Reasons for apparent 'xerophytic' adaptations are beginning to emerge. For example Ripley *et al.* (1999) suggest that apart from reducing water use and improving instantaneous water use efficiency, the hair layer on *Arctotheca populifolia* leaves filters out ultraviolet radiation and so increases assimilation rates due to the reduction of photoinhibition. Water may therefore not be as scarce, and the environment not as xeric as previously thought. It is certainly an environment which is subject to specific stresses which exclude many species found immediately inland of the pioneer dunes, but it is probably more complicated than simply a xeric/mesic division.

Chapter 2

Estimating transpiration rates of *Scaevola plumieri* and *Ammophila arenaria* leaves.

Data for *S. plumieri* presented in this chapter form the basis of a paper entitled "An empirical formula for estimating the water use of *Scaevola plumieri*," accepted for publication in the *South African Journal of Science* (Peter & Ripley in press).

Introduction

This chapter attempts to answer question one listed above in the introductory chapter, "Is it possible to simply model transpiration rates of *A. arenaria* and *S. plumieri* from readily available climatic data?" The relationship of transpiration rates of *S. plumieri* and *A. arenaria* to atmospheric vapour pressure deficit is examined and shown to be useful for predicting water loss by transpiration in these two species.

In addition to describing empirical relationships between transpiration and VPD, this chapter also investigates explanations for the observed positive correlations of transpiration to VPD.

Transpiration

In order to absorb carbon dioxide (CO₂) for photosynthesis, plants need to have large, moist surfaces. These moist surfaces are susceptible to evaporative water loss (Kramer 1983). The gradient of water vapour from the leaf to atmosphere is about two orders of magnitude larger than the gradient of CO₂ from the atmosphere into the leaf, so there is inevitably a greater loss of water than assimilation of CO₂ (Schulze 1986).

This evaporative loss of water from the aerial parts of the plants is known as transpiration¹ and involves two stages. The first, the evaporation of water at the cell surface into the leaf air-spaces, is maintained primarily by energy from the sun which determines leaf temperature. In addition, advection may be a major source of evaporation in dry environments (Passioura 1982). This is followed by the diffusion of water vapour out of the leaves of the plant (Kramer 1983).

The diffusion of water vapour out of the leaves is driven by the difference in water vapour pressure within the leaf and the vapour pressure in the atmosphere. This gradient is described by the numerator in Equation 2-1 below. The vapour pressure of the atmosphere is determined by the ambient temperature and humidity, while the vapour pressure at the evaporative surfaces is determined by the leaf temperature and the water potential of the evaporative surface. If it is assumed that the water potential of the evaporative surface is zero and the cells from which evaporation is occurring are turgid, then the vapour pressure is the saturation vapour pressure at leaf temperature. However, cells of transpiring leaves are often in the range of between – 1.0 and –6.0 MPa, but this only introduces a small amount of error (Kramer 1983). For example, at a leaf temperature of 30°C the vapour pressure at the cell surface is 4.24 kPa when the cells have a water potential of 0.0 MPa. The vapour pressure falls to 4.16 kPa at a cell water potential of –3.0 MPa, a decline of only 2%.

Water moves from the leaf to the air along a concentration gradient and is restricted by cuticular resistance, boundary layer effects and stomatal resistance. In many cases the boundary layer is removed even by light winds. Because the cuticular and stomatal pathways for water loss are in parallel, cuticular transpiration is likely to be very low when the stomata are open – cuticular transpiration is only important when stomata are closed (Schonherr 1982, Fitter & Hay 1995). In many cases stomatal resistance is the main barrier to transpiration and stomata play an important role in regulating water loss from aerial parts of plants (Kramer 1983).

¹ Evapotranspiration is the evaporation of water from an 'ecosystem' and includes transpiration as well as the evaporation of water from the soil.

Transpiration rates therefore rely on a supply of energy to vaporise water within the leaf and the gradient of water vapour concentration or pressure between the leaf air spaces and the atmosphere. Transpiration rates also depend on the size of the various resistances (stomatal, boundary layer, cuticular) which contribute to reducing the movement of water out of the leaf (Kramer 1983). More formally, transpiration rates (E) may be described as;

$$E = \frac{e_{T_l} - e_{T_a} \times \frac{RH_a}{100}}{r_l + r_a}$$

(Equation 2-1, modified from Gates 1976)

where e is vapour pressure at leaf temperature (T_l) and ambient temperature (T_a), and RH_a represents ambient relative humidity. The terms r_l and r_a represent resistance to water vapour movement in the leaf and atmosphere respectively. Note that r_l includes resistance to water vapour movement by the stomata and the cuticle, but as discussed above cuticular resistance is generally negligible (Gates 1976, Kramer 1983).

Transpiration is considered by many to be of vital importance to higher plants. Negative pressure, which causes water to move up the soil-root-xylem-leaf gradient, is generated by the evaporation of water in the mesophyll of the leaf (Passioura 1982). This force supplies the aerial parts of the plant with water and the various nutrients taken up by the roots from the soil. Evaporation of water from the leaf is one of the chief means of cooling the leaf in many plants, and is thought to be important in maintaining optimal leaf temperatures (Gates 1968 & 1976, Raschke 1970 & 1975).

However, Kramer (1983) suggests that the beneficial role of transpiration is overstated. He points out that leaves are rarely injured in full sunlight when leaf temperatures rise due to temporary wilting and midday closure of stomata. In addition, this researcher cites examples of studies where it is shown that growth rates are accelerated with increased humidity. Increased humidity would be expected to lower transpiration and hence the uptake of nutrients due to the lowered water movement through the soil-plant-atmosphere continuum.

The suggestions of Kramer (1983) are contrary to the detailed investigations by Gates (1968, 1976) and Raschke (1970, 1975). Raschke (1975) shows that above temperatures of about

35°C, stomata of plants well supplied with water become insensitive to CO₂ concentration. The stomata open even if CO₂ assimilation has stopped and CO₂ is being evolved from the leaf at temperatures above 40°C (Raschke 1970). Schulze *et al.* (1973) show that stomatal apertures of desert plants increase with increased temperature, as long as water is not limiting. As Raschke (1975) suggests, this loss of sensitivity to CO₂ and the continued high transpiration rates can be beneficial in avoiding overheating when water is available as well as in maintaining leaf temperatures near the optimum for photosynthesis (Raschke 1970, Drake *et al.* 1970).

Raschke (1975) also observes that in many species where the leaves of the plants are strongly illuminated, leaf temperatures are near air temperature when the air temperature is approximately 33°C. Below an air temperature of 33°C, leaf temperatures are higher than ambient, while when air temperature is higher than 33°C, leaf temperatures are below ambient. He attributes this to the exponential increase of water vapour pressure with increased temperature, which results in increased negative feedback of transpiration as well as the increased stomatal aperture with temperature.

Lange (1959, cited in Raschke 1975) reported substantial transpirational cooling of leaves of *Citrullus* sp. growing at an oasis in north Africa. The leaves of this plant were 15°C cooler than the air which was at 50°C.

The control of transpiration by stomata

Stomata are pores formed by a pair of specialised guard cells and are found in the epidermis of aerial parts of the majority of higher plants. As a result of unequal thickness of the cell walls, and the arrangement of cellulose microfibrils, the shape of the guard cells is altered by changes in their turgor pressure. Changes in the shape of the guard cells alter the pore aperture and hence regulate the amount of water vapour leaving the leaf and the amount of CO₂ entering it (Esau 1977, Bolhar-Nordenkamp & Draxler 1993). Stomata are most numerous on the leaves of higher plants, particularly on the abaxial surface in many tree species (hypostomatous leaves). In many herbaceous plants, stomata occur on both abaxial and adaxial surfaces of the leaves. Such leaves are termed amphistomatous, but in many cases stomatal densities are higher on the abaxial surface (Willmer 1983).

The stomata are situated at the point of the greatest decrease in water potential in the soil-plant-atmosphere continuum. As such they may be considered to be in the most advantageous position in the continuum to control the movement of water from the soil, through the plant, to the atmosphere (Jarvis & Morison 1981). Raschke (1975, 1979) gives extensive reviews of the mode of stomatal movement to bring about the opening and closing of stomatal pores.

While much is known about the detailed molecular processes involved in stomatal movement (e.g. Raschke 1975), there is still uncertainty about the physiological control or inducement of these responses and how the guard cells 'sense' changes in various external and internal factors (Jones 1998). Stomatal regulation has been the focus of considerable research, and debate continues as to the exact stimuli to which stomata respond (Bunce 1996, Franks *et al.* 1997). Papers presented in a book edited by Jarvis & Mansfield (1981) give an overview of many of the factors contributing to stomatal movement and stomatal control of assimilation and transpiration, as do Schulze & Hall (1982) and Raschke (1975).

A change of stomatal aperture is thought to be related to photosynthetic demand for CO₂ (Raschke 1975). In many cases stomata open in the light and close in the dark, although there are important exceptions such as species with Crassulacean Acid Metabolism (CAM). Stomata also open in many species if the CO₂ concentration in the sub-stomatal cavity falls below a certain critical value, the value of which may be species specific or dependant on the photosynthetic pathway employed (C₃, C₄ or CAM: Fitter & Hay 1995). Light and CO₂ are therefore both thought to make a significant contribution to the opening and closing of stomata on a daily basis, although it may be difficult to resolve the importance of these two factors in isolation (Mansfield *et al.* 1981).

The opening response of stomata to light may be linked to the intercellular CO₂ concentration which declines in the light as assimilation proceeds, although this is not always the case (Schulze & Hall 1982). However, opening responses to CO₂ are not limited to conditions of light. CAM plants open their stomata in the absence of light. Light also induces opening responses that are independent of CO₂ concentrations, but it is likely that stomata respond to a combination of both light and CO₂ concentrations in non-CAM plants (Mansfield *et al.* 1981).

High temperature may cause stomatal closure by increased respiration, which results in higher CO₂ concentrations in the leaf air spaces (Fitter & Hay 1995).

Stomata may also respond to such variables as humidity, plant water status, temperature and growth substances. Lösch & Tenhunen (1981), for example, show that stomata can respond directly to changes in the water vapour content of the atmosphere, altering the aperture before changes in leaf water potentials have occurred. Mechanisms for such responses remain unresolved (Schulze & Hall 1982) and there has been recent debate as to whether stomata respond directly to the humidity of the atmosphere (Bunce 1996) or to the rate of transpiration (Monteith 1995). Stomata of plants suffering from water stress normally respond by closing to some degree. This is thought to be a result of increasing concentration of abscisic acid which occurs as water stress increases (Lösch & Tenhunen 1981). The stomata are also thought to respond to leaf water potentials and close at a threshold level. The value of this threshold varies with species and conditions experienced by the plant (Fitter & Hay 1995). The role of temperature may be complex and influence the response of stomata to many other environmental factors (e.g. Lösch & Tenhunen 1981).

Stomatal aperture may therefore be influenced in a complex manner by such factors as solar radiation, CO₂ concentration primarily within leaf air spaces, humidity, water stress, wind, growth substances and endogenous rhythms (Jarvis & Mansfield 1981). Fitter & Hay (1995) suggest that the success of a species in a particular environment depends on the manipulation of the plants response to these factors so as to provide a favourable balance between assimilation of CO₂ and the loss of water by transpiration.

Modelling transpiration

Mathematical models can be objective and efficient systems for integrating and summarising available information, and they are useful for expressing and testing hypotheses (Hall 1982). However, “mathematical models of biological systems are works of art combining both fact and fiction, and they only occasionally and partially simulate reality” (Passioura 1973, cited in Hall 1982). These models may be seen as merely gross representations of complex natural systems. While it may not be possible to develop mathematical models that perfectly mimic biological systems, it is possible to construct useful models to help understand subsystems

within plants and ecosystems (Loomis *et al.* 1979). In many cases, models for predicting transpiration rates have practical applications such as determining the water use of crops (Thornley 1996, Alves *et al.* 1998) and irrigation scheduling for crop plants.

Reynolds *et al.* (1993) identifies three groups of models: empirical, phenomenological and mechanistic models. Empirical models are based on statistical formulations which correlate a set of observed variables to some response variable that is of interest. These models are simple, easily formulated and straightforward to apply, however, they lack generality and thus are of restricted use. Phenomenological models describe the system or process at the level of interest and, in contrast to empirical models, are derived from a general understanding of the system in question. Finally, mechanistic models decompose a system into its component parts and describe the behaviour of the entire system through the interaction of these different parts. Generally, mechanistic models are composed of a subset of empirical and phenomenological models.

Reynolds *et al.* (1993) point out that the question of scale is very important in modelling. A mechanistic model at one scale may only form a phenomenological model component of a mechanistic model at a larger scale. They note that the development of a hierarchy of models, each of which describes a particular scale and draws on outputs from lower levels, is important in accounting for the translation of effects from the physiological level to the ecosystem level.

There have been two approaches to calculating transpiration in the past. The first, favoured by meteorologists, entails describing transpiration in relation to potential evaporation. This is because transpiration is driven primarily by the environment, specifically the amount of light which is the energy source driving evaporation (Passioura 1982), as well as the dryness of the atmosphere which produces the gradient of water vapour pressure from within the leaf to the atmosphere (Monteith 1965, Kramer 1983).

For example, the rate of evaporation from a canopy is described by the Penman equation, which relates the evaporation to the available radiant energy and the humidity deficit, and less directly to air temperature and wind speed. This equation assumes the absence of advection

and low stomatal resistance (Monteith 1965). The equation does not hold when stomatal resistances are high. To circumvent this, terms for stomatal resistance have been added to the original equation, although this is perhaps not ideal (Passioura 1982). In addition to low stomatal resistances, this model requires open, well-ventilated canopies where the transpiration of individual leaves are coupled to the environment (Jarvis & McNaughton 1986).

The second approach holds that potential evaporation is important in driving transpiration (creating the gradient from leaf to atmosphere so that transpiration can occur), but stomata play an essential role in controlling transpiration, such that the inclusion of terms for stomatal conductance is imperative. Stomatal regulation of transpiration is important and is seen as the primary factor controlling transpiration by proponents of this approach (Jarvis & McNaughton 1986).

The above two processes may be valid at different scales and in vegetation of different structures. For example, the size of the water vapour gradient from leaf to air is important in explaining transpiration at the stomatal level, while at the canopy level stomatal regulation may be important in regulating overall transpiration. Alternatively, potential evaporation models may be acceptable in open, well-ventilated canopies which are not water stressed, but fail in cases where there is a more complex canopy structure (Jarvis & McNaughton 1986).

Essentially this study uses the former approach, comparing transpiration to potential evaporation, transpiration in this case being driven by the gradient of water vapour from the leaf air spaces to the atmosphere. This gradient is easily described from measured climatic variables, making subsequent predictions of transpiration possible. Modelling transpiration is discussed further in Chapter 3, specifically scaling predictions of transpiration from the level of individual leaves to the canopy level.

Study Sites

This study was undertaken primarily on the dunes west of the Old Woman's River mouth, (just to the east of the Fish River), Eastern Cape, South Africa during various seasons between 1997 and 1999 (Figure 2-1). Additional data were collected on dunes at various beaches of the

Eastern Cape. These include West Beach, Port Alfred and Gulu River mouth, south of East London. In KwaZulu-Natal, additional *S. plumieri* transpiration data were collected at Southbroom during June 1998.

Table 2-1: Co-ordinates of the study sites where this work was conducted.

Study Site	Longitude	Latitude
Southbroom	30° 18' 39"E	30° 54' 55"S
Nahoon Point	27° 56' 59"E	32° 59' 51"S
Gulu River Mouth	27° 43' 44"E	33° 07' 03"S
Old Woman's River Mouth	27° 08' 49"E	33° 28' 59"S
Port Alfred west beach	26° 52' 36"E	33° 37' 14"S
Kenton-on-Sea	26° 41' 45"E	33° 39' 50"S

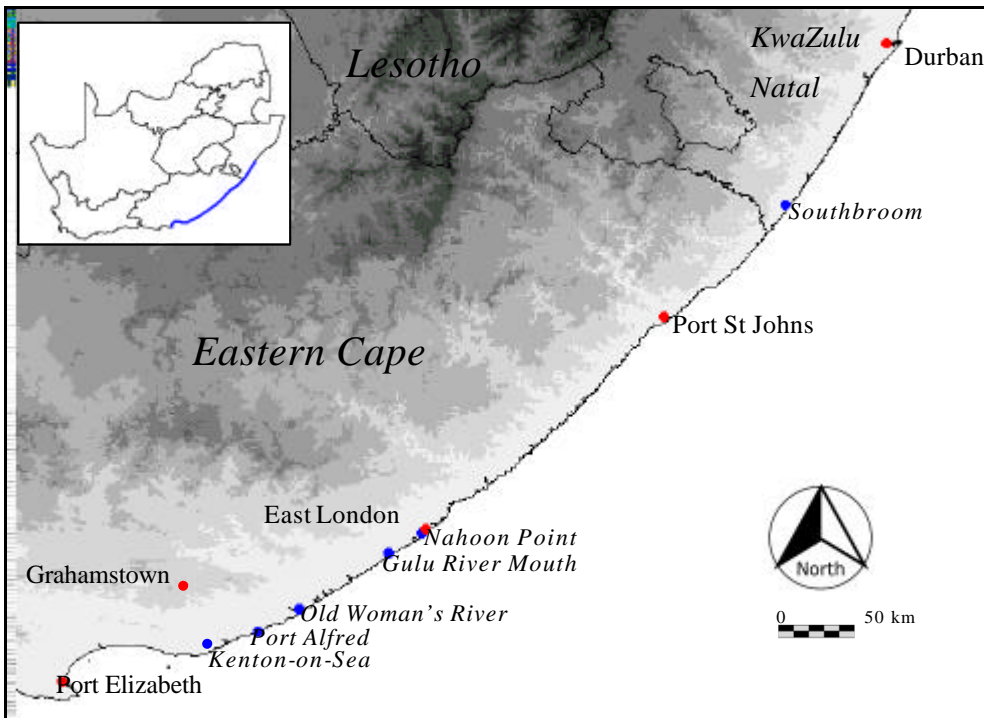


Figure 2-1: Position of various study sites (blue) along the south-east coast of South Africa, in relation to major centres (red). Altitude increases with darker shades of grey. Inset shows the position of these sites in relation to the entire country.

Materials and Methods

This chapter primarily describes the response of transpiration to vapour pressure deficit at the leaf level. These data were collected mainly in the field at the Old Woman's River study site.

The transpiration data were collected as part of a suite of various gaseous exchange data, some of which were used to calculate other parameters such as assimilation rates. Additional experiments were conducted to help explain the observations made.

In most cases similar data were collected for both *S. plumieri* and *A. arenaria*. Where methods differ slightly between species, these differences are explained.

Calibration and configuration of the IRGA

All gaseous exchange measurements were using an LCA2 portable infrared gas analyser (IRGA), mass flow controller and Parkinson broad-leaf chamber (PLC: Analytical Development Corporation, Hoddeson, UK). In a few cases a narrow-leaf PLC was used to measure transpiration rates of *A. arenaria*.

The CO₂ reading on the LCA2 IRGA was calibrated using certified calibration gas at a concentration of 406 ppm. The relative humidity reading of the LCA2 was calibrated using a dew point apparatus set-up in a Lauda RC6 water bath (Lauda Instruments, Germany). Zero relative humidity was determined by blowing dry air through the Parkinson Broad-leaf chamber directly from the Mass Flow meter. The relative humidity of the air entering the PLC was adjusted by altering the temperature of the Lauda water bath. The span was checked at various relative humidities. Relative humidity of the air within the PLC was calculated according to the equation:

$$RH = \frac{\text{Saturation Vapour Pressure (Dewpoint Apparatus Temperature)}}{\text{Saturation Vapour Pressure (PLC Temperature)}} \times 100$$

(Equation 2-2)

The LCA2 calibration was checked periodically throughout the course of this study, however, no subsequent alterations to the original calibration were required.

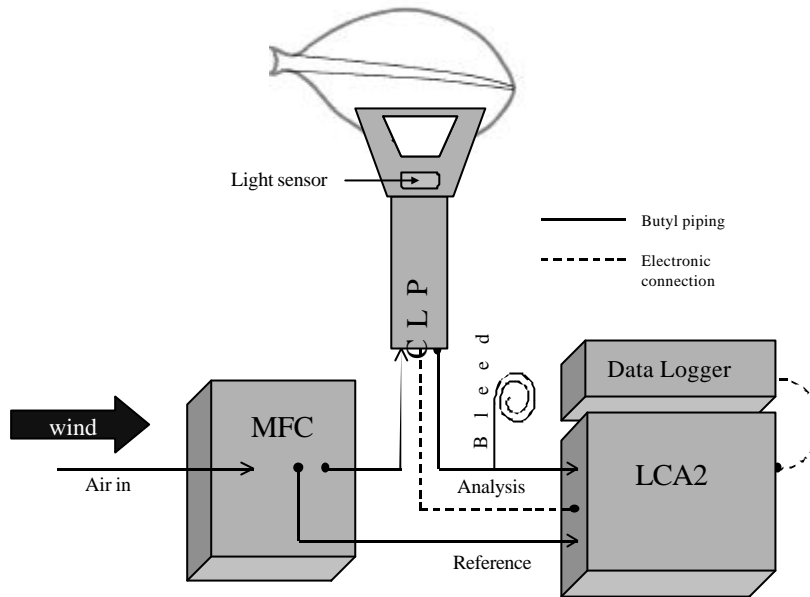


Figure 22: The LCA2 portable IRGA was set up in an open configuration. The Mass Flow controller (MFC) was positioned upwind from where measurements were being made, to avoid CO₂ contamination from the user. The MFC provided a constant stream of dry air at known flow rate to the Parkinson leaf chamber (PLC) where it is passed over the leaf. The PLC measures photosynthetically active radiation in the same orientation as the leaf. The PLC also measures the ambient air temperature and the relative humidity of the air after passing over the leaf. After passing over the leaf, the air is returned to the Leaf chamber analyser (LCA2) where CO₂ concentrations are compared to ambient air (also provided by the MFC). Data was logged using a DL-2 data logger connected to the LCA-2. All instruments from the Analytical Development Company, Hoddeson, UK.

The IRGA was set up in an open configuration (Figure 2-2). The mass flow controller was placed upwind and set to provide a flow rate of between 300 and 500 ml. The air was passed over Drierite and magnesium perchlorate to remove all water vapour from the air. The air was then directed either to the reference inlet on the LCA-2, which measures the ambient CO₂ concentrations, or to the inlet on the PLC. After passing over the leaf in the PLC, the air is returned to the LCA-2 analysis inlet. An outlet bleed was provided on the return from the PLC to avoid over pressurising the LCA-2 detector column.

The PLC measures the air temperature, relative humidity of the outflow air (after passing over the leaf) and incident PAR in the orientation of the leaf. The PLC also contains a small stirring fan and, because of the small cuvette volume, boundary layer resistances within the cuvette are low (ADC 1985).

Because the MFC dries the air, it is possible to calculate the change in water vapour concentration between the inflow air (0%) and the outflow air which has been passed over the leaf. From this change in water vapour concentration and the area of the leaf enclosed within the PLC (6.25 cm² if the broad leaf cuvette is filled), transpiration can be calculated.

The change in CO₂ concentration in the air that has passed over the leaf in the PLC is determined by the difference in CO₂ concentration measured in the reference air line and the analysis line.

The data recorded in the field were logged on the LCA2 data logger (DL-2) and downloaded for subsequent analysis, using the software Possim 1.0 (Sphynx Ink. 1996). This software was also used to calculate photosynthetic parameters, such as stomatal conductance and transpiration, according to the equations of von Caemmerer & Farquar (1981).

Field measurements

Transpiration rates of *S. plumieri* were recorded in the field on the 30-01-97, 23-07-97, 24-07-97, 10-09-97 and the 14-02-99 (Summer, Winter and Spring) at the Old Woman's River study site. Additional field data were collected at Southbroom on the 21-06-98 (Winter). *A. arenaria* transpiration data were collected at Old Woman's River on the 12-11-1999, 14-02-1999, 14-03-1999, 30-04-1999 and the 15-09-1999 (Summer, Autumn and Spring).

Transpiration rates of *S. plumieri* and *A. arenaria* were recorded in the field over a wide range of environmental conditions. Measurements were taken at approximately hourly intervals from dawn until after sunset over a number of seasons (see dates above). Leaves were selected in the vicinity of automatically logging temperature and humidity sensors. Leaves were also chosen from various points along the length of the stem. In *S. plumieri* leaves were typically selected between the 4th leaf from the apex and the first yellow leaf (about leaf 15 to 20). The youngest three to four leaves were not used as they are not big enough to fit into the PLC, while the yellowing, senescing leaves showed negligible transpiration rates (data not shown). In the case of *A. arenaria* green leaves were chosen randomly from a population of leaves on a single culm as well as from various culms in a stand. Leaves typically ranged from 7 mm wide in the oldest most unrolled leaves to only 2 or 3 mm in the youngest emerging

leaves. Older dead leaves (dry grey leaves) were assumed not to be transpiring. An individual leaf was inserted into the PLC and held in its natural orientation.

In both species only one leaf per shoot was selected when recording gaseous exchange data. A total of 226 *S. plumieri* leaves and 145 *A. arenaria* leaves were measured, each from a separate shoot. There was no formal randomisation in the selection of shoot (and hence leaves). However, only three to five shoots (and therefore leaves) were measured in a particular area of the dune, before moving a short distance and taking further measurements. All leaf measurements, collected from different parts of the sand dunes, were pooled and analysed together for each species.

Concurrent with the collection of gaseous exchange, ambient temperature and relative humidity were recorded automatically every five minutes using Weather Monitor II data loggers (Davis Instruments, Hayward, California, USA). These climatic data were downloaded using the Weather Monitor program, Weatherlink 3.01 (Davis Instruments Corporation 1994). From the climatic data the atmospheric vapour pressure deficit (VPD) was calculated according to the equation:

$$VPD = SVP_{T_a} - \left(SVP_{T_a} \times \frac{RH_a}{100} \right)$$

(Equation 2-3)

Here SVP_{T_a} is the saturation vapour pressure at ambient temperature (T_a), and RH_a the ambient relative humidity. Saturation vapour pressure at a specific temperature, for example T_a , was calculated according to the equations of Goff & Gatch (1946):

$$SVP_{T_a} = \frac{6.1375 \exp \left(T_a \times \left[18.564 - \left(\frac{T_a}{254.4} \right) \right] \right)}{T_a + 255.57} \times \frac{1}{10}$$

(Equation 2-4)

Atmospheric VPD was used instead of leaf-to-air VPD. This makes it possible to predict transpiration rates from measurements of ambient temperature and humidity without the added complication of measurements of leaf temperature. Additional climatic data were obtained from the Great Fish Point weather station of the South African Weather Bureau.

Weight loss experiment

As the LCA2 dries air before the air enters the PLC, and because the PLC stirs the air to break down the boundary layer, transpiration rates measured with this instrument were probably overestimates. Consequently, rates measured with the LCA2 were compared with leaf transpiration rates calculated by weight loss experiments on excised leaves. Individual leaves were excised and weighed using a Cahn 4100 four-place balance (Cahn Instruments, California, USA). After about five minutes, the leaf's transpiration rate was recorded using the LCA2 before being reweighed. Transpiration rates calculated by weight loss were compared to transpiration rates measured with the LCA2. Transpiration rates ($\text{mol m}^{-2} \text{s}^{-1}$) were calculated from weight loss data according to the equation:

$$E = \frac{\Delta \text{weight}}{18} \times \frac{1}{t} \times \frac{1}{a}$$

(Equation 2-5)

where Δweight is the difference between the starting and ending weights of the leaf in grams, t is the time between weighings in seconds and a is the leaf area, in square metres, of the leaf in question. Ambient temperature and relative humidity were recorded automatically using a Weather Monitor II data logger.

Water potential

Leaf water potentials of *S. plumieri* and *A. arenaria* were collected using a pressure bomb (Hall *et al.* 1993). Whole shoots with 4 to 8 leaves were selected, covered with a transparent plastic bag and excised. Loose leaves near the point of excision were removed. Using a cork borer, the cut end of the shoot was threaded through a hole in a rubber stopper. The stopper was then inserted into a hole in the lid of the pressure bomb with the leaves inside the chamber

of the pressure bomb. After sealing, the chamber was gradually pressurised until the water was observed, using a magnifying glass, emerging at the cut surface. As with the collection of gaseous exchange and gravimetric data, ambient temperature and humidity were recorded concurrently using the automatic Weather Monitor II data logger.

Water potentials of *S. plumieri* were collected by B.S. Ripley (unpublished data) concurrently to the collection of many of the gas exchange data. Water potentials of *A. arenaria* were collected at different times to the gas exchange data.

Integrated light data

Because the PLC measures instantaneous photosynthetically active radiation (PAR) in the same orientation as the leaf, a large range of PAR measurements were recorded. While assimilation might be expected to respond to the instantaneous PAR incident on the leaf, stomatal conductance is likely to be more strongly correlated to the integrated overall solar radiation incident on the plant. For this reason, solar radiation data were obtained from the automatic SAWB Port Elizabeth weather station. This station records radiation with a horizontally placed Li-cor pyranometer at standard instrument height and these measurements represent MJ m⁻² integrated over an hour. These values were converted to W m⁻² by multiplying by 277.8 (D. Esterhuysen pers. com.) and plotted against time. A fourth- to sixth-order polynomial regression line was fitted to the points, depending on fit. The regression was used to calculate irradiance at the same time each of the gas exchange measurements were made. This was repeated for each of the days on which field data were collected.

CO₂ Experiment

There is evidence that stomata respond to elevated CO₂ concentrations by closing (e.g. Willmer 1983, Morison 1987, cited in Weyers & Meidner 1990). Fitter & Hay (1995) note that one possible reason for midday stomatal closure, observed in many species, is the increased temperature at these times. This elevated temperature increases the rate of respiration and hence the CO₂ concentration within the leaf air spaces. The stomata respond by closing, which can lead to improvements of water conservation.

For this reason it was thought that by exposing the leaves to elevated CO_2 it might be possible to close the stomata artificially, revealing relationships between leaf conductance and transpiration.

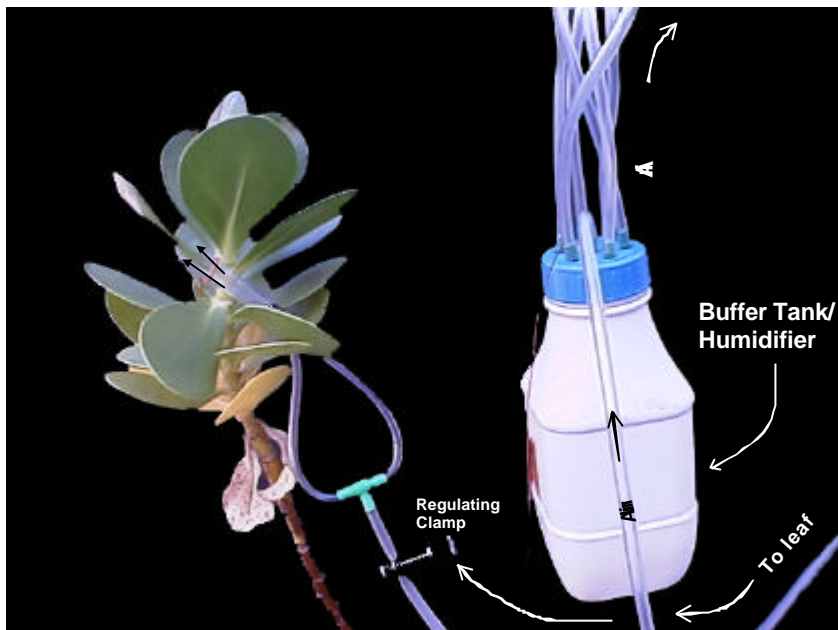


Figure 2-3: Rigging scheme for piping air with elevated CO_2 to individual *S. plumieri* leaves. Air from a cylinder made up to the desired CO_2 concentration is blown through a buffer tank which contains water to humidify the air. The humidified air then exits via six separate pipes to individual leaves, blowing air over both surfaces of the leaf. All outlet pipes are the same lengths. Clamps were used to set the flow rate at the mouth of the pipes. Changing the temperature of the water in the buffer tank altered the humidity of the outflowing air.

Figure 2-3 shows an overall scheme of how CO_2 was piped to individual leaves. Air with a specific CO_2 concentration (1000 ppm) from a cylinder was humidified in a buffer tank before being piped to the leaves via one of six out flow lines. The flow rate at the mouth of the pipes was balanced by bubbling all the tubes in water at the same depth and visually altering the flow rates until the pipes bubbled at approximately the same rate. Each pipe was split and positioned so that air was blown over both the abaxial and adaxial surfaces of the chosen leaf. An additional outflow tube was reserved as a reference line for the LCA2 when recording measurements with this instrument.

The humidity (and therefore VPD) of the outflow air was altered by changing the temperature of the water in the buffer tank. This was achieved by immersing the buffer tank in crushed ice or water of different temperatures. The humidity of the outflow air was determined by

blowing it through the PLC. Air temperature was assumed to be the same as ambient and was recorded using the Davis weather monitors. For practical reasons related to leaf morphology this experiment was not repeated on *A. arenaria*.

Results

Transpiration in relation to vapour pressure deficit

A comparison of transpiration rates measured using the LCA2 with values determined by weight loss yields a straight line (Figure 2-4A, $r^2=0.93$) in *S. plumieri*, showing that the LCA2 overestimates the actual transpiration rate by about 40% in this species. In the case of *A. arenaria* the overestimation by the LCA2 is considerably larger, about 70%, and the data is more variable (Figure 2-4B, $r^2=0.61$).

The equations of the straight lines in Figures 2-4A and 2-4B were used to adjust the values of the transpiration rates in both *S. plumieri* and *A. arenaria*. However, in the case of *A. arenaria*, the equation of the original regression line in Figure 2-4B resulted in negative transpiration rates being calculated at low VPDs, the intercept being -0.81. For this reason, a modified regression line was used with the intercept set to zero ($r^2=0.54$). This was also done for *S. plumieri*, changing the r^2 value fractionally.

The adjusted transpiration rates were then related to VPD. In the case of *S. plumieri* there is a strong, nearly linear relationship (Figure 2-5). A straight-line regression has an $r^2=0.86$, while the second-order polynomial regression used in Figure 2-5 has an $r^2=0.88$. The majority of the data are in the VPD range of 0 to 2 kPa and, over this range, are probably linear. Above a VPD of 3 kPa the transpiration rates begin to saturate and the regression becomes curvilinear.

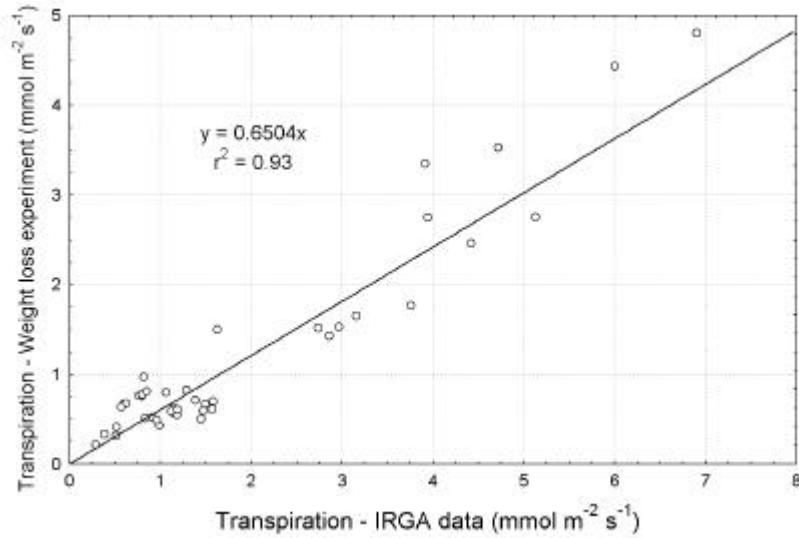


Figure 2-4A: Transpiration rates of individual excised *S. plumieri* leaves calculated by weight loss compared to transpiration rates measured with the LCA2 IRGA (n = 43, $\hat{r}^2=0.93$, p=0.0000).

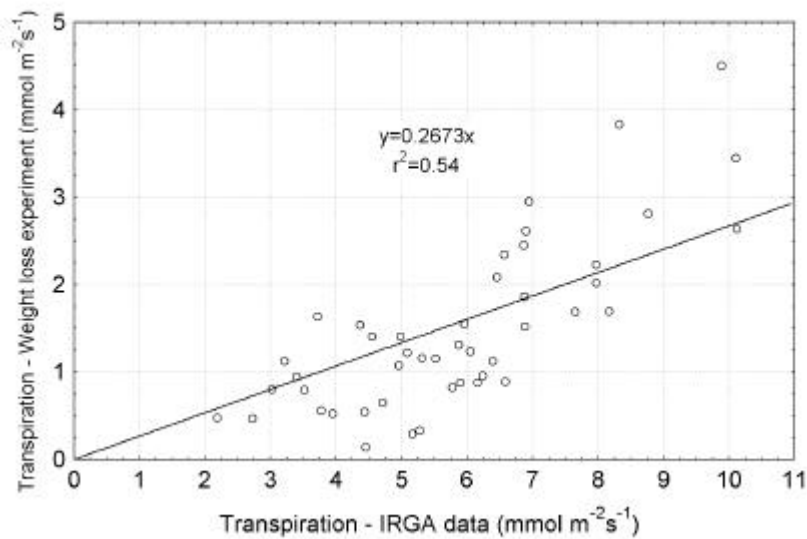


Figure 2-4B: Transpiration rates of individual excised *A. arenaria* leaves calculated by weight loss compared to transpiration rates measured with the LCA2 IRGA (n = 46, $\hat{r}^2=0.61$, p=0.0000).

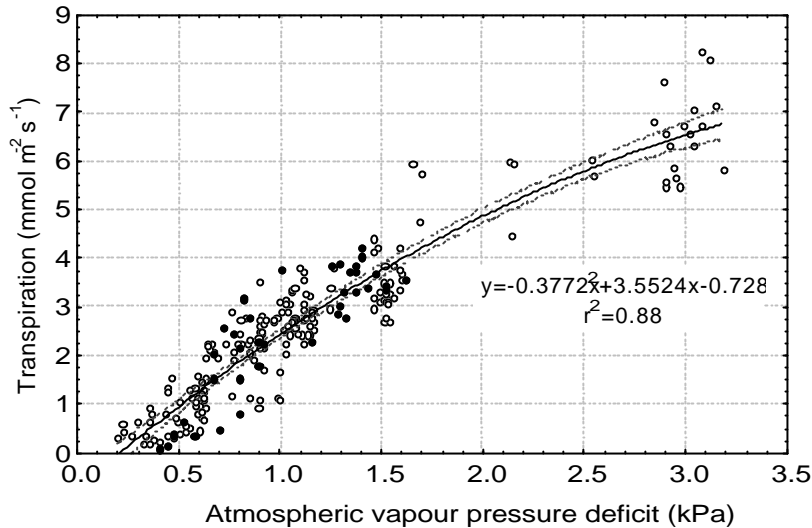


Figure 2-5: Transpiration of *S. plumieri* as determined from gaseous exchange data (corrected according to the relationship in Figure 2-4A) related to VPD calculated from weather data collected at Old Woman's River (○) on various dates from 1997 to 1999 and Southbroom (●) on 21-06-98. Data were collected at approximately hourly intervals from dawn until sunset on the days indicated in the text (n=226, $r^2=0.88$, p=0.0000). The equation refers to the mean regression line (solid black). Dotted lines are the 95% confidence limits for the regression line.

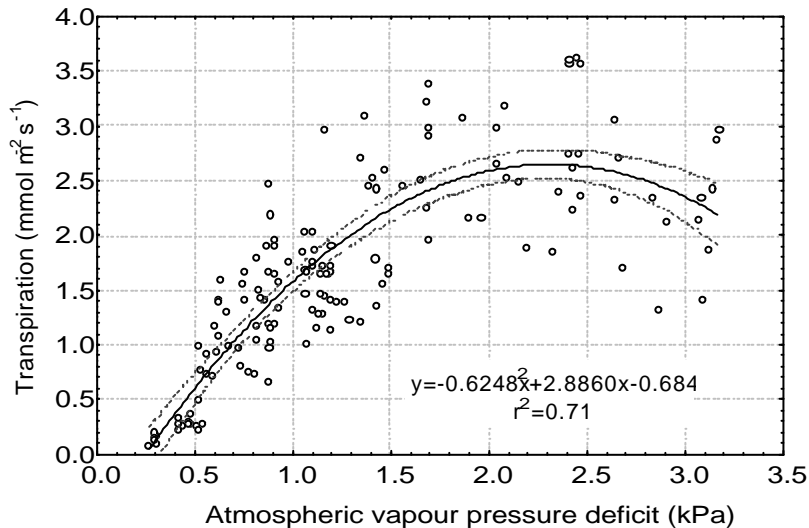


Figure 2-6: Transpiration of *A. arenaria* as determined from gaseous exchange data (corrected according to the relationship in Figure 2-4B) related to VPD calculated from weather data collected at Old Woman's River on various dates in 1998 & 1999. Data was collected at approximately hourly intervals from dawn until sunset on the days indicated in the text (n=145, $r^2=0.71$, p=0.000). The equation refers to the mean regression line (solid black). Dotted lines are the 95% confidence limits for the regression line.

The relationship in the case of *A. arenaria* is clearly curvilinear, with transpiration rates saturating at a VPD of about 1.8 kPa (Figure 2-6, $r^2=0.71$). There is more spread in the data as

compared to *S. plumieri*. This is possibly a function of the low transpiration rates and the variable degree of unrolling, with the associated variable boundary layer conditions within the PLC as discussed above.

These relationships between E and VPD for both species may be used to predict the E of individual leaves where the VPD is known. VPD in turn is easily calculated from measurements of ambient temperature and humidity, data that is readily available from many coastal weather stations.

Physiological explanations for the relationship of E to VPD in *S. plumieri*

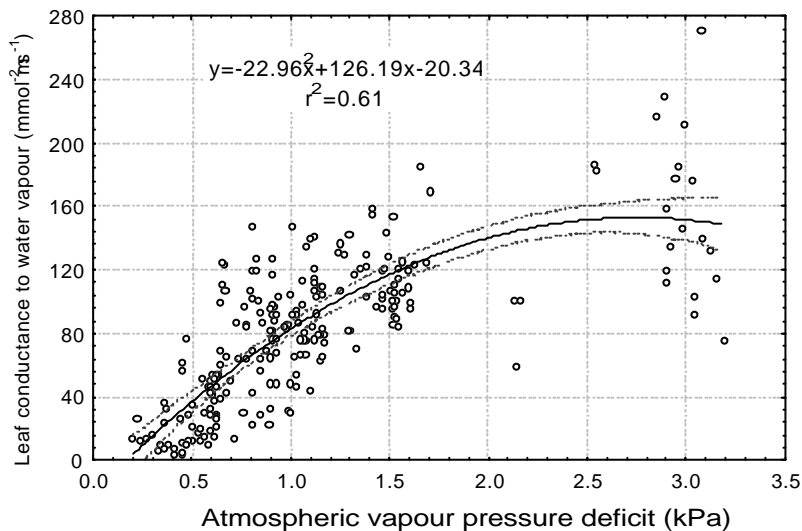


Figure 27: *S. plumieri* leaf conductance to water vapour related to VPD calculated from weather data collected at Old Woman's River on various dates from 1997 to 1999 as well as at Southbroom on 21-06-98 ($n=226$, $r^2=0.61$ $p = 0.0000$). The equation refers to the mean regression line (solid black). Dotted lines are the 95% confidence limits for the regression line.

The strong, nearly linear relationship between E and VPD suggests that transpiration is unlimited by leaf conductance over most of the VPD range measured, and that water moves out of the leaf air spaces in response to the size of the water vapour concentration gradient. However, this is not a passive evaporation phenomenon, and leaf conductance to water vapour increases with increased VPD up to 1.7 kPa, above which leaf conductance to water vapour saturates. As a result this relationship is best described by a second-order polynomial

(Figure 2-7, $r^2=0.61$) as opposed to a straight-line function ($r^2=0.52$) and may represent leaf conductances approaching maximal attainable values when stomata are fully open. This suggests that leaf conductance to water vapour saturates at a lower VPD compared to E and that leaf conductance does markedly affect the relationship of E to VPD at high VPDs (Figure 2-5). Specifically, the stomata limit transpiration rates at high VPD and might represent conditions of maximal stomatal aperture.

It is likely that the relationship of E to VPD might be a result of other physiological processes responding to environmental variables which co-vary with VPD. Specifically it was thought that physiological processes of these plants might respond to changes in light as has been suggested by Pammenter & Smith (unpublished manuscript).

PAR plays an important role in determining ambient temperature and relative humidity and leaf temperature. These three variables in turn contribute to determining the transpiration rate of a leaf. However while incident light can change rapidly, these other variables respond more slowly and hence transpiration is poorly correlated with instantaneous PAR measured with the PLC ($r^2=0.21$, data not shown).

The instantaneous PAR measurement recorded with the PLC where made in the orientation as the leaves. Pammenter & Smith (unpublished manuscript) show that the azimuth angles of leaves on a shoot are evenly distributed around individual shoots. As a result PAR measurements recorded in the orientation of various leaves are variable – some measurements being made facing the sun, other away from the sun, with a range in between these two extremes. Instantaneous PAR measurements made with the PLC are therefore a poor summary of light impinging on a leaf because this instrument shades much of the leaf and so light shining on the underside of the leaf may not be recorded. Therefore there is likely to be poor correlation between instantaneous PAR and factors such as ambient temperature and relative humidity as well as leaf temperature which determine transpiration rates. Longer term integrated measurements of solar radiation may better reveal relationships between E and light as there is sufficient time for the plants to respond to the light environment.

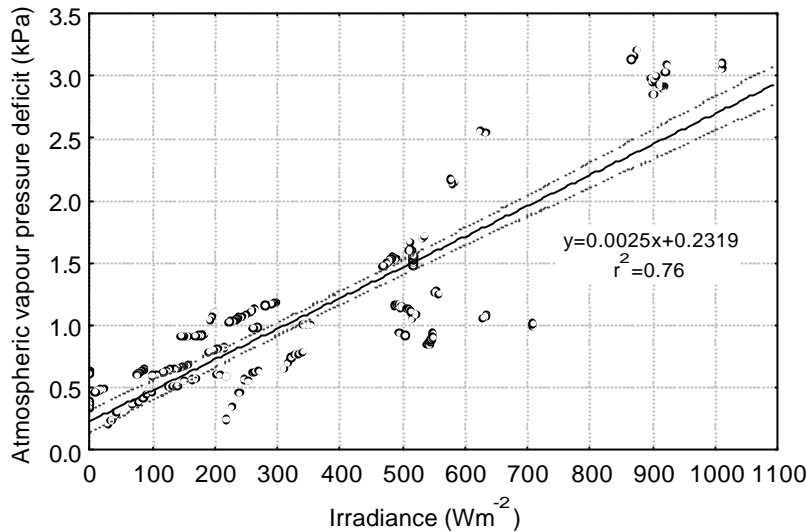


Figure 28: Atmospheric vapour pressure deficit, calculated according to Equation 2-3, is correlated to solar radiation. Solar radiation integrated over an hour was measured at the South African Weather Bureau Port Elizabeth station. Variability in the data may be a result of variable relative humidity near the sea ($n=187$, $r^2=0.76$, $p=0.0000$). The equation refers to the mean regression line (solid black). Dotted lines are the 95% confidence limits for the regression line.

Comparing atmospheric VPD to PAR measured by the quantum sensor on the PLC yielded a weakly positive relationship ($r^2=0.18$) as did the relationship of E to atmospheric PAR. As a result, VPD was compared to solar irradiance recorded at Port Elizabeth. These measurements represent solar irradiance integrated over an hour and measured on a flat surface. In this case there is a strong correlation, VPD increasing with increased irradiance (Figure 2-8, $r^2=0.76$). Solar radiation probably influences both ambient temperature and ambient relative humidity as, in the case of the latter, radiation drives the evaporation of water vapour from the sea. As a result VPD, which is calculated from saturation vapour pressure at particular temperatures, may be strongly correlated to solar radiation. However, the proximity to the sea, which is of variable temperature as discussed in Chapter 1, probably results in variable relative humidity which may account for the variability shown in Figure 2-8.

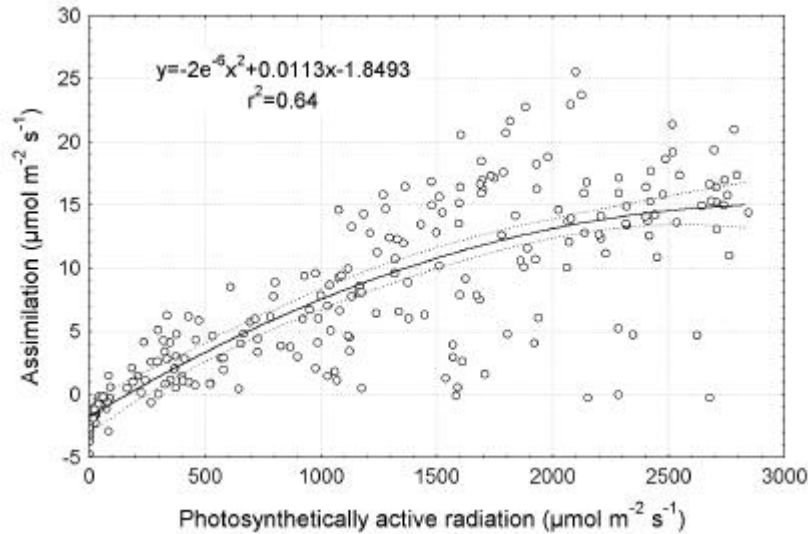


Figure 2-9: *S. plumieri* assimilation rates, measured concurrently to the collection of transpiration data and related to photosynthetically active radiation measured in the same orientation as the leaf by the PLC, collected at Old Woman's River and Southbroom ($n=226$, $r^2=0.64$, $p=0.0000$). The equation refers to the mean regression line (solid black). Dotted lines are the 95% confidence limits for the regression line.

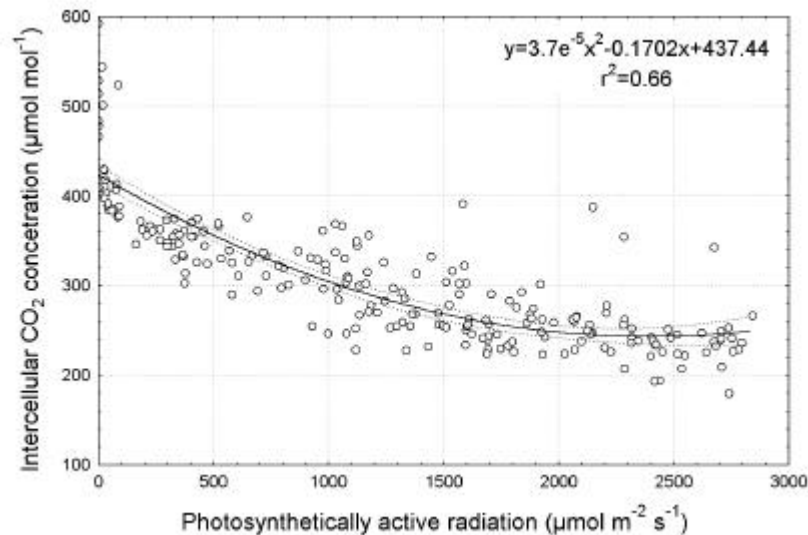


Figure 2-10: Intercellular CO_2 concentration of *S. plumieri* leaves calculated from gaseous exchange data in relation to photosynthetically active radiation measured in the same orientation as the leaf by the PLC. The data was collected at both Old Woman's River and Southbroom ($n=226$, $r^2=0.66$, $p=0.0000$). The equation refers to the mean regression line (solid black). Dotted lines are the 95% confidence limits for the regression line.

Assimilation is strongly correlated with PAR incident on the leaf as PAR provides the energy for CO_2 assimilation which, unlike transpiration, has a quick response time to changes in light intensity. Assimilation increases continuously over the range of PAR measured (Figure 2-9).

Data presented here are similar to those collected by Pammenter & Smith (unpublished manuscript) and suggest that assimilation is unsaturated, even at high light levels.

Intercellular CO₂ concentration (C_i) decreases with increased PAR (Figure 2-10) over most of the range of PAR levels measured. This trend corresponds with the positive correlation of assimilation to PAR. As CO₂ assimilation increases, C_i is depleted and declines. Minimum C_i concentrations are between 210 and 250 μmol mol⁻¹ which is within the operational range of intercellular CO₂ concentrations given by Fitter and Hay (1995) for C₃ plants.

Leaf conductance increases with increased solar irradiance (Figure 2-11). This is possibly in response to declining CO₂ concentrations within the leaf, which in turn is a result of increasing assimilation rates. Mansfield *et al.* (1981) discuss the response of stomata to light and CO₂. They note that stomata respond primarily to declining C_i concentrations, while light plays a secondary role in this response.

Increased solar radiation resulted in both increases in leaf conductance (Figure 2-11) and transpiration rates (Figure 2-12). High transpiration rates may therefore be seen as a side effect of maintaining high assimilation rates in a high light environment. This response is complicated as stomata possibly open with increased irradiance, providing the potential for high transpiration rates. However, coupled to this are high VPDs produced by high solar irradiance (Figure 2-8) which provide the gradient of water vapour concentration from the leaf to the atmosphere, allowing high rates of transpiration to occur.

These observations suggest that *S. plumieri* maximise assimilation at the expense of conserving water. The cost of water per gram of CO₂ fixed is generally high. On average, 747.0 g of water were used to fix one gram of CO₂ although the standard deviation is high (1524.9 g). The maximum recorded cost of water per gram of CO₂ fixed is 8049 grams. These values are calculated from instantaneous measurements and are thus variable due to the variable instantaneous light conditions that drive assimilation rates. These values are considerably higher than data collected for a range of C₃, C₄ (Fitter and Hay 1995) and desert plants (Caldwell 1977).

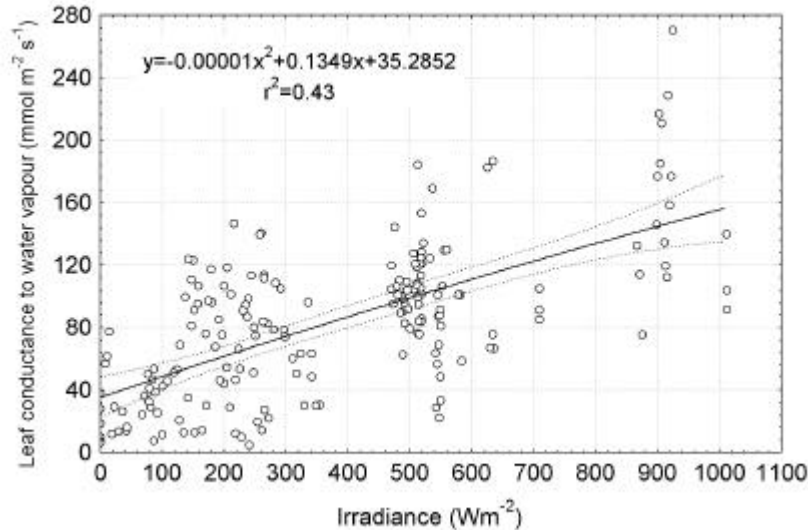


Figure 211: *S. plumieri* leaf conductance to water vapour in relation to solar radiation integrated over an hour as measured at the South African Weather Bureau Port Elizabeth station (n=187, $r^2=0.39$, $p=0.0000$). The equation refers to the mean regression line (solid black). Dotted lines are the 95% confidence limits for the regression line.

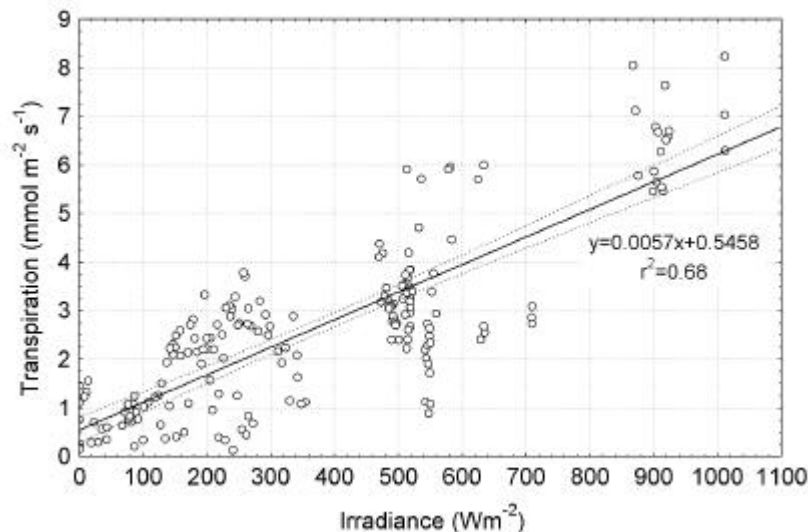


Figure 2-12: *S. plumieri* transpiration rates in relation to solar radiation integrated over an hour, as measured at the South African Weather Bureau Port Elizabeth station (n=187, $r^2=0.68$, $p=0.0000$). The equation refers to the mean regression line (solid black). Dotted lines are the 95% confidence limits for the regression line.

Elevated CO₂ experiment results

CO₂ is known to be one of the factors influencing stomatal aperture. Increasing CO₂ concentration causes stomata to close in many species (Willmer 1983). The aim of this

experiment was to expose individual leaves to elevated concentrations of CO₂ which was hoped would artificially close the stomata. It was hoped that this would reveal relationships between transpiration rates and leaf conductance. Specifically this experiment attempted to make the relationship between E and VPD more curvilinear as reduced leaf conductance to water vapour at a particular VPD should result in reduced transpiration rates if stomatal conductance to water vapour is limiting transpiration rates.

By piping air with elevated CO₂ concentrations to individual leaves the only environmental conditions altered are ambient CO₂ concentration and ambient relative humidity. Otherwise, leaves are exposed to the ambient light and temperature conditions.

Leaf conductance to water vapour was reduced under elevated CO₂ suggesting that the stomata of *S. plumieri* do indeed close under conditions of elevated CO₂ (Figure 2-13). The shapes of the regression line in both the ambient CO₂ readings and elevated CO₂ readings are similar. At comparable VPDs leaf conductance is reduced by 80 to 100 mmol m⁻² s⁻¹ (for example at 2.0 kPa) over the linear section of the regression lines.

Leaf conductances of leaves exposed to elevated CO₂ saturate slightly higher (180 mmol m⁻² s⁻¹) than leaves of plant at ambient CO₂ concentrations (150 mmol m⁻² s⁻¹), but this may be a function of the more variable data collected (Figure 2-13). Leaf conductances measured in both cases do not exceed about 200 mmol m⁻² s⁻¹, which may represent maximal rates for this species.

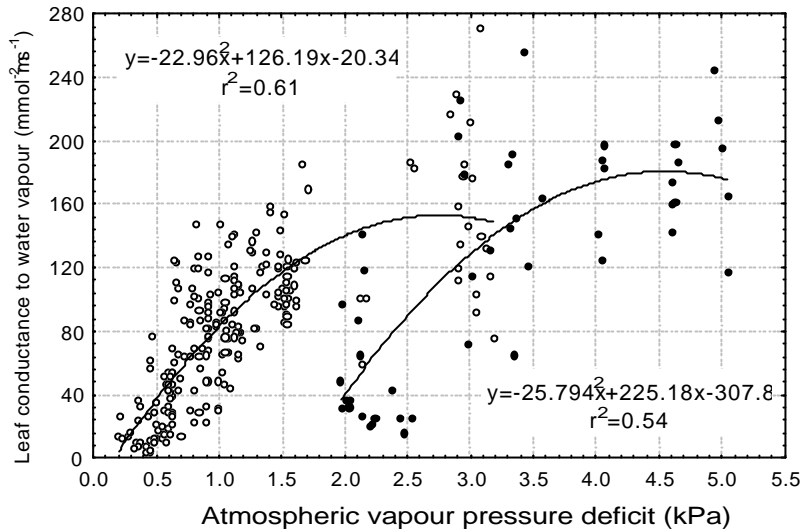


Figure 2-13: Leaf conductance to water vapour related to atmospheric VPD of *S. plumieri* leaves exposed to (○) ambient CO₂ (n=226, r²=0.61 p=0.0000) and (●) elevated CO₂ (r²=0.54, n=49, p=0.0000).

The reduced leaf conductances result in reduced transpiration rates (Figure 2-14). At comparable VPDs transpiration rates are reduced by about 2.5 mmol m⁻² s⁻¹. This effect is more pronounced at lower VPD and may be due to low light levels corresponding with low VPDs. Under such conditions, increasing C_i results in a relatively large stomatal closure when assimilation is low. When assimilation rates are higher the effect of stomatal closure is less marked.

Maximum transpiration rates at both ambient and elevated CO₂ concentrations are comparable at between 7 and 8 mmol m⁻² s⁻¹. However, in the case of the leaves at elevated CO₂ the maximal rates were only obtained at VPDs of 5.0 kPa. This may represent maximal transpiration rates obtainable by this species when stomata are at their maximum aperture. Unfortunately transpiration rates do not saturate at high VPDs so this remains unresolved. It may be enlightening to repeat this experiment with ambient CO₂ concentrations, with the aim of exposing the leaves to VPDs higher than those encountered in the field.

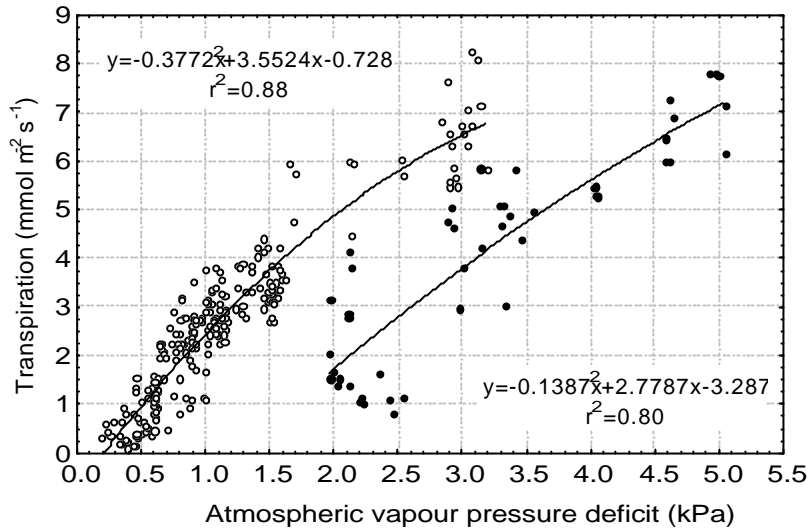


Figure 214: Transpiration rates related to atmospheric VPD of *S. plumieri* leaves at (○) ambient ($n=226$, $r^2=0.88$, $p=0.0000$) and elevated (●) CO_2 ($r^2=0.80$, $n=49$, $p=0.0000$).

Physiological explanations for the relationship of E to VPD in A. arenaria

A. arenaria leaf conductance increases over the range 0.2 kPa to 1.5 kPa (Figure 2-15). At a VPD of 1.5 kPa leaf conductance is about $110 \text{ mmol m}^{-2} \text{ s}^{-1}$ which is comparable to leaf conductances of *S. plumieri* at this VPD ($120 \text{ mmol m}^{-2} \text{ s}^{-1}$, Figure 2-7). However, above a VPD of 1.5 kPa leaf conductances saturate and then begin declining over the range of 2 kPa to 3 kPa.

The saturation of leaf conductance corresponds with the marked saturation of transpiration at VPDs above 2.0 kPa (Figure 2-6). This suggests that this species shows a more classical response to increased VPD, the stomata possibly closing as the gradient of water vapour from the leaf to the atmosphere increases to conserve water. This response to high VPDs is coupled with morphological traits which are traditionally equated with water conservation such as involute leaves.

As with *S. plumieri*, assimilation increases with increased PAR (Figure 2-16) and the data collected suggests that assimilation might not saturate over the range of PAR measured. Although, as with much of the data collected for this species, there is considerable variability in the points. However, maximum assimilation rates of about $20 \text{ } \mu\text{mol m}^{-2} \text{ s}^{-1}$ are similar to

midday assimilation rates measured by Pavlik (1983a) in the field and may therefore represent peak assimilation rates.

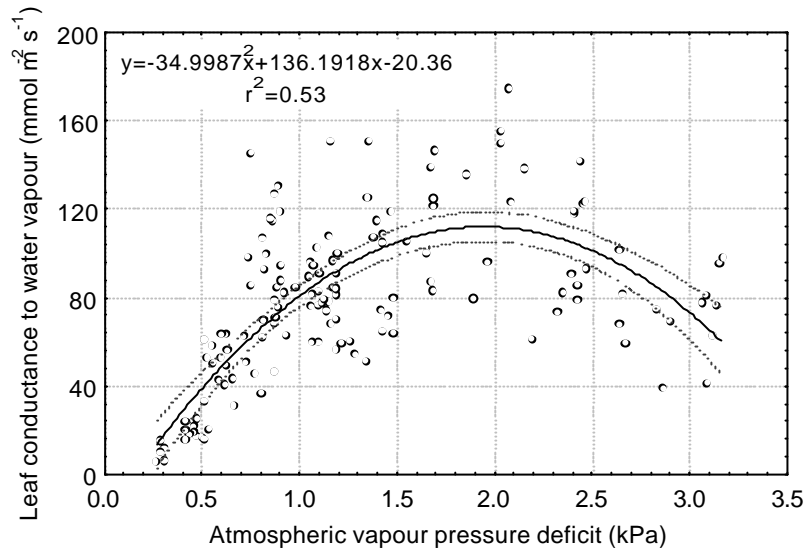


Figure 2-15: *A. arenaria* leaf conductance to water vapour related to VPD calculated from weather data collected at Old Woman's River on various dates in 1998 and 1999 ($n=145$, $r^2=0.53$, $p=0.0000$). The equation refers to the mean regression line (solid black). Dotted lines are the 95% confidence limits for the regression line.

In response to increasing assimilation rates, intercellular CO_2 concentration declines from about $400 \mu\text{mol m}^{-2} \text{s}^{-1}$ at low PAR levels to a constant level around $300 \mu\text{mol m}^{-2} \text{s}^{-1}$ at maximum assimilation rates at high PAR (Figure 2-17). These measurements, which are the lowest intercellular CO_2 concentrations measured, possibly correspond with lowered leaf conductances observed at high VPD. VPD is shown above to be correlated to incident solar radiation. However, in the case of *A. arenaria*, leaf conductances are poorly correlated to solar irradiance ($r^2=0.03$), with conductances across all light concentrations being between 50 and $150 \text{ mmol m}^{-2} \text{s}^{-1}$. Similarly, transpiration rates for *A. arenaria* show only a weak positive correlation to incident solar radiation ($r^2=0.12$).

These data suggest that assimilation increases with increased PAR and possibly becomes saturated at the maximum PAR levels measured. The corresponding decline of C_i to constant levels suggests that leaf conductances decrease at high VPDs or PAR.

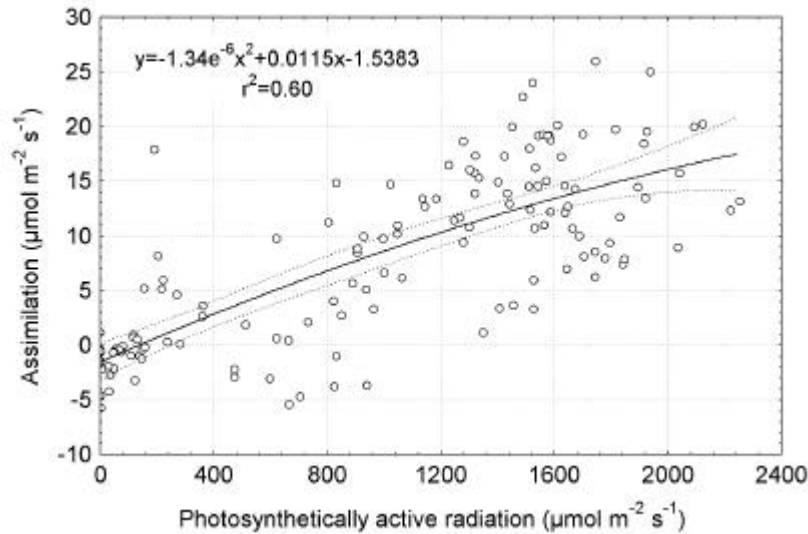


Figure 216: *A. arenaria* assimilation rates related to photosynthetically active radiation measured in the same orientation as the leaf by the PLC ($n=145$, $r^2=0.60$, $p=0.0000$). The equation refers to the mean regression line (solid black). Dotted lines are the 95% confidence limits for the regression line.

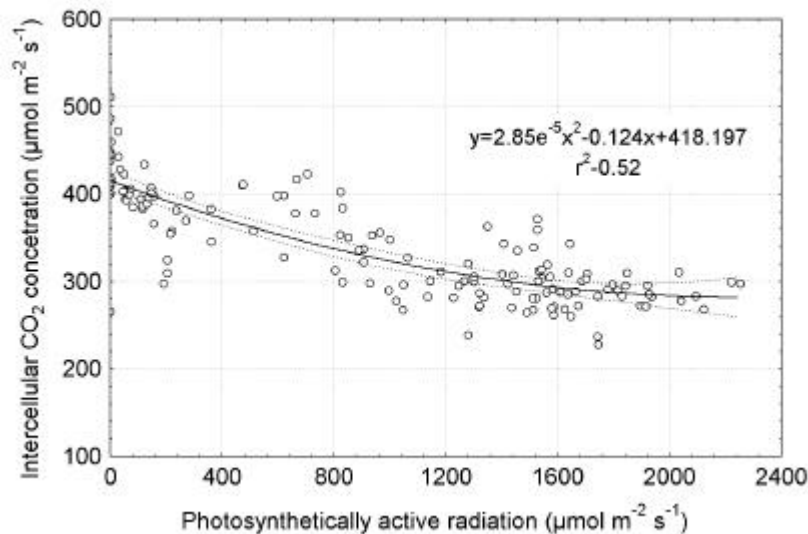


Figure 2-17: Intercellular CO_2 concentration of *A. arenaria* leaves calculated from gaseous exchange data in relation to photosynthetically active radiation measured in the same orientation as the leaf by the PLC ($n=145$, $r^2=0.52$, $p=0.0000$). The equation refers to the mean regression line (solid black). Dotted lines are the 95% confidence limits for the regression line.

This also suggests that in *A. arenaria* there is some degree of optimisation between carbon gain and water loss. On average, *A. arenaria* transpires 315.2 grams of water per gram of carbon fixed, although these values are from instantaneous measurements and therefore

variable as noted above. This is considerably lower than in the case of *S. plumieri*, and comparable to a number of C₃ crop plants but higher than desert plants (Caldwell *et al.* 1977, Fitter & Hay 1995).

In addition to varying leaf conductances, which may be a function of optimising carbon gain while reducing water loss through transpiration, boundary layers are likely to develop along the grooved adaxial surface of the leaf. This may be important in reducing transpiration rates while allowing relatively high assimilation rates.

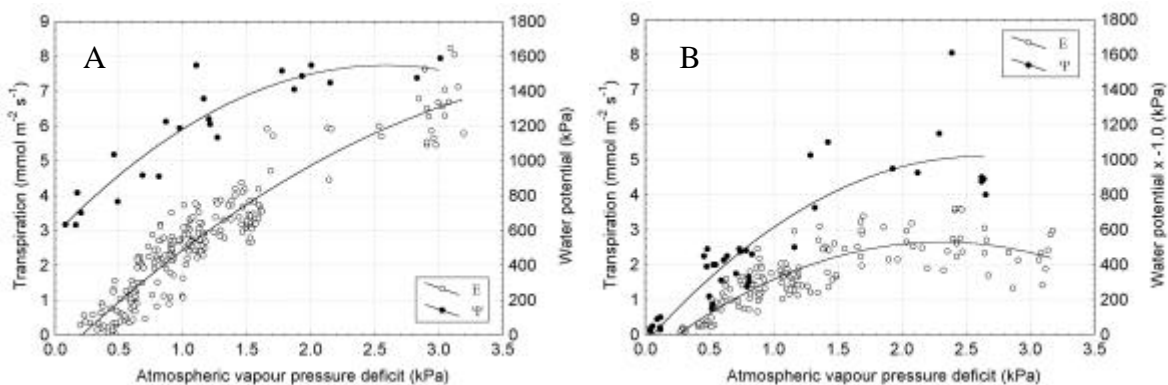


Figure 2-18: Leaf water potential (●) and transpiration rates (○) for *S. plumieri* (A) and *A. arenaria* (B) in relation to VPD. Each point for *S. plumieri* water potential represents the mean of five measurements. Water potentials for *A. arenaria* represent individual measurements.

In both species, water potentials do not become excessively negative at midday when maximum VPDs and hence transpiration rates are experienced (Figure 2-18). Maximum leaf water potentials of *A. arenaria* reach between -1000 and -1200 kPa at midday. In *S. plumieri*, leaf water potentials reach -1600 kPa at midday.

However, at low VPDs and transpiration rates the two species show different responses. Leaf water potentials of *A. arenaria* decline to around 0 kPa at dawn VPDs. *S. plumieri* leaf water potentials only reach about -600 kPa at dawn.

Discussion

Transpiration data was collected at the leaf level from various position on the sand dunes, during different times of the day and in a variety of seasons. These measurements were confirmed by weight loss experiments and yielded strong relationships of transpiration to atmospheric vapour pressure deficit. Vapour pressure deficit is calculated from measurements of ambient temperature and humidity, hence, where these two environmental variables are known, transpiration can be calculated.

A possible reason for the linear relationship of transpiration to vapour pressure deficit may be a function of the stomata opening with increased irradiance. As irradiance increases, so does the rate of photosynthesis and the internal CO₂ concentration declines. To correct the decreased internal CO₂ concentrations the stomata open to maintain high rates of photosynthesis. Concurrent to the opening of the stomata in response to increased irradiance, is increased vapour pressure deficit which is linearly related to irradiance. As a result transpiration rates increase. The linear response of transpiration to vapour pressure deficit may therefore be a response to increased irradiance.

Extensive use was made of the LCA2 IRGA for the collection of gaseous exchange data. While this is a relatively quick and convenient way of collecting such data in the field, this instrument may overestimate transpiration rates considerably as a result of using dry air in the determination of transpiration. This is probably a result of the dry air used by the LCA2 system as well as the stirring of the air within the PLC by the fan. Both factors contribute to elevating transpiration rates. By using dry air, the vapour pressure deficit between the leaf and the atmosphere is increased considerably, increasing the gradient of water vapour from the leaf to the atmosphere. This is likely to effect transpiration rates over the time period in which transpiration measurements are made (one to two minutes). Over the same period, stomata are unlikely to respond significantly enough to reduce transpiration.

The PLC is designed to reduce boundary layers, being a low-volume cuvette with a fan for stirring the air within the leaf chamber (ADC 1985). The reduced boundary layer, coupled

with the dry air, are also likely to contribute to increased transpiration rates. The effect of reduced boundary layer in increasing transpiration is probably more evident in the case of *A. arenaria*. *S. plumieri* has a more open canopy than *A. arenaria* and as a result the canopy is probably well ventilated with less marked boundary layers. Individual leaves of *S. plumieri* are therefore exposed to a low boundary layer environment to which they acclimatise. The low boundary layer conditions within the PLC are therefore probably not foreign. The dense clumps of *A. arenaria* probably develop high canopy boundary layers which contributes to high boundary layers of individual leaves which are rolled. As a result the low boundary layer conditions within the PLC can be regarded as alien and hence the overestimate of leaf transpiration rates by the IRGA. Transpiration measurements made gravimetrically are less likely to affect the local leaf boundary layer and so these measurements can be regarded as more representative than those made by the IRGA.

While care was taken to insert the leaves of *A. arenaria* into the PLC without affecting the degree to which they are rolled, some degree of unrolling was inevitable once the leaves were clamped in the PLC and 'squashed' flat. This 'unrolling' no doubt contributes to reducing the boundary layer of the leaf in the PLC and the associated increase in transpiration rates which were measured.

The transpiration measurements were therefore re-calibrated by comparing them to transpiration rates measured gravimetrically. Weight loss measurements are considered more accurate because the leaves are not exposed to a high VPD environment during the measurement as occurs when using the LCA2. In addition, the leaf experiences more natural boundary layer conditions, unlike in the PLC which is a low volume cuvette that minimises the leaf boundary layer.

Data for *S. plumieri* and *A. arenaria* show that if ambient temperatures and relative humidities are known, then the transpirational water losses from the leaves of these two species can be predicted due to the predictable response of transpiration to atmospheric VPD. This goes some way to answering question one as listed in Chapter 1 and suggests that it is possible to predict transpiration rates at the leaf level from readily available environmental

variables. The relationship of E to VPD presented here forms the basis of subsequent work described in Chapter 3 and Chapter 4.

The data collected here for both species is from a wide range of conditions. Transpiration rates, as shown in Figures 2-5 and 2-6, were collected over a number of seasons, from leaves at various positions along the length of shoots, and throughout the day from before dawn until after dusk. Transpiration rates were also recorded from leaves which were growing at various positions on the sand dunes, including the seaward side, landward side and crest of the sand dunes. Finally, in the case of *S. plumieri*, transpiration rates were recorded at two remote sites, the Old Woman's River study site and at Southbroom (Figure 2-1). This all suggests that the relationships of E to VPD at the leaf level hold under a wide variety of conditions. Chapter 3 investigates methods for scaling these leaf level predictions to the entire canopy, which is a more functional scale at which to investigate the interaction between water use and water availability.

Comparing transpiration rates to atmospheric VPD is valid as atmospheric VPD describes the gradient of water vapour concentration from the leaf airspaces to the bulk atmosphere (Kramer 1983). It would be more desirable to predict transpiration rates from the leaf-to-atmosphere VPD as this is a more accurate estimation of this gradient. However, this would remove the predictive power of the relationship as, in addition to inputs of ambient temperature and relative humidity, inputs of leaf temperature are required. As yet there is no accurate method for estimating leaf temperatures of either *S. plumieri* or *A. arenaria* remotely, nor is there historical data of this nature, and the use of leaf-to-atmosphere VPD for modelling purposes was therefore rejected.

Due to the fact that this model is based on the understanding that the gradient of water vapour from the leaf airspaces to the bulk atmosphere drives transpiration, this approach may be considered a phenomenological model as defined by Reynolds *et al.* (1993).

This approach is similar to 'meteorological' models such as the Penman-Monteith equation described in the introduction (Jarvis & McNaughton 1986). It is assumed that the input of energy is important to drive transpiration which is described in terms of potential evaporation.

This may be more valid in the case of *S. plumieri*, as stomatal limitations of E are negligible and the leaves of this plant are thought to be closely coupled to the atmosphere. In *A. arenaria* stomatal regulation of E may be more important but this response is predictable and therefore does not complicate predictions of E from measurements of VPD. Ventilation of the canopy and leaves may be important in producing the observed response of E to VPD at the leaf level.

In the case of *S. plumieri*, E is nearly linearly related to VPD, which suggests that there is little stomatal limitation of transpiration rates. This is evident over the lower range of VPD measured, which corresponds with the most common conditions encountered in the field. This near-linear response is also probably a result of the open, well-ventilated nature of the *S. plumieri* canopy. The boundary layers of shoot as well as leaves are removed, therefore increasing transpiration rates. This idea is discussed further in Chapter 3.

The response of *A. arenaria* is clearly non-linear, with transpiration rates saturating and indeed declining at high VPDs. This is probably a direct function of the higher boundary layer resistance, due to involute leaves. Leaf conductances are also reduced at higher VPDs, which may be in response to decreased plant water status. While the water potential data presented here suggest that the plants do not develop particularly negative water potentials, Pavlik (1985) measured water potentials of -2.0 MPa which were associated with partial stomatal closure at midday.

The simple empirical relationship presented here suggests that for both species transpiration is strongly related to light, atmospheric vapour pressure deficit and possibly other covarying environmental conditions. This is more evident in the nearly-linear response of E to VPD in *S. plumieri*, but also apparent in the predictable response of *A. arenaria*. While the data are insufficient to clearly elucidate which environmental factors are driving the transpiration rates in the predictable manner described above, the following may partly explain the observed response of transpiration to atmospheric vapour pressure deficit:

In *S. plumieri* this relationship may be a function of its response to light, maximising assimilation rates. Data collected here agree with that presented by Pammenter & Smith

(unpublished manuscript). Assimilation is apparently light limited, remaining unsaturated at midday irradiances (maximum sunlight).

Pammenter & Smith explain this as a function of the isobilateral leaves of this species. Photosynthetic tissue (“two to three layers of palisade cells and some chlorophyllous mesophyll”) underlies adaxial and abaxial surfaces of the leaves. They suggest that even though assimilation at the illuminated surface of the leaf may become saturated, increased PAR might then be transmitted through the leaf to the other “photosynthetically competent” surface, resulting in non-saturating light responses in this species.

Indeed, this photosynthetic competence of both abaxial and adaxial surfaces may explain some of the variability shown in the data (e.g. Figure 2-9). The PLC was positioned on individual leaves corresponding with the adaxial surface. This is the surface which normally receives most solar radiation. However, in some cases leaves were selected where the abaxial surface was receiving the majority of the incident radiation. In these cases the PLC possibly shades the leaf from the sun and measured assimilation rates might be lowered.

Speculation regarding this species response to light is supported by additional physiological evidence collected here. As assimilation increases with increased irradiation, intercellular CO₂ concentrations are depleted and stomata respond by opening to maintain relatively constant C_i concentrations so as to avoid limiting assimilation through the lack of suitable substrate. Increased transpiration rates brought about by high leaf conductances are a consequence of maintaining constant C_i concentrations to maximise assimilation rates.

Water use data suggest that in terms of grams of carbon fixed per gram of water transpired, this species is ‘wasteful’. A comparison of instantaneous water use efficiencies of *S. plumieri* to other species suggests that on a gram of CO₂ fixed to gram water transpired basis, this species has poor water use efficiencies. Fitter & Hay (1995) list water use efficiencies of different plants: C₃ about 500; C₄ about 250 to 300; while desert plants have water costs as low as 99.8 grams per gram of CO₂ fixed (Caldwell 1977).

Possible reasons for maximising assimilation rates may include the fact that carbon acquisition is important for rapid growth which might be important in rapidly accreting sands so as to outgrow the deposition of beach sand around the plant.

The straight-line relationship between E and VPD may hold only in circumstances where water supply (as rain or groundwater) is unlimited and the stomatal response is mainly to meet photosynthetic demand for CO₂ rather than optimising CO₂ gain, or minimising water loss. This appears to be the case over the entire range of VPDs measured in this study at all study sites investigated. However, Pammenter (1983) found that transpiration became constant above a VPD of about 1.5 kPa (12g m⁻³) under laboratory conditions with pot-grown plants. It is possible that water was limiting in these studies.

Fitter & Hay (1995) list water potentials of plants from different habitats. Desert plants are mainly in the range of -6 to -10 MPa, but water potentials may get as low as -16 MPa. Plants from areas that experience periods of drought may have water potentials in the range of -3.2 to -7 MPa, while woody plants and herbs from mesic sites have water potentials from about -1.5 to -4 MPa. Measured water potentials for both *S. plumieri* and *A. arenaria* are in the lower range of water potentials measured for plants from mesic sites, this suggests that water is freely available to these plants. Similarly, the most negative water potentials recorded in the review by Barbour *et al.* (1985) was about -2.2 MPa. This is despite suggestions by many workers (e.g. Hesp 1991, Oosting 1954) that coastal plants experience drought.

The stomatal response to VPD observed in this study for *S. plumieri* is contrary to what has been previously reported in many species under controlled conditions, but at a variety of leaf temperatures and irradiances (Bunce 1996, Schulze & Hall 1982). This increasing stomatal conductance with increasing VPD maximises water loss and replacement and, under non-water limiting conditions, may be advantageous for several reasons. Firstly, it would increase the uptake of essential nutrients which are found in low concentrations in beach sand (Harte & Pammenter 1983) and aquifer water (Campbell *et al.* 1992).

Secondly, high transpiration may be required to lower leaf temperatures (Gates 1968). Pammenter (1985) showed that optimal leaf temperature for maximal carbon assimilation is

around 25°C for *S. plumieri*, which is typical for C₃ plants (Fitter & Hay 1995). One can speculate that under conditions of sufficient water the plant maintains maximal transpiration rates such that leaf temperatures are maintained closer to optimal temperatures for photosynthesis (Drake *et al.* 1970, Raschke 1970). More likely, high transpiration rates may be necessary to reduce leaf temperatures and so avoid damage by high temperatures (Raschke 1975). Midday ambient temperatures certainly exceed 25°C in summer and many other months (data not shown). Assimilation rates are highest under maximum conditions of irradiance. It may not be coincidental that this corresponds with maximum leaf conductances and VPDs, which in turn lead to high transpiration rates which create the maximum potential for evaporative cooling.

A preliminary experiment was conducted to prevent transpiration with the aim of investigating the relation between transpiration and leaf temperature. Leaves were covered in either clear lacquer or petroleum jelly. Transpiration rates were low, while leaf temperatures of these leaves were higher than those of the controls (data not shown). However, once again the various leaf angles resulted in the leaves receiving varying amounts of radiation. As a result, leaf temperatures measured were variable and obscured the effects of reduced transpiration rates. By carefully selecting leaves of corresponding orientation it may be possible to resolve this question more fully.

In *A. arenaria* the response of E to VPD is perhaps more conventional, increasing as VPD does until shoot water potential becomes excessively negative. As water potential decreases the stomata begin to close, reducing water loss. Support for this is given by the higher water use efficiencies measured for this plant which is comparable to C₃ plants as listed by Fitter & Hay (1995). This suggests that in the case of *A. arenaria*, water is less readily available over the course of the day. It is likely that this species is less deeply rooted and may not have access to as much water as *S. plumieri*. Salisbury (1952) and Huikies (1979) report that *A. arenaria* does not root deeper than about two meters.

Chapter 3

Scaling from leaf to canopy and investigations into the interaction between plant water use and sand water availability

Introduction

This chapter forms a link between the physiological work and the GIS study and addresses questions two and three listed in the introduction:

2. Can transpiration rates be scaled up to whole dunes or larger areas?
3. Can budgets of water use and water availability be constructed?

It primarily describes how physiological measurements (specifically transpiration rates) were scaled from individual leaves, the level at which measurements were made and described in Chapter 2, to the canopy level which is the basic unit used in the modelling of regional transpiration rates using a GIS in Chapter 4. It also investigates the possible role soil water plays in supporting these plants.

Finally, this chapter acts as a ‘service chapter’ describing how leaf areas and leaf area index, were calculated. These are used in Chapter 4 in the calculation of regional water deficits for both species.

Scaling up

In the introduction to Chapter 2, transpiration and modelling transpiration were discussed in general terms introducing the two main schools of thought regards modelling transpiration: the ‘meteorologists’ idea that transpiration is controlled primarily by the supply of energy to drive the evaporation of water, as opposed to the ‘physiologists’ view that transpiration is strongly regulated by stomata (Jarvis & McNaughton 1986).

Jarvis & McNaughton (1986) have extensively reviewed this conflict between ‘physiologists’ and ‘meteorologists’ and conclude that “it is not a conflict of scientific evidence but of interpretation. It is a consequence of the different scales at which the evidence has been obtained and the results interpreted. The results from either group are not applicable to the plant system studied by the other, unless proper allowance is made of the change of scale.” These authors suggest that, as a generalisation, stomata may be important in controlling transpiration rates at small scales such as at the leaf level. At broader scales such as at the scale of the entire canopy, transpiration might be more strongly influenced by climatic factors and the supply of energy to drive evaporation.

Predicting the rate of transpiration from a canopy is complex, primarily because of the complex structural and environmental characteristics of canopies. This includes indigenous vegetation but also relatively simple systems such as monospecific crop stands. Models for estimating the transpiration rates of complex canopies (e.g. Claus *et al.* 1995, Harley & Baldocchi 1995 & Schelde *et al.* 1997) require numerous inputs such as data on the orientation and energy budget of individual leaves, clumping of leaves within a canopy, specific leaf-area index, ventilation within the canopy and importantly, data on stomatal conductance. The fact that most canopies are extremely heterogeneous further complicates modelling canopy transpiration rates. Even monospecific crop canopies may vary structurally and morphologically as a result of different genotypes within the stand and the numerous weeds that are invariably present (Jarvis & McNaughton 1986).

The inclusion of terms for stomatal conductance makes modelling transpiration considerably more complicated. This is primarily due to the fact that as yet there is no consensus as to what controls stomatal conductance and to which factors stomata respond (Jones 1998). For example, there has been recent debate as to whether stomata respond to humidity or the vapour pressure deficit of the air (Bunce 1996), or whether they respond to the rate of transpiration – the rate of water vapour movement through the stomatal pore (Monteith 1995).

Monteith (1965) reworked Penman’s original work which formalised the importance of atmospheric humidity in studies of evapotranspiration. Monteith, for example, includes terms for stomatal conductance and the resultant ‘Penman-Monteith equation’ remains the basis for

most applications and research in evapotranspiration, despite the numerous derivatives and modifications (Norman 1993). Stanhill (1970, cited in Norman 1993) makes the light-hearted suggestion that subsequent papers are more useful reducing evaporation from the soil surface as a mulch, than by virtue of their content.

The first step in the derivation of the Penman-Monteith equation is to reduce the original three-dimensional canopy to a single one-dimensional ‘Big-Leaf’, hence these models are often termed ‘Big-Leaf models’ as the canopy is summarised as a single large leaf surface. The basic model assumes that the original canopy is homogeneous, level, continuous and extensive. This one-dimensional canopy absorbs all the radiation and loses water vapour and heat (Alves *et al.* 1998).

In a number of photosynthesis and transpiration models the canopy is divided into multiple layers with many different leaf angle classes. While such multiple-layer models produce ‘good’ results, they are complex to develop and involve numerous calculations which make them less suitable (Jarvis & McNaughton 1986, de Pury & Farquhar 1997), particularly when forming a part of a larger mechanistic model (Reynolds *et al.* 1993). Useful results have been obtained by summarising these different layers into only two, a sun layer and a shade layer, which significantly simplifies calculations (Harley & Baldocchi 1995, de Pury & Farquhar 1997).

Reynolds *et al.* (1993) suggest that significant error may be introduced if information used at a “lower level in the hierarchy” is used directly to make predictions at a higher level because of the increasingly complex systems involved. Direct extrapolation may break down as scale increases or when extrapolations are made for novel conditions not recorded in the original observations. However, direct extrapolation from observed trends may be valid where there is a relatively small change in scale as suggested by Levin (1993).

Water relations of fore-dune vegetation

De Jong (1979) found that on the Californian coast soil water content was generally around 4%, but this decreased in the surface layers. This value is similar to data from the United Kingdom (Salisbury 1952), the Florida coast on the south-east coast of the United States² (Oosting 1954) as well as the south-east coast of South Africa (present study). These constant soil water values appear to be unrelated to rainfall, although rainfall events may cause transient increases in soil water content (Salisbury 1952). Reasons for this consistency at remote sites may relate to similar physical properties of beach sands (Campbell *et al.* 1992) or to particular mechanisms which act to recharge the sand water content (De Jong 1979).

Besides relatively constant water contents in different sand columns, plants growing on sand dunes in different parts of the world have relatively high water potentials and in many cases do not wilt even during periods of low rainfall (De Jong 1979, Barbour *et al.* 1985).

Salisbury (1952), for example, conducted weight loss experiments to calculate the transpiration rates of individual plants of different species growing in containers placed in the sand dunes. He then estimated the volume of sand the roots occupied, presumably by excavating each experimental plant. The volume of water lost by transpiration, based on these transpiration measurements, was subtracted from the amount of water held in the volume of sand the roots occupied, assuming that this sand contained about 4% water by volume. This work suggests that in the absence of rainfall plants growing on sand dunes in the United Kingdom might be expected to exhaust the water contained in the sand volume occupied by their roots within about five days. However, over the period that this work was done, stretches of up to six weeks without rain did not induce wilting of the dune plants. Salisbury therefore invokes the idea of internal dew formation to meet the plants' water demand. He suggests that "moisture-laden air... [is] drawn into the pore spaces of the soil" where it condenses at night when the sand temperature drops below the dew-point temperature. Mechanisms for drawing the air into the sand from the atmosphere above are not clear.

² *S. plumieri* is found along this coast.

Additional work has been conducted to investigate the source of water in beach sands. In 1865 Kerner (cited in Olsson-Seffer 1909a) investigated the idea that water might be drawn up through the sand column by capillarity. However, capillary rise in beach sand is limited to about 30 cm because of the coarse-grained nature of this substrate. Olsson-Seffer (1909b) suggests that internal dew formation may be important but, unlike Salisbury (1952), proposed that the source of moist air is the wetter soil at greater depths within the sand column.

To test this problem De Jong (1979) excavated two holes, one of which was lined with plastic. Soil pycnometers were buried below and above the plastic barrier as well as in the control hole and then the holes were refilled. In the experimental hole, the water potential was -36 bar above the plastic barrier, as low as -3 bar below the barrier and -10 bar in the control. This experiment suggests that water moves up from the ground water in response to the soil water potential gradient. Where there was a barrier, the soil water potential is raised above that of the control (below the barrier) and becomes significantly more negative above the barrier where the movement of water is impeded. De Jong (1979) also found that soil water potential was higher at depth than nearer the surface (<-15 bar at 100 cm, -30 to -85 bar at 10 cm). He suggests that this gradient of soil water potential may account for the consistent distribution of water in the sand column, with water moving from a high to low water potential.

Because of the small amount of water that can be stored in the sand column and used by the plants, Barbour *et al.* (1985) suggest that the temporal distribution of the rainfall is very important. For example, regular even rainfall that contributes to recharging the sand and aquifer water may result in a more 'mesic' soil water balance than limited periods of very high rainfall. Regular rainfall also contributes to decreasing physiological water stress by periodically leaching wind-blown salts out of the sand.

Study Sites

The study sites for work described in this chapter are essentially the same as those for Chapter 2. The majority of the work described here was conducted at the Old Woman's River study site in the Eastern Cape. Leaf areas and leaf area indices were determined for *S. plumieri* plants growing at Old Woman's River. For *A. arenaria* leaf areas were determined for plants growing at Old Woman's River and Kleinemonde (between Port Alfred and the Old Woman's

River site at 27°02'44"E 33°32'32"S, see Figure 2-1 for map). Leaf area indices for *A. arenaria* were determined for three separate stands of plants growing at various points on Port Alfred's west beach.

The majority of the holes for determining the sand water profiles were dug at Old Woman's River. Additional holes were dug at Port Alfred and the Kenton-on-Sea side of the Bushman's River mouth. See Figure 2-1 for the location of Kenton-on-Sea south of Port Alfred.

Materials and Methods

In this study a relatively simple approach was taken to scaling from the leaf level to the canopy level. The leaf area for the canopy was summed and transpiration predicted for the entire leaf area as if the canopy were one large leaf. Methods are presented for calculating the leaf areas of both individual leaves and the canopy, so that predictions of the canopy transpiration rates can be made.

Being able to predict the water loss from a canopy of either species then allows estimates to be made of the interaction between water use and water availability in the form of rain, sand water or aquifer water.

Leaf area calculations

Individual leaves were removed from the shoot and the leaf's length and breadth recorded. These measurements were correlated with leaf area (figures 3-1 and 3-2). Leaf areas were calculated as a percentage of the area of an A4 sheet of paper based on the weight of the A4 sheet and the weight of a cut-out paper replica of the specific leaf (see equation 3-1).

The area of the A4 paper was determined (length×breadth) as well as its mass in grams to four decimal places. Individual leaf shapes as traced from the original leaves were then cut out and weighed on the same balance, also to four decimal places. From this the leaf areas of the individual leaves were calculated as follows:

$$\text{Leaf Area} = \left(\frac{\text{Mass Paper Leaf Replica}}{\text{Mass A4 Sheet}} \right) \times \text{Area A4 Sheet}$$

(Equation 3-1)

Because *A. arenaria* has long, narrow involute leaves which are difficult to trace, leaves of this species were copied on a photocopier. Leaf area data were kept separate for each individual shoot so the entire leaf area of individual shoots could be determined by summing the leaf areas of all the leaves on that shoot.

A total of 110 *S. plumieri* leaves were measured and the individual leaf areas determined. The leaves were collected from a number of different positions on the dune (including the seaward side, crest and landward side) as well as from two different beaches (Old Womans' River and Port Alfred). Only 15 leaves were measured in the case of *A. arenaria* as the relationship of leaf area to length multiplied by breadth was clear. Leaves were also collected from different positions on the beach and at different beaches (Old Womans' River and Kleinemonde).

Shoot area determinations

Leaf areas of entire shoots were determined by summing the leaf areas of all the leaves on a shoot. In some instances the leaf areas were measured directly as described above. Additional shoot areas were calculated using the allometrical relationship between leaf length and breadth, and leaf area (Figures 3-1 and 3-2). Lengths and breadths of both *S. plumieri* and *A. arenaria* leaves on a shoot were measured and the areas were calculated according to these relationships. Shoot leaf areas were calculated for 72 *S. plumieri* shoots and 35 *A. arenaria* shoots. These shoots were collected from a number of sites as described above in the previous section.

Leaf Area Index

Leaf area index (LAI) is the leaf area per unit ground area and can be expressed as:

$$LAI = \frac{s}{G}$$

(Equation 3-2)

where s is the total leaf surface area of shoots on one square metre of sand dune and G is the ground area which, in this case, is one square metre. Because the same units are used for both s and G , LAI is dimensionless (Beadle *et al.* 1993).

LAI was calculated for both species by counting the number of shoots (or culms) per square metre quadrat and multiplying this number by the mean shoot leaf area calculated above (see Table 3-1) to get the leaf area per square metre of vegetated sand dune. In most cases, the canopies of either *S. plumieri* or *A. arenaria* dunes are monospecific, with very few other species contributing any cover. These canopies can therefore be considered to be homogenous, allowing LAI to be calculated in this fashion.

Scaling from leaf to shoot

It was assumed that an individual shoot within the canopy is the basic unit making up the canopy. Because of the regular monospecific structure of canopies dominated by either *S. plumieri* or *A. arenaria* it was assumed that canopies of either species respond as a collective of individual shoots. Therefore, to investigate the validity of scaling transpiration measurements from individual leaves to whole shoots and hence the entire canopy, transpiration rates of whole shoots calculated by weight loss were compared to shoot transpiration rates predicted using the regressions between transpiration and vapour pressure deficit presented in Chapter 2. Shoots were excised, weighed using a two-place balance and returned to their original position in the canopy where they were exposed to the greater canopy-wide environment³. The shoot was reweighed after about five minutes and the transpiration rate for the whole shoot calculated from the change in weight, time in seconds between weighings and the leaf area according Equation 2-5. However, leaf area (a) was that of the entire shoot calculated as described above for each species based on the allometrical relationship of leaf area to leaf length and breadth. Transpiration for the shoot was predicted from the average temperature and humidity measured over the time between weighings. VPD was calculated from these two measurements and, in turn, transpiration was determined using

³ That is the greater micro-environment found within the greater canopy area, not just the micro-environment around the individual shoots or leaves

the relevant equations of the regression lines for each species which are given in either Figures 2-5 or 2-6.

Because of the problem of accurately weighing the long, thin culms of *A. arenaria*, this experiment was repeated using shoots which had been harvested and recut under water in the field. The shoots were returned to the base camp/laboratory where weight measurements could be made in a sheltered environment on a four-place balance. Between weighings the culms were returned to a 'simulated' clump of culms in a bucket, which was maintained outdoors where they experienced similar solar radiation and wind conditions to the original stand of plants.

Sand water

Holes between 1 and 3.5 metres deep were dug at various beaches including Port Alfred West Beach, the Kenton-on-Sea side of Bushman's River Mouth, but mainly at the Old Woman's River study site. Soil samples were collected at 250 millimetres intervals from the surface down to free ground water. These were sealed in two plastic sandwich bags and returned to the laboratory.

To determine the water content of the soil, first the crucible was weighed to two decimal places. Then approximately 20 to 30 grams of the sand sample was weighed into the crucible and placed in an oven at 50 to 60°C to dry. The percentage soil water content was calculated from the percentage weight change as follows:

$$\% \text{ Soil Water} = 100 - \left(\left[\frac{(\text{crucible} + \text{dry soil weight}) - \text{crucible weight}}{(\text{crucible} + \text{wet soil weight}) - \text{crucible weight}} \right] \times 100 \right)$$

(Equation 3-3)

Changing sand water concentration

The changing sand water concentration was investigated for vegetated sand dunes occurring near Port Alfred. Port Alfred was selected as there is a South African Weather Bureau first order weather station in this town. First order weather stations record hourly temperature, relative humidity and rainfall data. At the Port Alfred weather station this hourly data is

available for the last nine years. Two years were selected from this data-set to show the extremes of rainfall over this period. In 1995, 571.8 mm of rain fell, while in 1998, 733.6 mm were recorded.

Mean temperature and relative humidity were calculated from the hourly data for each day. These two values were used to calculate daily VPD according to Equation 2-3. Using the regressions of E to VPD (Figures 2-5 and 2-6 for *S. plumieri* and *A. arenaria* respectively), transpiration rates were calculated for each day. This value of transpiration was multiplied by the leaf area index for the particular species (Table 3-1), so as to express the result on a 'per square metre of vegetated sand dune' basis. Using these regression lines (Figures 2-5 and 2-6), negative transpiration rates were predicted on cool, humid days with very low VPDs. As a result the regression lines were altered and the y intercept set to zero (Figures 3-6 and 3-7).

The following assumptions were made when calculating the compound sand water volumes. The surface area of vegetated sand dune was one square metre, from which the transpiring leaf area of the plants extracted water. Over this area of one square metre, the amount of water entering the system as rain was calculated from the measured values. The plants occupying one square metre of sand dune were assumed to be part of a larger continuous homogenous canopy and so the water available to the plants is primarily from the column of sand below the square metre surface area⁴. The depth of the sand column below the surface was taken as three metres which is about the maximum depth at which the aquifer was recorded (Figure 3-5). Therefore the sand volume from which one square metre of canopy can extract water, if not making use of the aquifer water, is three cubic metres of sand.

Pammenter (1983) recorded a sand bulk density of 1.3 kg l^{-1} for beach sand. Using this value, a sand volume of three cubic metres (3000 litres) and a sand water content of 4% by weight as determined from Figure 3-5, was calculated to contain 156.5 litres of water in this column of sand⁵. Dune sand water potentials only drop appreciably at sand water concentration below

⁴ Surrounding sections of the canopy will have comparable demands of water from the sand column and therefore water from these neighbouring areas is used by other parts of the canopy.

⁵ One kilogram of water equals 1.00294 litres.

1.5%, therefore most of the water in dune sand is available to be used by plants (Pammenter 1983).

Water lost from one square meter of vegetated sand dune by transpiration was subtracted from this starting volume, while rainfall input to the system was added on a daily basis to revealing interactions between transpiration rates and sand water availability as affected by variations in rainfall both in time and intensity.

Results

Leaf and shoot areas

In both *S. plumieri* (Figure 3-1) and *A. arenaria* (Figure 3-2) there is a strong, linear allometrical relationship of leaf area to length and breadth of individual leaves. These relationships are useful as they make collecting leaf area data easier, allowing for many more measurements to be made than would be feasible by measuring the actual areas of individual leaves.

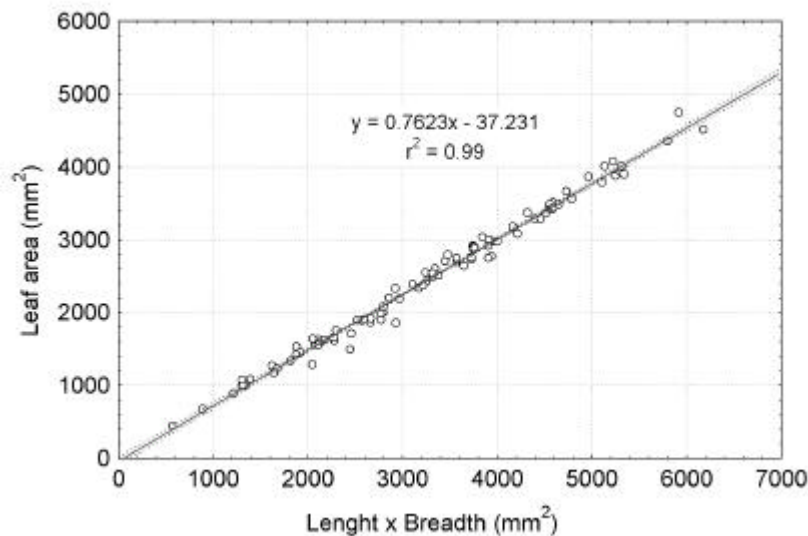


Figure 3-1: Allometric relationship of leaf area to length and breadth in *S. plumieri*. (n=110, $r^2=0.99$, $p=0.0000$). The equation refers to the mean regression line (solid black). Dotted lines are the 95% confidence limits for the regression line.

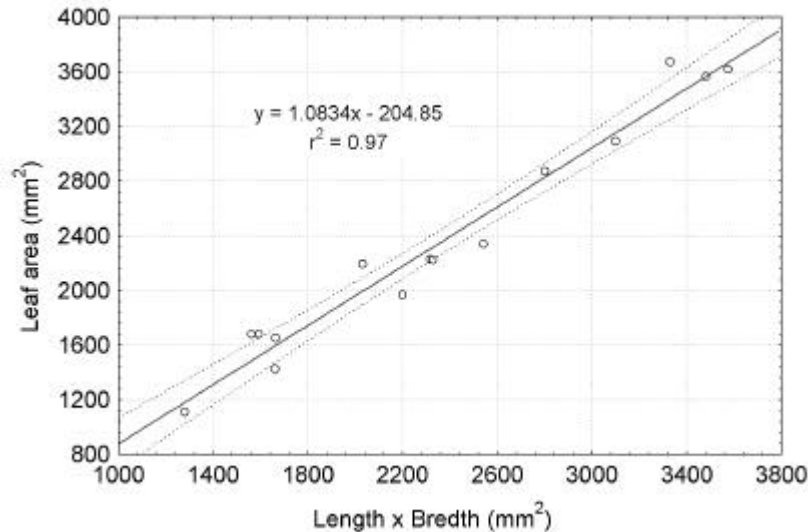


Figure 3-2: Allometric relationship of leaf area to length and breadth in *A. arenaria*. ($n=15$, $r^2=0.97$, $p=0.0000$). The equation refers to the mean regression line (solid black). Dotted lines are the 95% confidence limits for the regression line.

Using these allometrical relationships, the leaf areas of different leaves on a shoot were determined from measurement of length and breadth. These individual leaf areas of the different leaves on a shoot were summed to determine the leaf area of a shoot.

Table 3-1: Characteristics of *S. plumieri* and *A. arenaria* canopies.

	<i>S. plumieri</i>	<i>A. arenaria</i>
n of shoot leaf area determination	72	35
\bar{x} shoot leaf area mm^2	44670.69	8571.60 mm^2
n of shoots per m^2	10	25
\bar{x} shoots per m^2	21.43	210.45
LAI	0.95	1.80

Table 3-1 gives the average shoot leaf areas for the two species as well as the number of shoots used to determine this average shoot area. Individual shoots of *S. plumieri* have much higher leaf areas than *A. arenaria* (Figures 1-1 and 1-2). Also obvious in these two figures is the fact that the canopy of *S. plumieri* is more open than *A. arenaria*. This is quantified by LAI which is calculated according to Equation 3-2 by multiplying the mean number of shoots per square metre by the mean shoot leaf area and describes the structure of the canopy integrating the number of shoots as well as the leaf area of individual shoots. Because of high

shoot densities, *A. arenaria* has a higher LAI than *S. plumieri* despite having much lower individual shoot leaf areas (Table 3-1). *S. plumieri* has an open, sparse canopy (Figure 1-1) with a corresponding low LAI of 0.95.

Scaling from leaf to canopy

In the case of *S. plumieri* transpiration rates of individual shoots predicted from measurements of temperature and relative humidity using the regression equation established in Chapter 2 (Figure 2-5) compare closely to transpiration rates measured gravimetrically (Figure 3-3). This suggests that it is acceptable to scale transpiration rates from individual leaves to a whole stand simply by multiplying transpiration rates by the leaf area of the stand in question.

In the case of *A. arenaria*, shoot transpiration rates predicted from temperature and relative humidity according to the regression equation determined in Chapter 2 (Figure 2-6) are somewhat higher than transpiration measured gravimetrically.

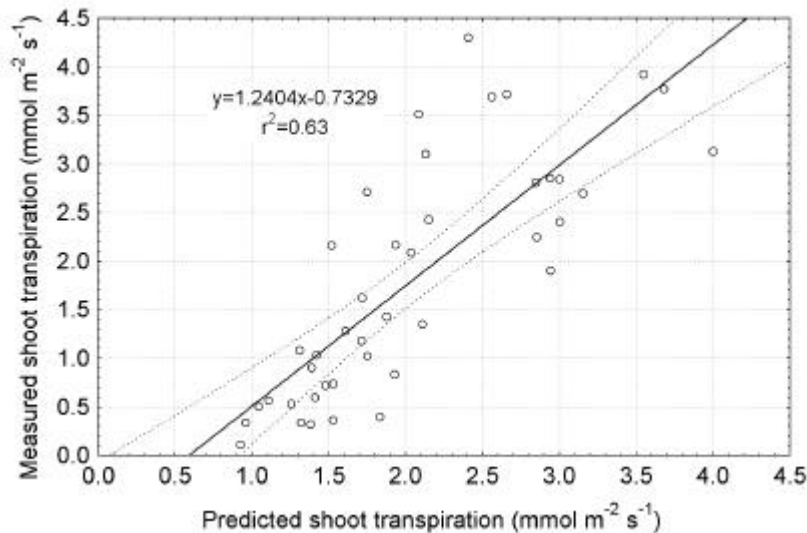


Figure 33: Transpiration rates of individual *S. plumieri* shoots calculated by weight loss, compared to transpiration rates calculated from measurements of ambient temperature, using the equation of the regression line in Figure 2-5 ($n=42$, $r^2=0.63$, $p=0.0000$). The equation refers to the mean regression line (solid black). Dotted lines are the 95% confidence limits.

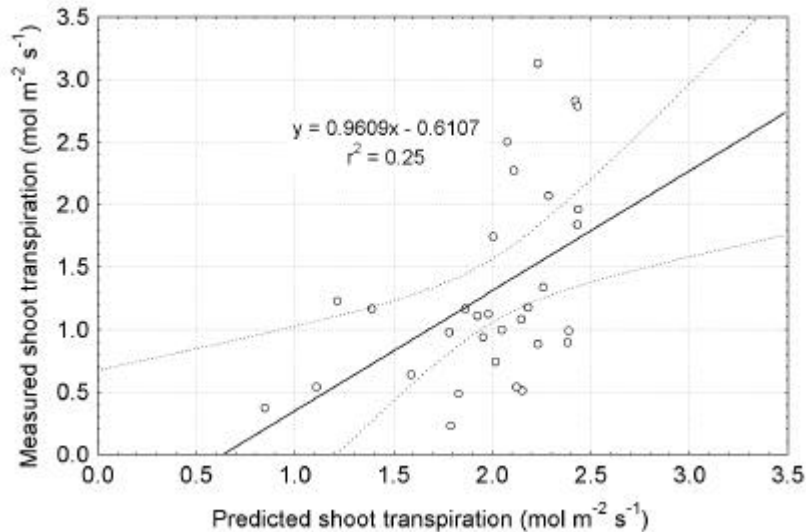


Figure 34: Transpiration rates of individual *A. arenaria* culms calculated by weight loss, compared to transpiration rates calculated from measurements of ambient temperature, using the equation of the regression line in Figure 2-6 ($n=31$, $r^2=0.25$, $p=0.0043$). The equation refers to the mean regression line (solid black). Dotted lines are the 95% confidence limits for the regression line.

The relationship between predicted and measured transpiration at the shoot level is poor ($r^2=0.25$) and there is considerable variation in the data (Figure 3-4). Both these factors suggest that boundary layer effects within clumps of *A. arenaria* are important – the canopy of *A. arenaria* possibly being poorly ventilated as a result of this species clumping growth form.

Sand water profiles

In the surface layer of sand reaching a depth of no more than 10 cm, soil water is effectively 0%. From 10 cm down to the dune aquifer, the water content of the sand is almost constant at around 4%, nearly all of this water being available to the plants (Campbell *et al.* 1992). At depths greater than one metre the water content jumps to around 20% and this represents the depth of the dune aquifer. The depth of the dune aquifer is variable and may be influenced by recent rainfall events and high tides, both of which might decrease the depth from the sand surface. This very constant water content of the soil is probably a function of the specific sand particle size (Campbell 1992).

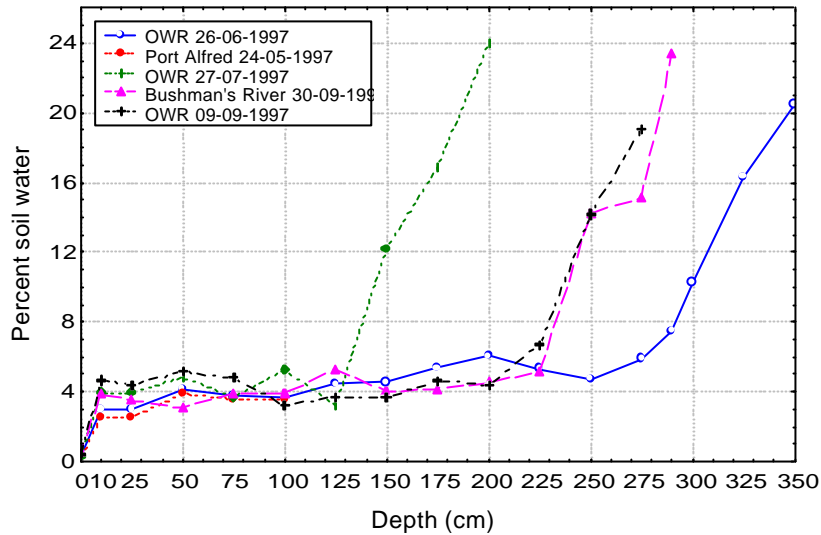


Figure 35: Percent sand water content at increasing depths in the sand column, from the surface down to the free aquifer water. Data collected at Old Woman's River (OWR), Port Alfred and Bushman's River mouth on the dates indicated.

Compound sand water content

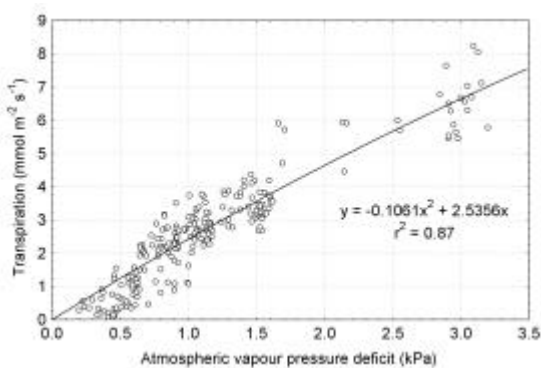


Figure 3-6: The regression equation of E to VPD for leaves of *S. plumieri*, modified to have a zero y intercept so as to avoid predicting negative transpiration values at low VPDs.

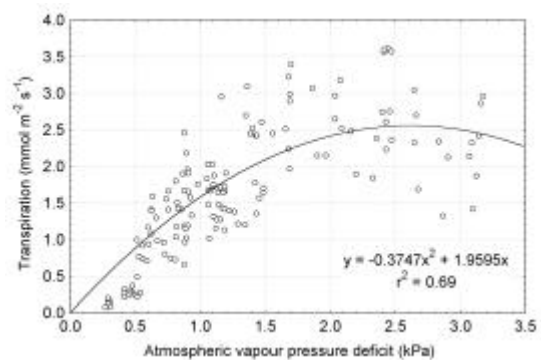


Figure 3-7: The regression equation of E to VPD for leaves of *A. arenaria* was modified to have a zero y intercept so as to avoid predicting negative transpiration values at low VPDs.

As already noted, transpiration rates predicted using the regression equation of E to VPD established in Chapter 2 for both species (Figures 2-5 and 2-6) were negative on cool humid days when VPD measurements are very low. To address this, the regression equations were recalculated with the y intercept set to zero (Figures 3-6 and 3-7).

Theoretically, this is more desirable as it is unlikely that the leaves of these species absorb water at low VPDs as predicted by the original regression equations. These modified regression equations were also used in subsequent estimations of transpiration rates for determining the compound sand water concentration in Chapter 4 where regional water deficits were predicted.

In both 1995 and 1998 the sand column below stands of *A. arenaria* was shown to potentially have a lower water content than *S. plumieri* (Figures 3-8A and 3-8B), although the uncertainty in predicting canopy water loss from *A. arenaria* dunes is acknowledged. This is due primarily to the higher leaf area index (Table 3-1) and the higher canopy leaf area of this species which result in higher canopy wide transpiration rates than in *S. plumieri*.

In the dry year of 1995, low rainfall from about May results in increasingly low sand water volumes in the second half of the year as the plants continue to extract water which is not replaced by rainfall (Figure 3-8A). The lower transpiration rates of *S. plumieri* mean that water extraction by this species is relatively low, and during this period rainfall is sufficient to balance the plant's demand.

A. arenaria on the other hand has significantly higher transpiration rates and so extract more water than is entering the system as rain. This result in the sand water content dropping below the starting volume in the second half of the year.

In 1998 higher rainfall results in more water entering the sand column, although low rainfall during January and February result in the sand water content dropping below the starting volume in both *S. plumieri* and *A. arenaria* dunes (Figure 3-8B). On the 1st March of that year 128 mm of rain fell, substantially elevating the sand water volume. In the case of *A. arenaria* high transpiration rates results in sand water volumes temporarily dropping below the starting volume in mid July when rainfall is low. During the rest of the year sand water content of the *A. arenaria* sand column is slightly higher than the starting value. The low

transpiration rates of *S. plumieri* results in increasingly sand water volumes as rainfall continues adding water to the sand column throughout the year.

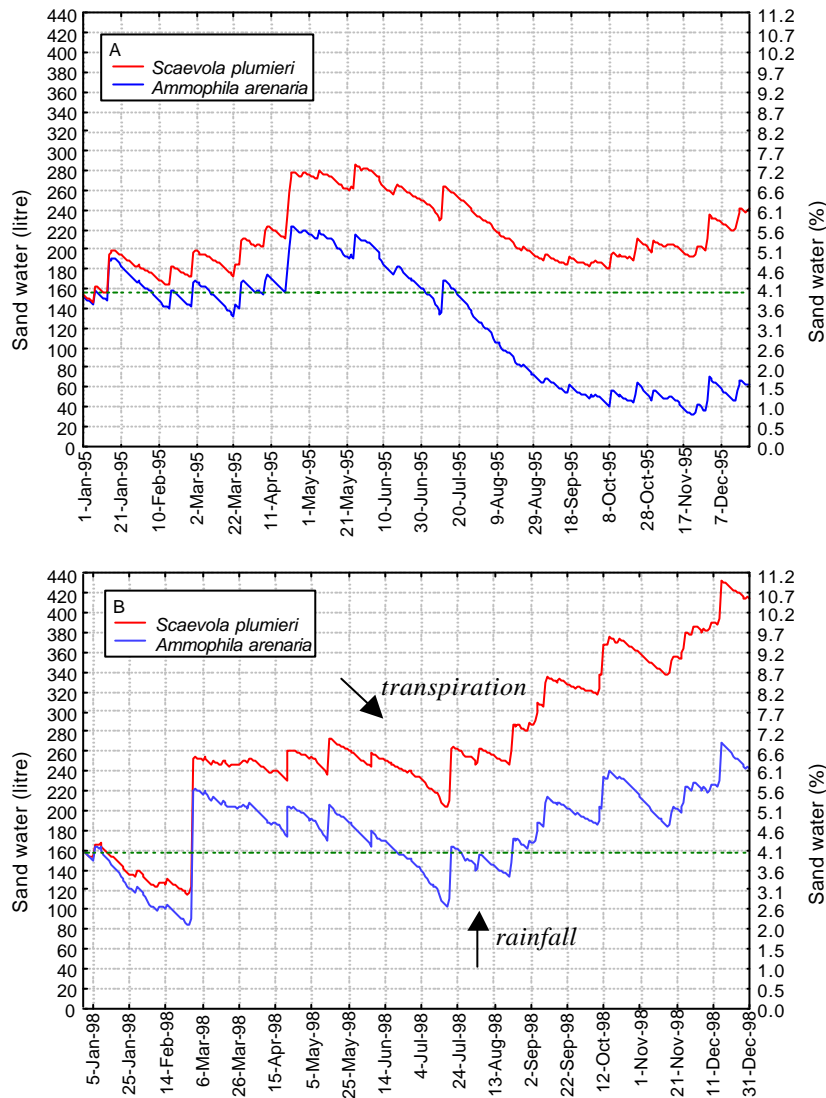


Figure 3-8: Compound sand water for one square metre of vegetated sand dune, with a sand column three metres deep, assuming that the dune aquifer is at this depth. The values presented are estimates calculated from climatic data for each day of the year. Inputs of hourly temperature and relative humidity were used to calculate mean daily values from which daily transpiration rates were calculated. From a starting value of 156 litres of water in this sand column (4% sand water from Figure 3-5 and a sand density of 1.3 kg l^{-1} after Pammenter 1983), water transpired by the canopy was subtracted, while rain falling on the one square metre of vegetated sand dune was added. The green line gives the volume of sand water assuming 4% sand water. A) Compound sand water in 1995 when 571.8 mm of rain fell and B) in 1998 with 733.6 mm of rain falling on the square metre of sand dune.

Comparing the volumes of water within the sand column to the corresponding percentage sand water on a weight basis (right y axis in Figures 3-8A and 3-8B), shows that the percentage sand water reaches about 10% in 1998 using calculations for *S. plumieri*. In the case of *A. arenaria* sand water fluctuates between three and six percent in 1998 while in 1995 it gets potentially as low as one percent.

Discussion

Scaling from leaf to canopy

A leaf area index of 0.95 for *S. plumieri* growing at Old Woman's River, as determined in this study, is comparable to that estimated by Pammenter and Smith (unpublished report) of about 1.0 for plants growing at Mtunzini. These low LAI values of *S. plumieri* are most comparable to desert plants as listed by Schulze (1982), with only a few temperate grasslands having lower values. The LAI value for *A. arenaria* determined in this study is also low and is similar to the lower values of tropical grasslands. The number of culms per square metre are comparable to values recorded by Willis (1965) in the United Kingdom.

One complication of modelling the transpiration rates of canopies is the fact that canopies are heterogeneous either in terms of species or genotypes present (Jarvis & McNaughton 1986). In both *S. plumieri* and *A. arenaria*, the canopy is particularly simple and, in most cases, can be considered monospecific as only one species may contribute significant cover in areas where either *S. plumieri* or *A. arenaria* occurs. The canopy of *S. plumieri* is made up of regularly spaced shoots all of which probably have the same or a very similar genotype as it is estimated that most dunes are made up of only one or two plants (Harman pers. com.). The fact that all *A. arenaria* plants in South Africa might be descended from one set of plants introduced from Europe (Hertling 1997) suggests that genetic variability might also be limited in this species, at least in South Africa. The INVASS programme is investigating the genetic variability of *A. arenaria* in

South Africa. The physical nature of the canopy of *A. arenaria* is more complex than that of *S. plumieri* due to the different densities of culms in various clumps (pers. obs.).

The approach used in this study is, in a sense, a simplified ‘Big-Leaf’ model, with the canopy of interest being reduced to a single large leaf area. This was done by first validating that the transpiration rate of a shoot within the canopy is simply the sum of the transpiration rates of the individual leaves on the shoot. The leaf area of all the shoots can then be summed to determine the leaf area of the canopy which is essentially reduced to a single large leaf. That is, predictions of transpiration made at the level of a single leaf are extrapolated to the leaf area of the entire canopy.

Jarvis & McNaughton (1986) suggest in broad terms that stomata might be important in controlling transpiration at the leaf level, while at the canopy level, the supply of energy to drive transpiration is more important. The fact that in *S. plumieri* stomatal conductance is relatively unimportant in determining the rate of transpiration and the transpiration rate is strongly related to atmospheric conditions (Chapter 2), suggests that individual leaves can be seen as discrete sub-units of the larger canopy. If this is so, scaling from these individual leaves to the larger canopy can be viewed as a simple extrapolation exercise from the leaf area of a single leaf to the leaf area of the canopy. Direct extrapolation from observed trends may be valid because there is a relatively small change in scale as suggested by Levin (1993), and both scales may be subject to similar environmental conditions and respond in the same manner.

Shoot transpiration rates as predicted from climatic data correlated closely to shoot transpiration rates measured by weight loss and allowed for the prediction of canopy transpiration rates. This correlation is possibly also due to the open, well-ventilated nature of the *S. plumieri* canopy and the frequent windy conditions on the beach, resulting in both leaf and canopy transpiration rates being closely coupled to the environment (Jarvis & McNaughton 1986).

The situation is somewhat different in the case of *A. arenaria*. It is likely that in this species boundary layer effects cannot be ignored. This is probably true at the level of individual leaf as well as at the canopy level. At the leaf level, involute leaves and the fact that the stomata are sunken into hair-lined grooves (pers. obs.) probably result in relatively large boundary layer conditions in the vicinity of the stomata. Related to this are the large boundary layer conditions which can be expected to develop within the dense clumps of culms (see Figure 1-2). The magnitudes of the boundary layers at these two different scales are probably quite different, making direct extrapolative scaling much less accurate in this species.

The predicted transpiration rates of *A. arenaria* shoots are higher than transpiration rates of the shoots measured by weight loss. This may be a result of the so-called Iwanoff effect (Iwanoff 1928, cited in Willmer 1983), but is more likely a result of the large boundary layer associated with shoots within a large clump of shoots (see Figure 1-2 for an example of the density of *A. arenaria* stands). Briefly the Iwanoff effect relates to the slight opening of the stomata following the excision of a leaf. This is followed by the steady, longer-term closure as water becomes limiting (Willmer 1983).

It is uncertain how this phenomenon applies to whole shoots, following excision (in the case of *S. plumieri*) and after being recut under water to remove air bubbles within the xylem vessels (*A. arenaria*). In the case of *S. plumieri*, the experiment is conducted quite quickly and relatively little effect is likely. The fact that *A. arenaria* shoots were maintained in a bucket of water for up to two hours following excision may contribute to the lower transpiration rates measured. It should be noted that this was unavoidable as accurate weight measurements could not be made in the windy conditions experienced on the dunes where these plants grow.

It is therefore possible to use the leaf level regression equations described in Chapter 2, to predict the transpiration rates of canopies of either *S. plumieri* or *A.*

arenaria. These models are simplified by the fact that the complicating effects of variables such as leaf angle, leaf area index and specific aspects of canopy structure are, to a greater or lesser extent, built into the model. This is a result of the collection of transpiration data from leaves of all ages and positions on a wide number of shoots with different positions on the sand dunes. Data was also collected at different times from before dawn until dusk, during different seasons and, in the case of *S. plumieri*, at two different sites, making the relevant regression equations widely applicable to these two species. In addition, the variable effects of stomatal regulation of transpiration are absent. Thus the considerable uncertainties associated with modelling stomatal regulation (Hall 1982) are removed.

Compound sand water

There are two assumptions made when calculating water loss using the above formulations. Firstly, it was assumed that the majority of the leaf area associated with a well-vegetated sand dune does not acquire water from roots that extend laterally beyond the area of the canopy. Secondly, direct evaporation from the sand surface was assumed to make an insignificant contribution to total water loss from a dune because the upper dry layer of sand on the dune forms a barrier to the evaporation of the water from below. This idea has been discussed by Hesp (1991).

It must be stated that these are calculations of potential water use based on the assumption that the plants maintain high levels of transpiration in the relatively dry year of 1995. It is likely that *A. arenaria*, for example, would adopt water conserving measures as the sand water volume decreases during the course of the year.

It is possible that this relatively high water content results in the excess water above the field capacity of the sand, draining into the dune aquifer and the water in the sand column is only reset to the volume in the sand at field capacity, making

these calculations less accurate. For example, if field capacity is at 5% and rainwater entering the system can only reset the sand water volume to this level, then sand water volumes might drop below the starting value even in the case of *S. plumieri* (Figures 3-8A and 3-8B).

Huiskes (1979) notes that the field capacity of mobile dune sands is about 7%, while Salisbury (1952) observes that wilting occurs when the sand water content reaches 0.5%. Such information may allow more accurate calculation to be made by setting the maximum water content that the sand column can achieve.

In most cases for *S. plumieri*, water loss, as calculated by the above formulations, is perhaps less than the input of water to the system by rainfall. It is likely that in most cases the amount of water contained within the sand is sufficient to meet the water demands of the canopy. Sand water content measured on five occasions, at various *S. plumieri* vegetated sites showed that water content from 10 cm below the surface down to the level of the permanent ground water remained relatively constant (mean percentage water content = 4.1 ± 0.8 %). This suggests that mechanisms may operate to maintain water concentrations in the sand column constant, ensuring a constant supply of water for dune species. These mechanisms may include the diffusion of water from areas of high water potential at depth to areas of lower water potential near the surface (De Jong 1979), or internal dew formation (Olsson-Seffer 1909b, Salisbury 1952). It is unlikely that capillary action is sufficient to move water up through three metres of the sand column (Olsson-Seffer 1909a). Alternatively, the even temporal distribution of rain on this and other coasts, where similar sand water content have been recorded, may result in relatively constant sand water volume in the sand column. It is also interesting to note that the dune aquifer depth on this coast is in the range of depths measured by De Jong (1979) on the Californian coast.

It is also interesting to note that the dune aquifer depth on this coast is in the range of depths measured by De Jong (1979) on the Californian coast, and suggests that common physical processes may be operating at these two sites. As noted in the

introduction of this chapter, the sand water concentration on South African dunes is also similar to that of other sand dunes in the USA and UK.

While water within the sand might be sufficient to support the plants growing in these ecosystems, the plants may tap the water in the dune aquifer. De Jong (1979) has noted that a number of dune species along the Californian coast have deep tap root systems. It is likely that *S. plumieri* is a deep rooted species which can potentially make use of the relatively deep aquifer water. Isotopic studies may be required to confirm the possibility that these plants use groundwater during drier periods.

If these plants do rely on the groundwater, then the human utilisation of coastal aquifer water described by Campbell *et al.* (1992) has the potential to adversely impact *S. plumieri* and any other species making use of this resource. Further research is required in this regard.

A. arenaria has a adventitious root system extending to a depth of between one (Salisbury 1952) and two (Huiskes 1979) metres and is perhaps more dependant on water contained in the sand column. Huiskes (1979), for example, notes that this species is found on dunes in the United Kingdom where the dune aquifer may be as deep as 26 metres which is probably deeper than the extent of this species root system.

Chapter 4

GIS investigation of factors which may limit the distribution of *Scaevola plumieri* and *Ammophila arenaria*

Introduction

This chapter draws on information from the two previous chapters to investigate factors which may limit the distribution of both *S. plumieri* and *A. arenaria*. As such it aims to answer question four, “Can budgets of water use and water availability be used to explain the observed distribution of these two species at a regional level?”

Distribution of vegetation and species

Von Humboldt & Bonpland (1805, cited in Woodward & Williams 1987) were the first to map the distribution of the world’s major vegetation types. This early work attempted to explain the observed distribution of vegetation in terms of global climatic patterns. The idea that climate is the dominant factor controlling vegetation development and distribution is therefore at least as old as the early descriptive vegetation maps (Woodward & Williams 1987). Indeed rough correlations between vegetation types and climate were appreciated by people in classical times and probably long before that (Box 1981, Woodward 1987).

Box (1981) investigated the correlation between climate and vegetation at a global scale using a low-resolution model with inputs of various measurements of temperature extremes and precipitation. From these, estimates of annual potential evapotranspiration were made. Annual precipitation was divided by potential evaporation to provide an annual moisture index. This researcher notes that, for many regions of the globe, temperature and precipitation are the most readily available climatic data. This may be due to the importance of these variables to human activities.

Box (1981) concludes that the basic features of world vegetation are determined primarily by the general levels and mean seasonal patterns of temperature and the “climatic water balance”. That is, there are very strong correlations between the distribution of different vegetation

types, based primarily on growth forms as opposed to species composition, and the equation of evapotranspiration subtracted from precipitation. This is despite the complexity of ecological systems, species interactions and plant-environment relations.

While Box (1981) has provided broad correlations between vegetation and climate at a global level, he does not establish a physiological basis for these observations. Woodward & Williams (1987) investigated the physiological mechanisms whereby climate may control distribution, focusing on the two most obvious features of climate, temperature and precipitation. Woodward (1987) expands these ideas and includes solar radiation, general water relations, low and high temperatures and frost in an ecophysiological modelling approach to global vegetation.

Woodward & Williams (1987) used an equation of rainfall minus transpiration and run off – the Hydrological balance – to predict the distribution of vegetation. They provide a ‘physiological link’ between leaf mass and hydrological balance. Specifically, they suggest that increased water availability results in increased leaf growth and leaf mass. Measurements of leaf mass can be used to predict vegetation types. For example, high leaf mass corresponds with forests in moist areas, while desert vegetation has very low leaf masses. In between these two extreme there is a range of decreasing leaf mass with decreasing water availability.

Temperature is also thought to affect the distribution of vegetation types in a fundamental way. Woodward (1987) and Woodward & Williams (1987) investigated the role of temperature in some detail. They suggest that annual minimum temperature may limit plant distribution and perhaps vegetation types by exceeding lethal threshold limits for survival. The impact of low temperature in controlling both species and vegetation types is obvious and much work has been conducted on the physiological response of plants to low temperature stress (see Berry & Raison 1982, Steponkus 1982, Larcher & Bauer 1982 for reviews).

However, it is not clear why species which tolerate low temperatures do not colonise warmer areas. One suggestion is that the cost of increased frost resistance is the loss of competitive ability in warmer locales (Woodward & Williams 1987). Tolerance to higher temperatures in tropical and desert vegetation may be important in allowing these plants to colonise warmer

areas. For example, CAM and C₄ species may require higher heat tolerance as they have reduced transpiration rates and hence higher leaf temperatures (Kappen 1982). Woodward and Williams (1987) therefore proposed that minimum temperatures limit the spread of vegetation towards the poles, while competition controls the equatorial spread of vegetation. However, temperature may play a more direct role in limiting vegetation physiologically, particularly in very warm areas (Kappen 1982).

Climate is therefore thought to fundamentally determine the distribution of plants and indeed most terrestrial organisms (Richardson & McMahon 1992), and climatic variables may define the broad geographic range of a species. Physiological responses to climatic variables are therefore often the primary factors producing distribution limits (Panetta & Mitchell 1991). Within this range other factors such as geology, soils, competition and environmental disturbance will determine the presence or absence of a species in an area, as well as its abundance (Lindenmayer *et al.* 1991).

Considering that climate may limit the range of an organism, studies of climatic variables can provide insight as to why a particular species (or taxon) is found in a particular area (Lindenmayer *et al.* 1991). The study of the distribution of taxa at various levels as well as assemblages of taxa forming, for example, different vegetation types has accelerated recently. This is due to the rapid increase in computing power and decrease in the cost of personal computers, as well as the development of powerful programs which can handle large volumes of spatial data (Elston & Buckland 1993). Coupled with this is the production of many long-term climatic databases for different regions, which are now available for general use.

Modelling the distribution of organisms

Models for predicting the distribution of organisms may be grouped into two main categories. The first method, termed here as the correlative approach, uses pattern analysis to investigate the correlation between environmental variables and the sampled distribution of the organism being investigated (Beerling *et al.* 1995). This correlative approach to distribution modelling is also known as homocline analysis, which seeks to define the physical limits of the distribution of an organism (Lindenmayer *et al.* 1991, Panetta & Mitchell 1991).

At its most simple, this approach involves defining a climatic envelope for a species based on the climate at sites where the organism has been recorded. Using this climatic envelope, other areas falling within this envelope are identified as being potentially within the range of the species in question.

Due to the ready availability of accurate species distribution data of some taxa, as well as the compilation of extensive databases of climatic variables for various regions or countries, there has been a considerable amount of work in terms of correlative modelling of organisms' distributions. In Australia, and now elsewhere, a widely applied correlative model is BIOCLIM (Nix 1986, Busby 1991). This model uses a set of climatic variables for each confirmed distribution point, as well as absence data, to derive a profile of suitable habitats for the organism based primarily on temperature and precipitation (Busby 1991). Carpenter *et al.* (1993) discuss a number of limitations of BIOCLIM and propose an alternative model, DOMAIN, which can operate using presence-only distribution records.

Robertson *et al.* (in prep) propose a system for predicting distributions of organisms using fuzzy classifications of presence data in relation to a number of available climatic variables. Instead of predicting presence or absence in a binary fashion, this approach predicts the possibility that a given area is suitable based on observed distributions and a number of different climatic variables such as those developed for South Africa by Schulze *et al.* (1997).

Predictions of the potential range of species using only climatic factors in correlative models frequently give good results (Richardson and McMahon 1992). As a result, a large number of correlative studies have been conducted on the distribution of various organisms including invasive or economically useful plants (Panetta & Mitchell 1991, Richardson & McMahon 1992, Beerling *et al.* 1995, Sykes *et al.* 1996) and threatened marsupials (Lindenmayer *et al.* 1991, Carpenter *et al.* 1993). However, the correlative approach to modelling distribution has been criticised as mechanisms limiting the organisms distribution may not involve the climatic variables used in the model. Rather, other variables which are coincidentally correlated with the variables used in the model may be the key limiting variables associated with the organism's distribution (Beerling *et al.* 1995).

While correlations are often regarded as poor substitutes for a mechanistic understanding of relationships, they can play an invaluable role in suggesting candidate mechanisms for investigation (Levin 1993, Stephenson 1998).

The second approach is mechanistic, modelling the “interactive processes between organisms and their environment using performance parameters” (Carpenter *et al.* 1993). This approach incorporates explicit models which simulate the mechanisms which might be considered to cause the observed correlations of distribution with environmental attributes (Beerling *et al.* 1995). The importance of the organism’s physiological tolerances and life-history traits in relation to the environment in predicting its distribution is therefore referred to as a mechanistic (Beerling *et al.* 1995) or ecophysiological (Stephenson 1998) approach to modelling organisms’ distributions.

This approach provides important biological and ecological information and insights (Carpenter *et al.* 1993). Sykes *et al.* (1996) suggest that plant species distribution limits should be expressed in terms of bioclimatic variables which represent physiologically limiting mechanisms as opposed to relying simply on correlations with standard climatic variables. However, because of the requirements for detailed information about aspects of the organism’s ecology and physiology, this approach is less practical in many circumstances where such detailed information is not accessible.

In addition, mechanistic models are based on underlying processes, allowing predictions to be made for the future as specific variables change. Correlative models are formulated on the assumption that previously observed relationships to variables will continue to hold in the future, and so may be considered static (Elston & Buckland 1993).

However, because of the lack of physiological information for particular organisms, relatively few mechanistic studies have been undertaken. One such mechanistic model, while not specifically modelling distribution, is that of Weiss & Weiss (1998). They modelled the phenology of the emergence adults of a threatened butterfly which was variable in different parts of the study site because of variable climate.

This study is an attempt at relating aspects of the physiology of *S. plumieri* and *A. arenaria* to long term climatic variables prepared by Schulze *et al.* (1997), with the aim of identifying factors which may limit the distribution of these plants.

Geographic Information Systems

The rapid development of computers and associated software has been one of the driving forces of scientific developments in the last ten years (Elston & Buckland 1993) and has undoubtedly spurred the advances in the analysis of spatial data. These developments in hardware and software allow for: the databasing of large data sets in readily accessible formats; the processing and manipulation of large data sets; and the graphic display of results in various digital and print formats (Elston & Buckland 1993).

A GIS can broadly be considered as a computer system with the ability to acquire, store, analyse and display geographic data, or data with associated spatial attributes. Central to a GIS is the relevant hardware (computers, digitising devices, printers etc.) and software for processing the data. Perhaps more important than these 'off-the-shelf items', is the database and expertise required for implementing a successful GIS, both of which may be considerably more expensive than the hardware and software in the long term (Eastman 1997a). Maguire (1991) note that producing a definition of GIS is difficult as a result of their rapid development, commercial orientation and the diversity of uses and users. This author suggests the very broad description of a GIS as "an integrated collection of hardware, software, data and 'liveware' which operates in an institutional context." More detailed definitions depend on particular applications of the GIS (Maguire 1991).

One of the advantages of GIS is the ability to integrate spatial data from different sources with different formats, structures, projections or levels of resolution and, as such, is a powerful aid to spatial analysis (Elston & Buckland 1993, Payn *et al.* 1999). GIS is not only a digital store of spatial objects (pixels, point, lines, and areas), but also a means of analysing the interactions within and between these spatial objects (Payn *et al.* 1999).

A GIS stores two types of data which are represented on a map. A geographic definition (position) of a feature as well as the attribute that may be found at that position. There are two

different methods used for representing this data - vector and raster representations (Eastman 1997a).

In vector representations a feature is identified primarily by a point with x and y co-ordinates (e.g. latitude and longitude co-ordinates) defining the position of this point. The point then has a set of attributes assigned to it and these are usually stored in a separate database file. Points may be linked by straight lines to form linear features such as rivers. Alternatively, points linked by straight lines may enclose an area known as a polygon. These features (lines or polygons) also have attributes linked to them as in the case of individual points (Eastman 1997a).

The second major form of representation is raster representation. Raster systems typically combine the position and attribute information into a single file. In this case features are not specifically identified. Rather, the entire 'study site' is subdivided into a regular grid of cells and the position of the entire grid is defined, from which the co-ordinates of individual cells can be inferred. Each cell of the grid is given a number which may be a unique number to which a table of attributes can be linked. Alternatively, this number might be a qualitative attribute code or a quantitative attribute value. Although the data stored in these grids does not necessarily represent phenomena which can be seen, these data grids are often thought of as 'images'. Usually separate images are constructed for each different attribute for the mapped area. These different images may be known as a layer (Eastman 1997a). The cells of the raster grids are often referred to as pixels and are similar in some sense to the pixels of digital images. Although in the case of raster images each pixel has a value associated with it rather than a colour as in digital images.

Raster systems are data intensive as data is recorded in all pixels regardless of whether that pixel holds useful data or not. The advantage, however, is that geographical space is uniformly defined in a simple and predictable manner. As a result, raster systems have considerably more analytical power than vector systems in the analysis of continuous space (Ball 1994). The structure of raster data is also closely matched to the architecture of digital computers, making them rapid in the evaluation of various mathematical combinations of different images or layers (Ball 1994, Eastman 1997a).

Vector systems have limited analytical capabilities over continuous spaces. They excel at problems involving the movement over networks. In addition, they have simple database management functions and are very good for mapping purposes (Eastman 1997a).

This study primarily uses raster data in the form of monthly or annual climatic raster surfaces developed by Schulze *et al.* (1997). A raster grid of pixels covers the land area of the country and each of these pixels has a value attributed to it. This value represents the monthly (or annual) value for the specific pixel of the climatic factor being investigated. The distribution data are vector point data. However, these points are converted into raster pixels for further processing with raster climatic surfaces.

Materials and Methods

This section describes the collection of distribution data for both *S. plumieri* and *A. arenaria*. These distribution data form the basis of investigation into factors which may control the distribution of both species. In many cases, the distribution data collected is extensive and of high resolution for certain sections of the coast where continuous presence or absence data for each species has been collected.

A GIS was used to construct regional maps of water use (transpiration rates) which were subtracted from rainfall to show potential water deficit. The production of these regional transpiration rate maps is based on the known response of both species to ambient temperature and humidity at the leaf level, as described in Chapter 2, and scaled to the canopy level as investigated in Chapter 3.

In addition, a discriminant function analysis was used to investigate other climatic variables which may play a role in limiting the distribution of these two species along the South African coast.

Distribution data

Distribution data for both *A. arenaria* and *S. plumieri* were collected from a number of sources. Distribution data for these two species in Southern Africa were gathered from herbarium specimens housed in the Schönland Herbarium (GRA), Natal Herbarium (NU) as well as the Pretoria Herbarium (PRE) via the PRECIS data base, although much of it is not particularly useful. This is because the data are at the quarter-degree square precision and, as such, are only useful for showing low-resolution representations of where the species are found. The continued collection of distribution data for all species at this course level should be discouraged as it is not compatible with modern modelling and mapping techniques⁶. More emphasis should be placed on high precision locality data for herbarium specimens, which can be scaled up to produce low resolution maps if required.

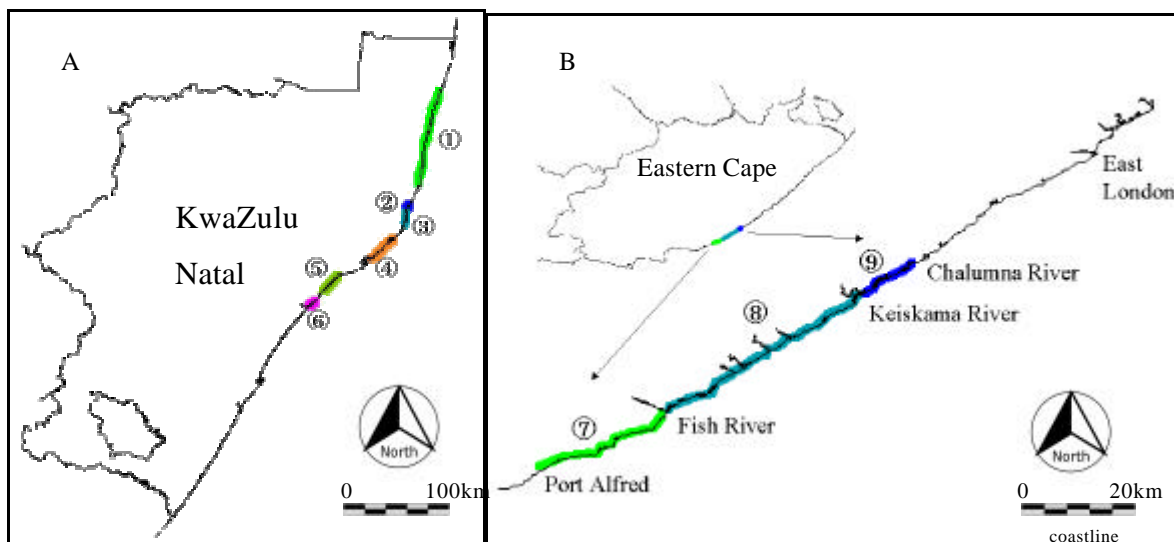


Figure 4-1: Routes surveyed along KwaZulu-Natal (A) and Eastern Cape (B) coasts. These stretches of the coasts were surveyed from a vehicle for continuous presence or absence distribution data of *S. plumieri* as well as *A. arenaria* in parts of the Eastern Cape. See text for definitions of numbered routes.

In the field, distribution data were collected for *S. plumieri*, *A. arenaria* and other dune pioneer species using a Magellan GPS 2000 and more recently a Magellan GPS 315 Global Positioning System (Magellan Corporation, San Dimas, California, USA). These were either

⁶ The PRECIS database has two records of *S. plumieri* distribution recorded to include degrees, minutes and seconds. There are no such records for *A. arenaria*. PRECIS data does include the original locality descriptions from which it may be possible to infer locality points possibly including degrees and minutes (E. Snyman pers. com.).

point data at beaches which are accessible by road or continuous data of presence or absence of the species which were collected by driving along the beach and recording starting and ending co-ordinates of sand dunes covered by the two species. This was done in KwaZulu-Natal from Mission Rocks south of Cape Vidal to mBibi (Hulley Point) south of Kosi Bay. This section of the coast includes Leven Point, the St Lucia Sanctuary area and Sodwana sections of the St Lucia marine protection area No. 1 (Figure 4-1A, -). Other routes include from St Lucia estuary north as far as First Rocks (-); from the mPelane side of the mFolozu estuary south to Lighthouse rocks (®); Richards Bay harbour north to Dawson's Rocks (-); mLalazi estuary south to the aMatikulu River (°); Tugela estuary north for 8 kilometres (±). In the Eastern Cape province, continuous presence or absence data were collected from Port Alfred in the south west to the Fish River (Figure 4-1B, ™); from Old Woman's River east of the Fish River to the Keiskama River (³) and from the Keiskama River north east to the Chalumna (Thyolomnqa) River (´).

Representative voucher specimens were collected at various points where distribution data were collected. These specimens are housed in the Schönland Herbarium, Grahamstown (GRA).

Additional methods were used to confirm species presence on various beaches. Photographs from family holidays confirmed the presence of *S. plumieri* on the sand dunes at Bungha neck, Kosi Bay. Aerial photos taken by R.A. Lubke (pers. com.) were also used to confirm the presence of *S. plumieri* along certain stretches of the Transkei coast. In all cases distribution points were only recorded if the photograph clearly corresponded with a feature on a 1:50 000 topographic sheet so that accurate co-ordinates could be determined. These records are important as they are in areas such as the Transkei where there are few distribution records.

In the case of *A. arenaria*, extensive use was made of Hertling's (1997) data recorded on 1:50 000 topographic sheets. This was supplemented by locality data recorded with a GPS as described above for *S. plumieri*. A total of 327 points were collected for *S. plumieri* and 123 points for *A. arenaria*. Lists of these distribution points are housed in the Schönland Herbarium (GRA).

Distribution points collected with the GPS as well as points determined from recent 1:50 000 topographic sheets use the WGS84 (World Geodetic System 84) co-ordinate reference system as does the digital system used in IDRISI to map both the raster grid and point and line features. Older 1:50 000 topographic sheets use the previous Cape Datum reference system. Differences of up to 300 metres can be expected between these two co-ordinate reference systems. Such error is perhaps insignificant in the context of the resolution of the surfaces used in this study. This is discussed further below.

Importing point data

Distribution data in the form of decimal degrees, determined from either GPS positions or from data recorded on 1:50 000 topographic sheets were imported, along with the point's unique identifier numbers, to IDRISI for Windows version 2 (Eastman 1997c). Decimal degrees were calculated from the recorded data which was in the form, degrees, minutes, seconds, east or south:

$$\text{Decimal Degrees} = \text{Degrees} + \left(\frac{(\text{Minutes} \times 60) + \text{Seconds}}{3600} \right)$$

(Equation 4-1)

The alignment of the climatic surfaces in relation to the coastline is not perfect and as a result most of the data points, as collected using both GPS and 1:50 000 topographic sheets, fell outside of the climatic surfaces used for modelling. As a result, these points did not correspond with valid pixels of the surfaces.

To circumvent this, new data points were assigned to the nearest pixel of the surface to the actual data point (Figure 4-2). This is not ideal and a better solution would involve re-interpolating the original point data to produce new surfaces according to the equations of Schulze *et al.* (1997) so as to overlay the coastal 'strip' which is not covered in the present surfaces. Another option would be to realign the available surfaces to overlap the coastline by shifting the surfaces down, towards the southern coast. This may be legitimate as the surface does overlap the northern border of the country by about half a pixel, suggesting that the surfaces are skewed north with respect to the data base of the coastline and provincial boundaries. The coastline may be considered relatively accurate, being digitised directly from

1:50 000 topographic sheets and the data points, as collected by both GPS and off 1:50 000 topographic sheets, correspond well with these lines (Figure 4-2).

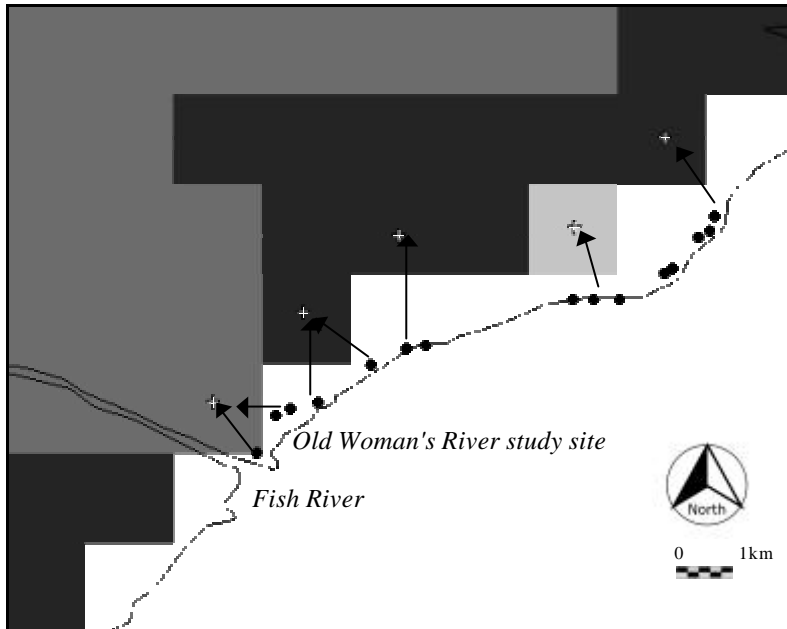


Figure 4-2: The climatic surfaces as produced by Schulze *et al.* (1997) end short of the coastline. Because of this, distribution points were assigned to the nearest raster pixel and the adjusted distribution data set was used to extract values from the surfaces.

Distribution data points collected using a GPS are accurate to within 150 metres, or better. The inaccuracy of positions is due to the United States department of defence's Selective Availability (SA) program, which introduces error to the satellite signals for security reasons (Herring 1996). More recent distribution data collected with a Magellan GPS 315 are more accurate as this receiver averages the position over time and so removes some of the errors introduced by SA (Magellan 1998).

Data recorded on 1:50 000 topographic sheets are also very accurate, although this relies on the careful estimation and marking of the original positions on the maps. If accurately positioned on the topographic sheets, accurate point data can be determined, probably to within one or two hundred metres (Figure 4-3).

While there is some error inherent in the distribution points collected using either a GPS or from estimation from 1:50 000 maps, the operational mapping unit use in this study is one

minute square (an area 1.6 km by 1.6 km). As a result error associated with distribution points is probably insignificant.

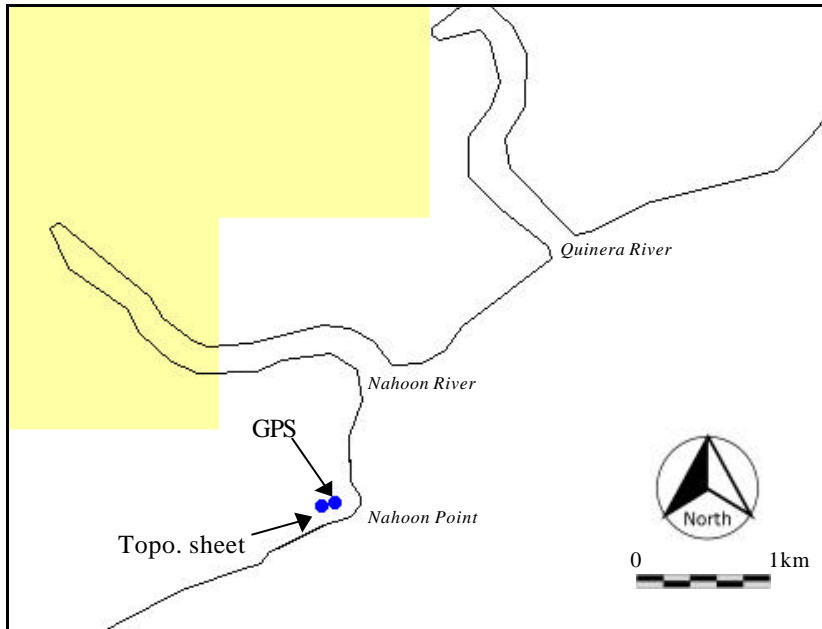


Figure 4-3: Comparison of data points collected with a Magellan GPS 315 and points inferred from 1:50 000 topographic sheets. Both points represent the same 'target point' on the ground as measured by the two methods. While accurate latitude and longitude data can be calculated from 1:50 000 topographic sheets, this relies on the accurate marking of the point in question on the map.

Climatic surfaces

Climatic surfaces developed by Schulze *et al.* (1997) were downloaded from the Department of Agricultural Engineering, University of Natal, Pietermaritzburg. Where necessary these surfaces were converted from ArcView Spatial Analyst format to IDRISI image format.

In this study, four principle sets of surfaces were used. Mean monthly maximum and minimum temperatures were used to calculate mean monthly average temperature. In addition, mean monthly relative humidity and median monthly rainfall surfaces were also used. Monthly surfaces were used as it is possible to then calculate annual values if needed. Additional surfaces were used for the discriminant function analysis and are listed below in that section.

The climatic surfaces represent a raster grid of 1021 columns by 781 rows. Each pixel in the grid is one minute of latitude by one minute of longitude (approximately 1.6 km x 1.6 km) and has a value associated with it. This value is the mean monthly value for the specific variable – for example, mean monthly maximum temperature.

The basis for the climatic surfaces is a grid of altitudes interpolated from about 437 000 points. Each point has various attributes associated with it and these attributes were used in the subsequent analyses to produce the secondary climatic surfaces of temperature and rainfall. The attributes for each point include latitude, longitude, altitude, aspect, 'continentality index', topographic exposure index, terrain roughness index and extraterrestrial radiation for each month. The country was then divided into a different number of homogeneous regions, depending on which climatic variable was being calculated. For example, 34 regions were used to produce the rainfall surfaces, but only twelve for the temperature surfaces. Using stepwise multiple regression equations and the attributes mentioned above (latitude, altitude aspect etc.), equations were developed to predict secondary climatic parameters (maximum and minimum temperatures and rainfall) for each month. These predicted variables were compared statistically to measured values to obtain a level of confidence for each equation which was then used to interpolate or extrapolate values where no observations have been made for the particular region. Measured variables are mean values of a number of years of continuous data collection (Schulze *et al.* 1997).

Once accepted, the equations were used to predict values at each point in the region with an overlap of fifteen minutes with the neighbouring region. Where two or more regions overlap the values were smoothed to eliminate differences which might be caused by the different equations being used in each region. The values produced were checked particularly when extrapolations which exceed the highest or lowest observations for that region were made (Schulze *et al.* 1997).

From the primary variables mentioned above (altitude, latitude, continentality, topography etc.), as well as the secondary surfaces of temperature and rainfall, various tertiary surfaces were calculated in much the same way as mentioned above. These tertiary surfaces include relative humidity and potential evaporation among others (Schulze *et al.* 1997). These authors

provide details about the derivation of the different regression equations used to interpolate variables in various regions as well as rationales for the different methods selected to produce these surfaces.

Calculations

The regression of transpiration rates to atmospheric vapour pressure deficit (VPD) for both species (Figures 2-5 and 2-6), as presented in Chapter 2, form the basis of the mechanistic modelling approach presented in this chapter. These regressions were modified as discussed in Chapter 3 so as to have zero intercepts (Figures 3-6 and 3-7). This is to avoid predicting negative transpiration rates. Upper and lower prediction limits were calculated for both the *S. plumieri* and *A. arenaria* data sets according to the formulae below from Wackerly *et al.* (1996):

$$\text{Regression equation} \pm t_{\alpha/3} S \sqrt{1 + \frac{1}{n} + \frac{(x - \bar{x})^2}{S_{xx}}}$$

(Equation 4-1)

Where $t_{\alpha/3}$ is the t value with α significance levels and $n-3$ degrees of freedom, S is the estimated standard deviation and is calculated according to the equation:

$$S = \sqrt{\frac{SSE}{n-2}}$$

(Equation 4-2)

Here SSE is the *sum of squares for error* and is calculated from the sum of the squares of the difference between the actual (y) and predicted (\hat{y}) values of y :

$$SSE = \sum_{i=1}^n (y_i - \hat{y}_i)^2$$

(Equation 4-3)

S_{xx} is calculated from the sum of squares of the difference between the x value and \bar{x} values:

$$S_{xx} = \sum_{i=1}^n (x_i - \bar{x}_i)^2$$

(Equation 4-5)

The upper and lower prediction limits are plotted below for *S. plumieri* (Figure 4-4) and *A. arenaria* (Figure 4-5). Table 4-1 gives a summary of the equations of the regression lines and prediction limit lines in each of these figures. These equations are used below to calculate transpiration rates below for the entire country from surfaces of mean temperature and humidity.

Table 4-1: Equations used in calculations of the mean regression lines and 95 % prediction limits.

	<i>S. plumieri</i>	<i>A. arenaria</i>
Mean regression	$y = -0.1061x^2 + 2.5356x$	$y = -0.3747x^2 + 1.9595x$
+95% prediction	$y = -0.1013x^2 + 2.5246x + 1.0333$	$y = -0.3700x^2 + 1.9470x + 0.8278$
-95% prediction	$y = -0.1109x^2 + 2.5466x - 1.0333$	$y = -0.3794x^2 + 1.9720x - 0.8278$

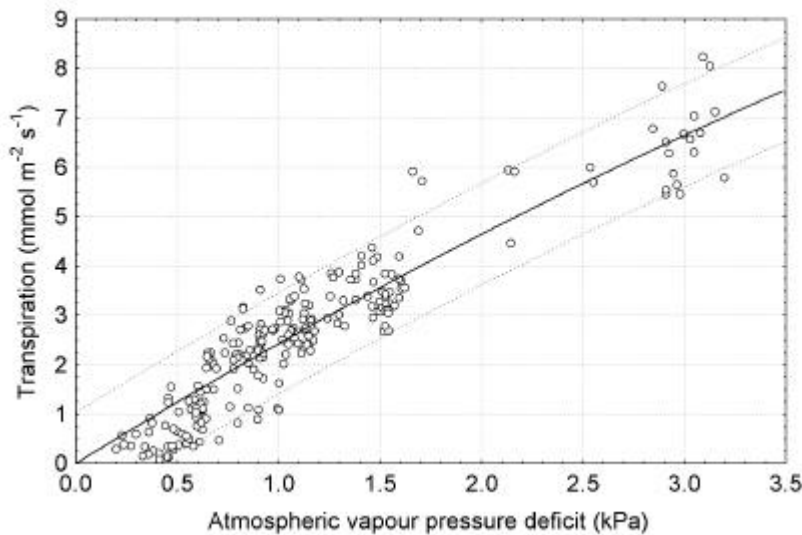


Figure 44: Transpiration rates of *S. plumieri* in relation to VPD as determined in Chapter 2 and modified to have a zero y intercept in Chapter 3 (Figure 3-6). Equations of the regression line (solid) and upper and lower 95% prediction limits (dotted) are listed in Table 4-2.

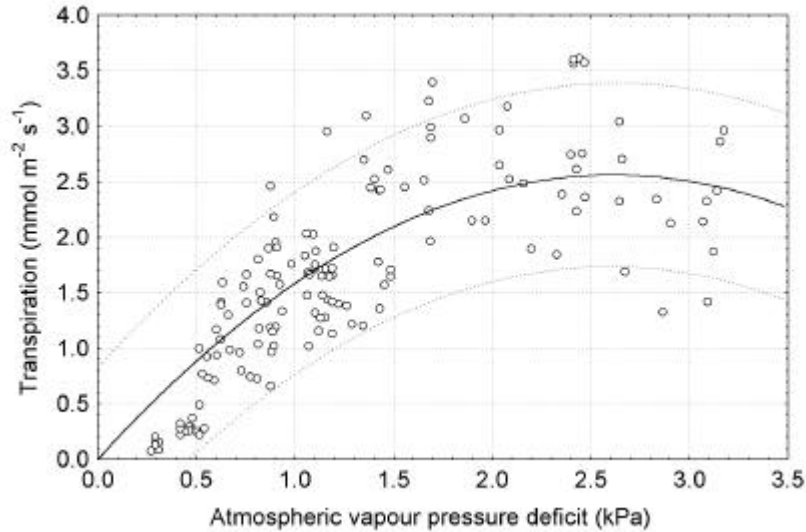


Figure 4-5: Transpiration rates of *A. arenaria* in relation to VPD as determined in Chapter 2 and modified to have a zero y intercept in Chapter 3 (Figure 3-7). Equations of the regression line (solid) and upper and lower 95% prediction limits (dotted) are listed in Table 4-2.

GIS processing

The general scheme for the calculation of regional deficits for each species from the different climatic surfaces is given in Figure 4-6. Input or primary surfaces as downloaded from the Department of Agricultural Engineering, University of Natal, Pietermaritzburg, include monthly maximum (T_{max}) and minimum (T_{min}) temperatures, monthly average relative humidity (RH_{ave}) and monthly median rainfall ($Rain$).

From surfaces of T_{max} and T_{min} surfaces of monthly average temperature (T_{ave}) were calculated. Average temperature was used as this integrates data from both T_{max} and T_{min} surfaces and probably better describes diurnal fluctuations than using extremes of either maximum or minimum temperatures alone. A surface representing saturation vapour pressure (SVP) was calculated according to Equation 2-4 using T_{ave} as an input surface. Using the surface of SVP and RH_{ave} , a surface of VPD was calculated according to Equation 2-3. The surface of monthly VPD was then used as the input surface from which monthly transpiration was calculated according to the various equations listed for each species in Table 4-1. These include the equation of the mean regression line as well as the equations of the positive and negative 95% prediction limits.

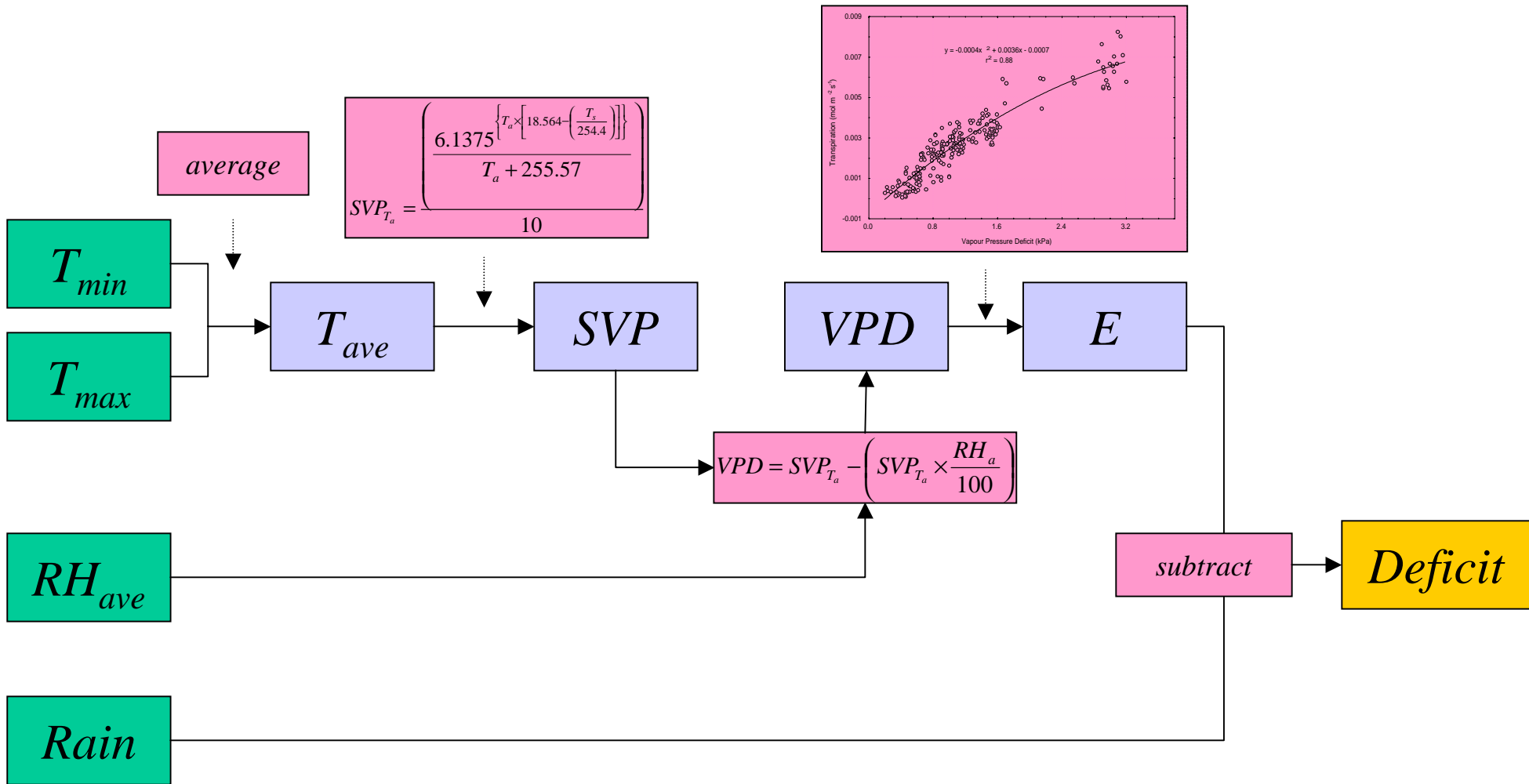


Figure 4-6: Schematic representation of the calculation of deficit surfaces. Input surfaces are given by , intermediate surfaces by , operations by and the output deficit surface by . This is necessarily simplified and each step shown here may entail more than one calculation. Text and Appendix 2 gives additional details as to how the various surfaces were calculated. See text for explanations of abbreviations.

The surfaces of transpiration rates were converted to litres per month by multiplying by 18, and then by 1.003 to get litres $\text{m}^{-2} \text{s}^{-1}$. This was then multiplied by the number of seconds in a specific month. Finally this was multiplied by the LAI (square metres of leaf area per square metre of sand dune area, as calculated and described in Chapter 3) to produce surfaces of transpiration (litres per month) over a square metre of vegetated sand dune. This resultant surface of monthly transpiration was then subtracted from the corresponding monthly median rainfall surface (also expressed in litres for a square metre of sand dune) to produce a surface of monthly water deficits on the basis of a square metre of vegetated sand dune.

These various steps can be easily calculated in IDRISI using the ‘Image Calculator’ module. However, because of the large number of surfaces to be processed, a macro sequence was written to process all the input surfaces and produce monthly deficit surfaces for each month of the year. Details of these calculations and the macro are given in Appendix 3.

Extraction of data from deficit surfaces

The above processing produced 36 deficit surfaces for each species. Twelve monthly deficit surfaces were produced from the mean regression line equation, as well as the lines of the positive and negative 95% prediction limits. Representative surfaces of the mean deficits are given for summer (January, Figures 4-8 and 4-12) and winter (June, Figures 4-9 and 4-13). In addition, surfaces of the average annual deficit (Figures 4-10 and 4-14) were calculated from the twelve monthly deficit surfaces using the IDRISI ‘Image Calculator’ module.

To better show the degree to which the deficits as presented in the surfaces are positive or negative, three-dimension scatter plots were produced to show the changing deficit along the coast. This was done by first digitising every second or third coastal pixel⁷ of a raster surface. These points were then used to extract the value of the deficit in the individual pixels. A macro was written which extracts the value of given pixels, as identified by the digitised points, to a value file which can then be imported to a spread sheet (see Appendix 4). This

macro was then used to extract values for the various pixels (identified by the digitised points) of the monthly surfaces which have been produced.

The extracted deficit value (z) was then linked to the latitude (x) and longitude (y) in decimal degrees of the original point. These three values were used to plot three-dimensional scatter plots which accompany the deficit surfaces presented below. The scatter plots were constructed using Statistica, a statistics software package (Statsoft Inc. 1999a)

There is a considerable amount of information available from both single monthly deficit surface as well as the set of twelve monthly surfaces for a year, all of which is difficult to synthesise visually. For this reason, data were extracted for a number of points around the coast and used to construct graphs of deficits as they change over time.

For both species 'stations' were assigned, more or less arbitrarily, along the length of the coast at roughly equal intervals, although in many cases, the stations correspond with a study site or a city that may be of importance and are generally comparable for both species. Figures 4-11 and 4-15 give the location of the stations that were selected and include stations from within the range of the species concerned (red points) as well as stations from areas where the particular species is known to be absent (blue points).

The deficit data were extracted from each monthly surface at each station as mentioned above and explained in more detail in Appendix 4. This was repeated for each of the three sets of monthly surfaces (mean, positive 95% prediction limits and negative 95% prediction limits). These 'station databases' were used to produce the various graphs included in Figures 4-11 and 4-15. These graphs track the change of deficits throughout the year as well as upper and lower prediction limits which describe the possible variation in the predicted deficits introduced by the possible error associated with the original data collected in the field.

⁷ Unfortunately there appears to be a limitation with IDRISI where there is a limit of about 1400 points which can be used to extract data from different pixels of a surface. As a result, when data is extracted for all coastal pixels, the final stretch of coast corresponding to the last 300 or so pixels is absent. Other users have noted this problem previously.

Discriminant Function Analysis

To further investigate factors limiting the distribution of these two species a discriminant function analysis (DFA) was carried out using a variety of climatic variables. DFA is used to determine which variables discriminate between two or more naturally occurring groups (Statsoft 1999b). The sets of monthly data used are listed below (Table 4-2). Apart from monthly minimum and maximum temperature, mean relative humidity and median rainfall surfaces already mentioned, surfaces of monthly solar radiation and monthly A-pan potential evaporation were also used.

Solar radiation surfaces represent $\text{MJ m}^{-2} \text{ day}^{-1}$. A-pan potential evaporation represents potential evaporation (in millimetres) expressed in terms of equivalence to a 'class-A' evaporation pan which is the most common evaporimeter in use world wide (Schulze *et al.* 1997).

In this case the variability within a group of 12 monthly surfaces of climatic variables was summarised in a principle component analysis (PCA) using the 'PCA' module in IDRISI. It should be noted that the original climatic surfaces in a real-binary (data/file) format were converted to byte-binary file types as required by the 'PCA' module of IDRISI.

PCA is a linear transformation technique, which transforms a set of variables (in this case, raster surfaces of twelve monthly climatic variables), to a set of 'component' indices (in this case a set of component surfaces). This subsequent set of component indices, which are uncorrelated with one another, are ordered in terms of the amount of variability of the original data-set they describe. The fact that the component are uncorrelated is also useful as the different components measure different dimensions of the original data set (Manly 1994). In the case of raster surfaces the first two or three components normally describe the majority of the variance contained in the original set of surfaces because the surfaces are often substantially correlated. As a result, the first two components summarise the variability (Eastman 1997a) and remove much of the redundancy present in the original twelve surfaces. Manly (1994) describes general principle component analysis calculations while Barker & Weisberg (1997) discuss the use of PCA in uncorrelating climatic surfaces.

Principle components for each set of climatic variables with eigenvalues greater than one were then selected for the DFA. Eigenvalues express the amount of variance explained by each component of a principle component set (Eastman 1997b). In all cases either the first, or the first and second components of a set of monthly surfaces account for more than 95% of the variance in the original set of twelve surfaces. The components with eigenvalues greater than one and which are used in the DFA are listed in Table 4-2.

Table 4-2: Components surfaces used in the discriminant function analysis. C1 and C2 refer to components one and two respectively.

Surface and component	Name	Eigenvalue	% variance explained
A pan Potential evaporation C1	ApanC1	11.8	98.3
Maximum temperature C1	MaxC1	11.92	99.32
Minimum temperature C1	MinC1	10.8	90.18
Minimum temperature C2	MinC2	1.08	9.03
Median rainfall C1	MrflC1	7.86	65.5
Median rainfall C2	MrflC2	3.63	30.24
Mean Relative Humidity C1	MrhC1	11.96	99.69
Solar radiation C1	SradC1	11.89	99.05

The component loadings of the different principle components listed in Table 4-2 are given in Appendix 5. These loadings refer to the contribution each original monthly surface makes to the final principle component summarising a particular set of variables. In cases where most of the variability of a set of monthly surfaces is summarised in a single component, then all twelve contribute to the production of this single component. However in the case of monthly minimum temperature and monthly median rainfall, two components are required to adequately summarise the original twelve surfaces. In such cases, the first components are strongly defined by the summer surfaces, while the second components are more strongly defined by the winter surfaces.

Data was extracted from pixels of each of the components surfaces listed in Table 4-2 using points for presence or absence and the macro sequence explained in Appendix 4. Due to the extensive surveying of the coast, both during this study and that undertaken by Hertling (1997), there is considerable confidence that the distribution limits are accurate and comprehensive for both species (Figures 4-7A and 4-7B).

For *A. arenaria* only pixels with confirmed presence of the plants were used to extract presence data from the different surfaces. No absence data were included within the extremities of the presence points (Langebaan in the west and East London in the east). This is to avoid introducing error as a result of false absence data being included with true absence values. False absences may be a result of poor sampling along inaccessible parts of the coast or along parts of the coast where the climate may be suitable for the plants but the substrate (for example) is not. Rocky parts of the coast are an example of areas where the climate is suitable but these plants cannot grow.

All pixels to the east of East London and to the west of Langebaan were considered to be localities where *A. arenaria* is absent. Points were digitised in each of the 'absence' pixels. The different sets of distribution points (presence or absence) were used to extract the values of the climatic variables from each of the component surfaces listed in Table 4-2.

The extracted data from either presence or absence pixels were kept separate. Absence data for *A. arenaria* were separated into absence along the east coast and absence along the west coast, as it is possible that different climatic variables may be limiting distribution along these two separate stretches of the coast, since the climate in these two regions differ considerably.

In the case of *S. plumieri* all points to the west of Arniston, the western most location of this species (Figure 4-7A), were considered absence points. Essentially, the same procedure was followed for *S. plumieri*, except that the absence data was *a priori* divided into two areas, the moist high rainfall area of the south-west coast where substantial water surpluses are recorded in winter, as well as the much drier west coast, north of Cape Columbine (Figure 4-10).

The extracted data were partitioned and coded into the different categories (presence or absence in different regions). The DFA was undertaken using the 'Discriminant Analysis' module in Statistica (Statsoft 1999a).

Results

At a purely descriptive level this study documents the distribution of *S. plumieri* in considerably more detail than other work (Figure 4-7A). This is particularly true along the

east coast of South Africa, and while there is data missing for the former Transkei coast, data collected along parts of the Eastern Cape coast, including the former Ciskei coast (Cape Padrone to Kei River mouth) as well as the KwaZulu-Natal coast, are extensive. This study has also investigated its occurrence on the south coast and has identified Arniston as the southwestern most occurrence of *S. plumieri* in Africa. Along the south coast the distribution of *S. plumieri* becomes increasingly patchy moving westwards.

While Hertling (1997) has extensively surveyed the occurrence of *A. arenaria* in South Africa, this study has identified a number of additional sites where this species occurs. These include, for example, the sand dune blow-out at Nahoon Point, East London, Rufane's River mouth east of Port Alfred and the beaches at Natures Valley where it appears that these plants are altering the shape of the beach. Using a GPS, the locality data collected can be considered more accurate than those inferred from 1:50 000 topographic sheets as collected by Hertling (1997) and used in this study where GPS data is not available. This is primarily because of the error involved in recording the position precisely on the 1:50 000 topographic sheets. If the points are marked accurately on the topographic sheets, this data can be almost as precise as the GPS data subject to selective availability as is discussed above (Figure 4-3).

At low resolution (Figure 4-7) this data is only a slight improvement on the 'pixelated' distribution maps produced from quarter-degree squares such as the data provided by PRECIS. However, when in the form of an electronic or high-resolution map these data sets are considerably more useful. The fact that these are coastal plants, restricted to no more than a '500 metre strip' around the coast, makes the collection of this data somewhat easier as the plants are essentially part of a linear feature. The importance of this is also evident in the deficit surfaces constructed for both species below.

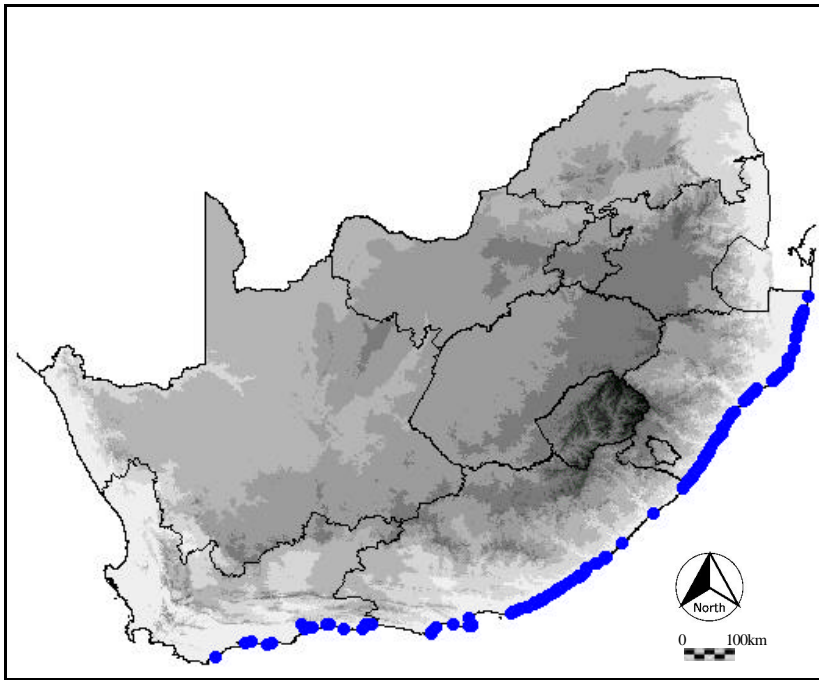


Figure 47A: Distribution of *S. plumieri* in South Africa. Altitude increases with darker shades of grey.

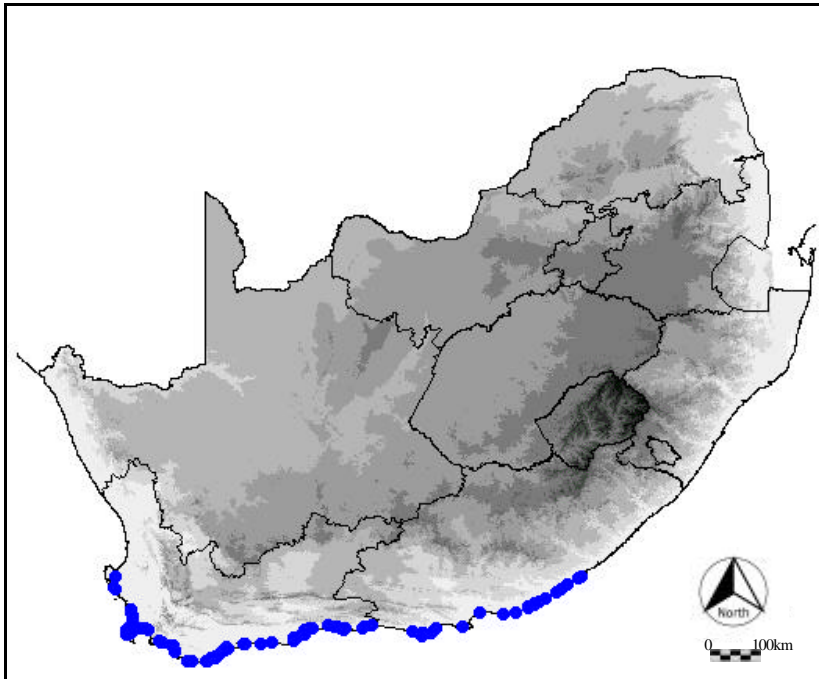


Figure 47B: Distribution of *A. arenaria* in South Africa. Altitude increases with darker shades of grey.

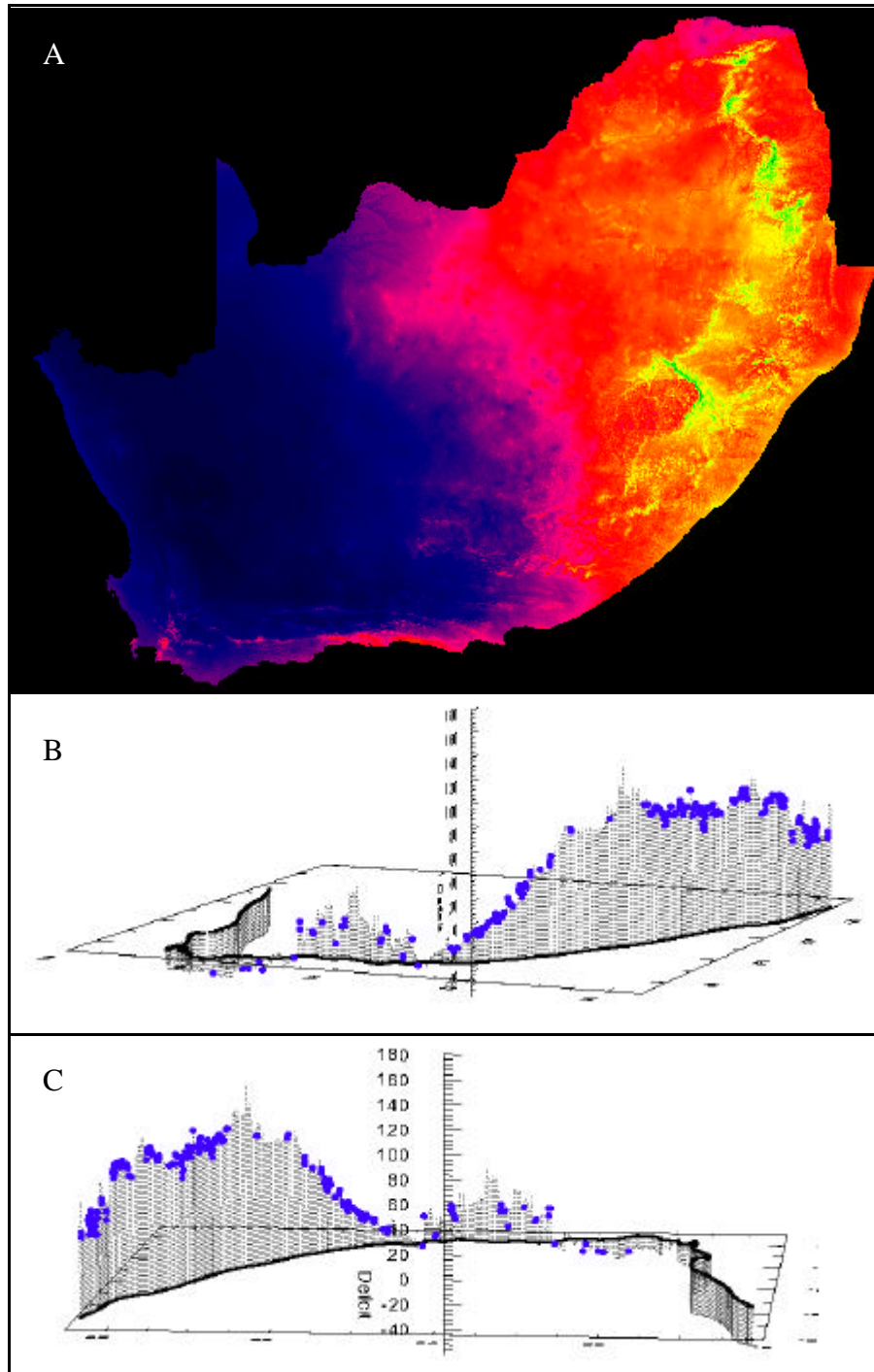
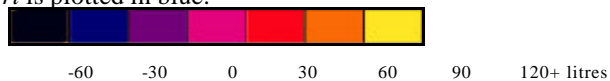


Figure 4-8: A) January monthly deficit for *S. plumieri* calculated from the mean regression of E to VPD (see Table 4-1). Inputs of temperature and relative humidity were used to calculate E from this regression. E was subtracted from rainfall to give the water deficit on a 'litres per square metre of vegetated sand dune' basis. Data was then extracted from coastal pixels in Figure 4-8A, to show water surpluses and deficits graphically along the coast, x-axis: latitude, y-axis: longitude, z-axis: water balance (litres). Perspectives from the south-east (B) and from the north (C). Corresponding distribution of *S. plumieri* is plotted in blue.



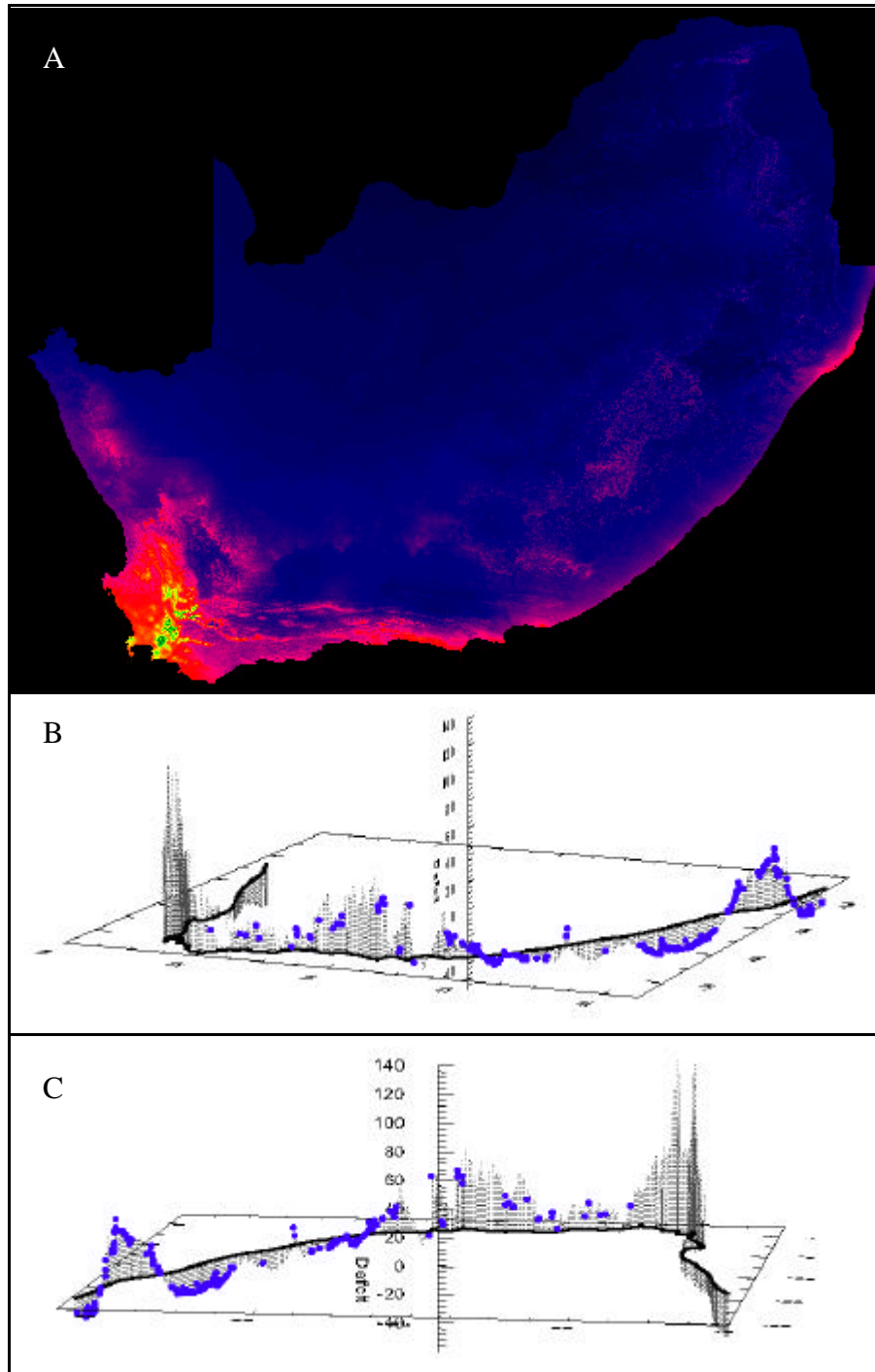
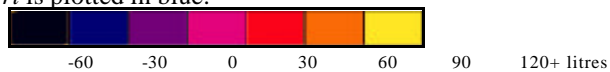


Figure 4-9: A) June monthly deficit for *S. plumieri* calculated from the mean regression of E to VPD (see Table 4-1). Inputs of temperature and relative humidity were used to calculate E from this regression. E was subtracted from rainfall to give the water deficit on a 'litres per square metre of vegetated sand dune' basis. Data was then extracted from coastal pixels in Figure 4-8A, to show water surpluses and deficits graphically along the coast, x-axis: latitude, y-axis: longitude, z-axis: water balance (litres). Perspectives from the south-east (B) and from the north (C). Corresponding distribution of *S. plumieri* is plotted in blue.



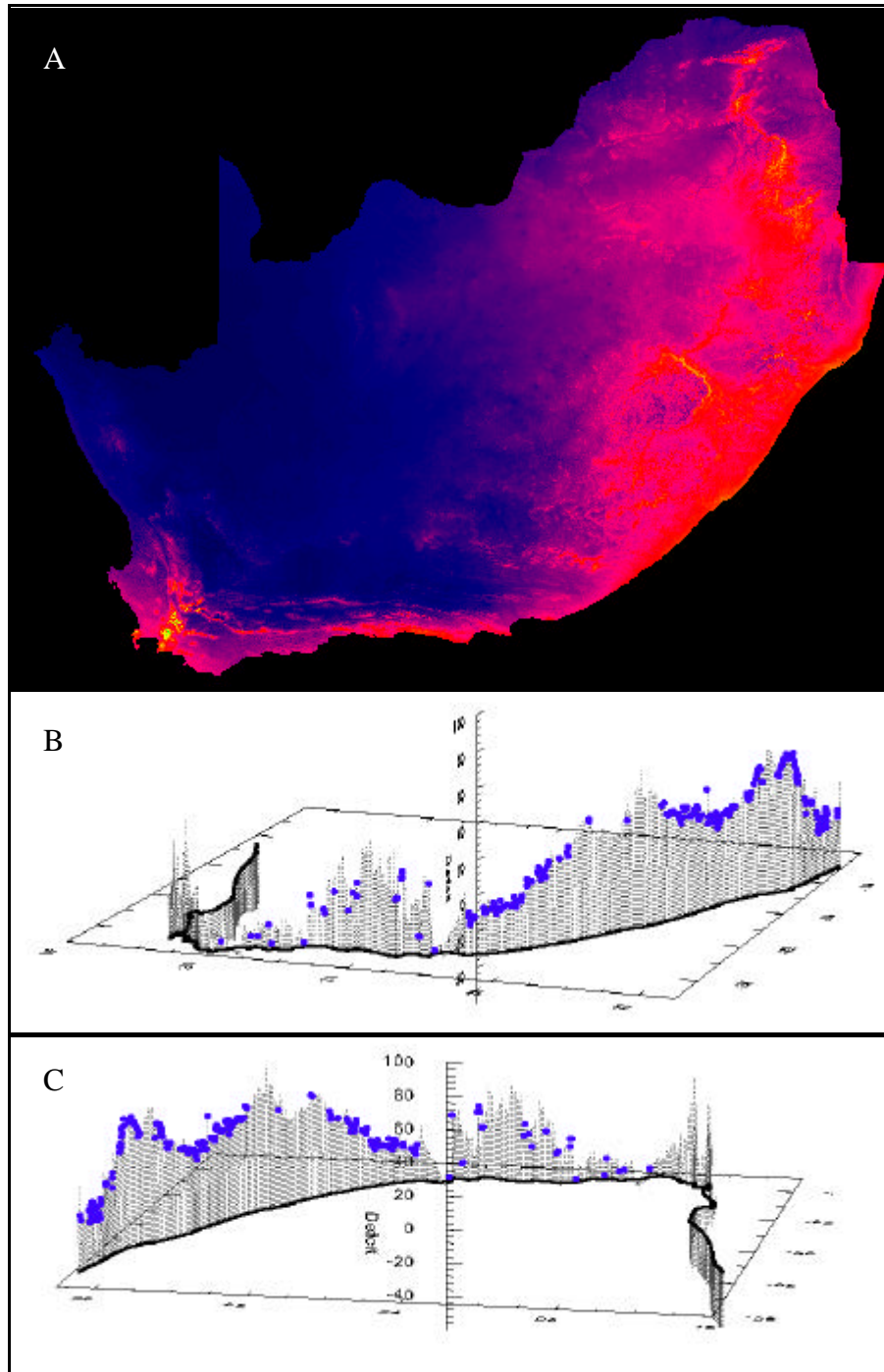


Figure 4-10: A) Annual average deficit for *S. plumieri* calculated from the mean regression of E to VPD (see Table 4-1). Inputs of temperature and relative humidity were used to calculate E from this regression. E was subtracted from rainfall to give the water deficit on a 'litres per square metre of vegetated sand dune' basis. Data was then extracted from coastal pixels in Figure 4-8A, to show water surpluses and deficits graphically along the coast, x-axis: latitude, y-axis: longitude, z-axis: water balance (litres). Perspectives from the south-east (B) and from the north (C). Corresponding distribution of *S. plumieri* is plotted in blue.

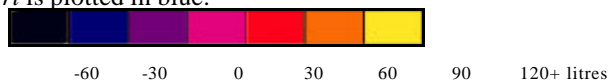
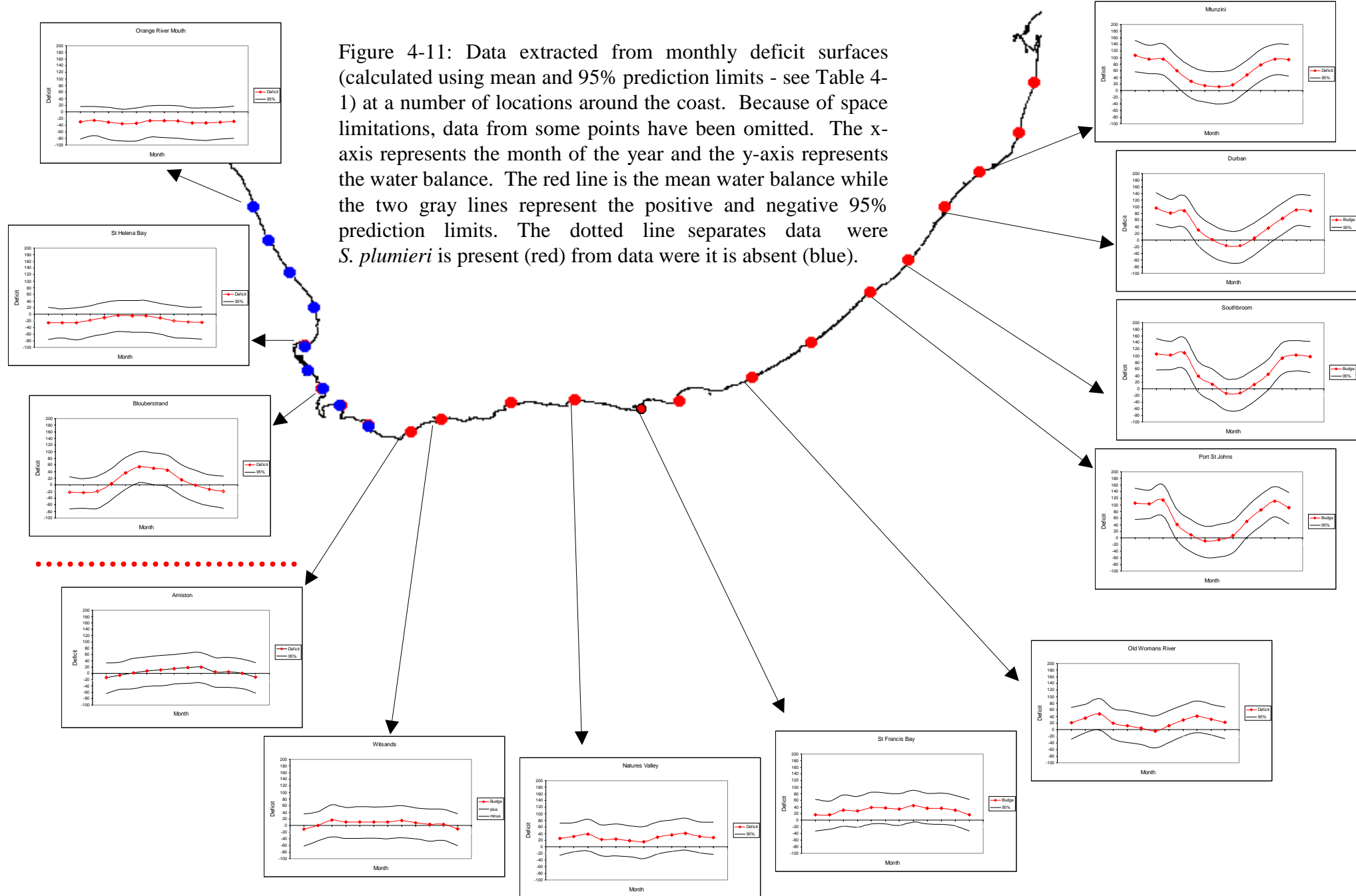


Figure 4-11: Data extracted from monthly deficit surfaces (calculated using mean and 95% prediction limits - see Table 4-1) at a number of locations around the coast. Because of space limitations, data from some points have been omitted. The x-axis represents the month of the year and the y-axis represents the water balance. The red line is the mean water balance while the two gray lines represent the positive and negative 95% prediction limits. The dotted line separates data where *S. plumieri* is present (red) from data where it is absent (blue).



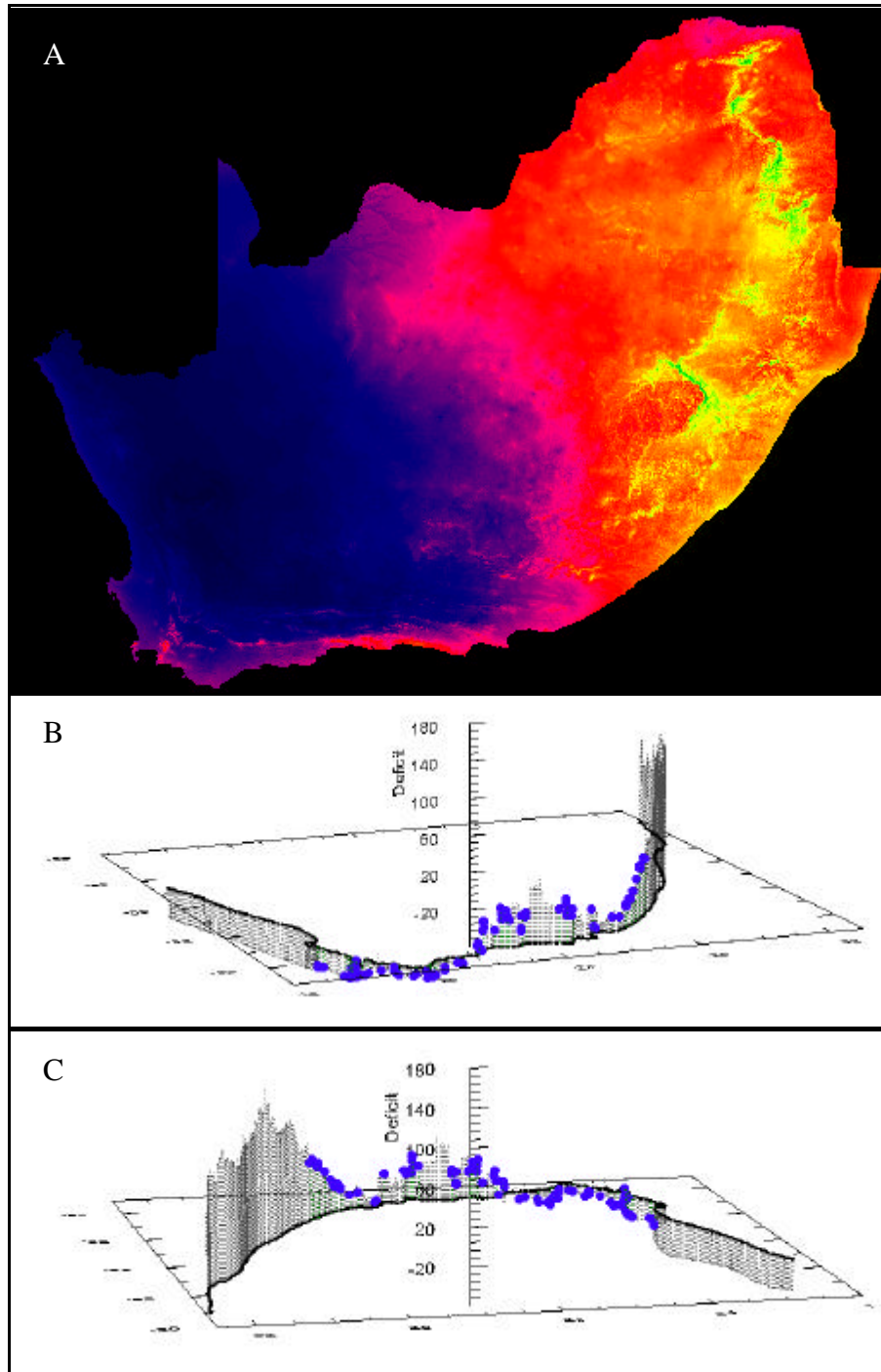


Figure 4-12: A) January monthly deficit for *A. arenaria* calculated from the mean regression of E to VPD (see Table 4-1). Inputs of temperature and relative humidity were used to calculate E from this regression. E was subtracted from rainfall to give the water deficit on a 'litres per square metre of vegetated sand dune' basis. Data was then extracted from coastal pixels in Figure 4-8A, to show water surpluses and deficits graphically along the coast, x-axis: latitude, y-axis: longitude, z-axis: water balance (litres). Perspectives from the south-west (B) and from the north (C). Corresponding distribution of *A. arenaria* is plotted in blue.



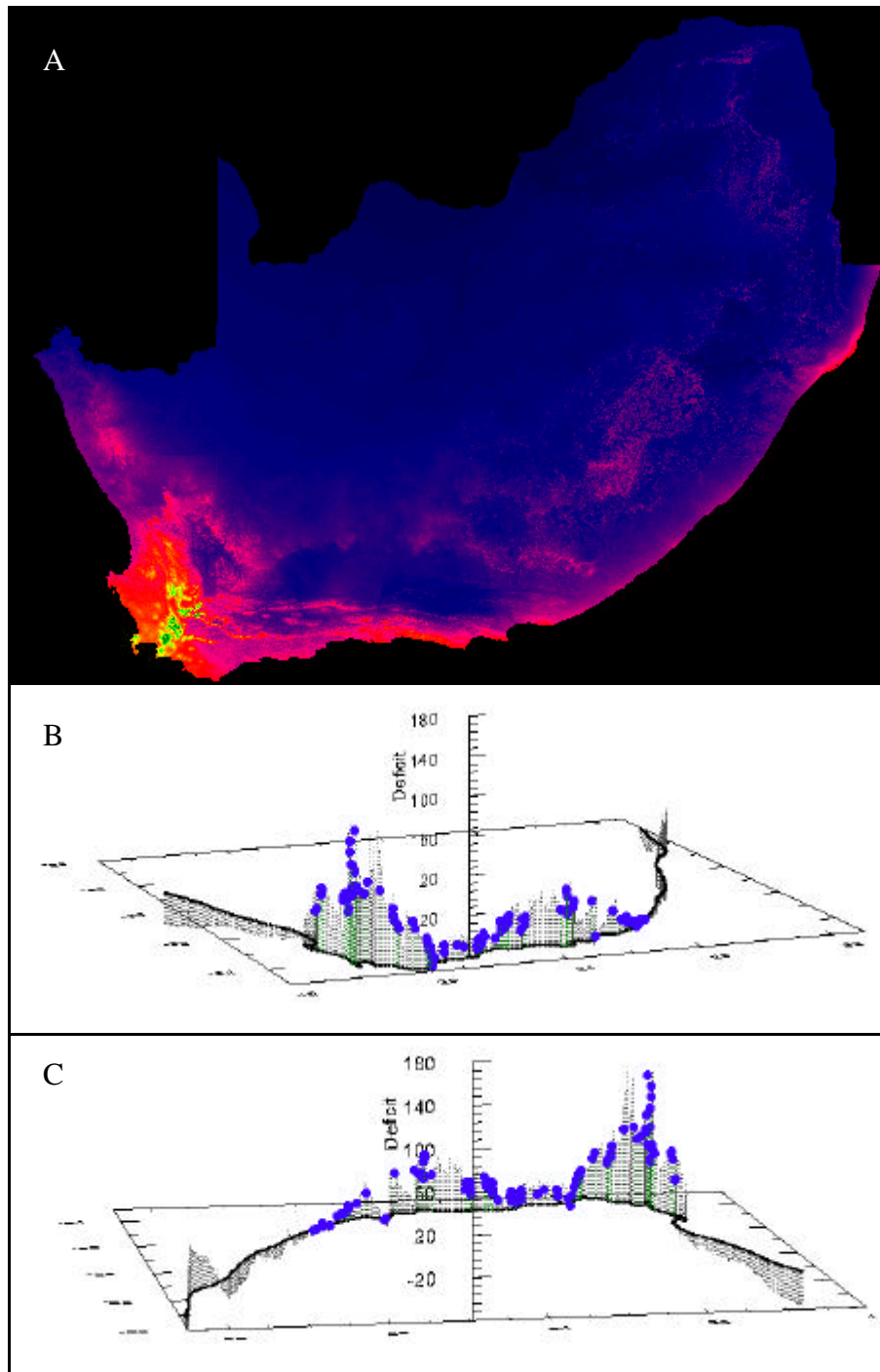
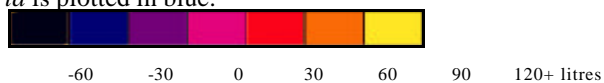


Figure 4-13: A) June monthly deficit for *A. arenaria* calculated from the mean regression of E to VPD (see Table 41). Inputs of temperature, and relative humidity were used to calculate E from this regression. E was subtracted from rainfall to give the water deficit on a 'litres per square metre of vegetated sand dune' basis. Data was then extracted from coastal pixels in Figure 4-8A, to show water surpluses and deficits graphically along the coast, x-axis: latitude, y-axis: longitude, z-axis: water balance (litres). Perspectives from the south-west (B) and from the north (C). Corresponding distribution of *A. arenaria* is plotted in blue.



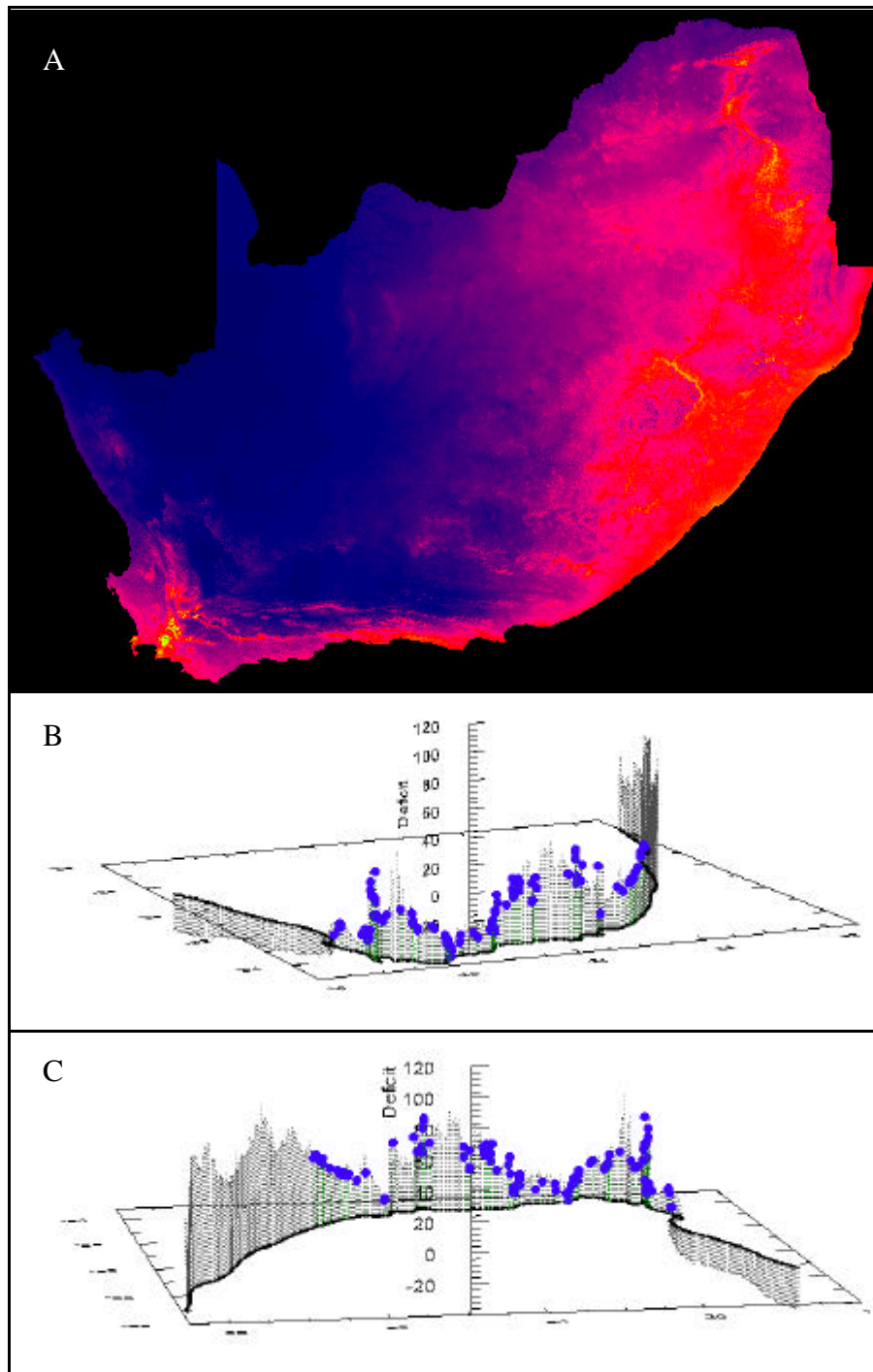
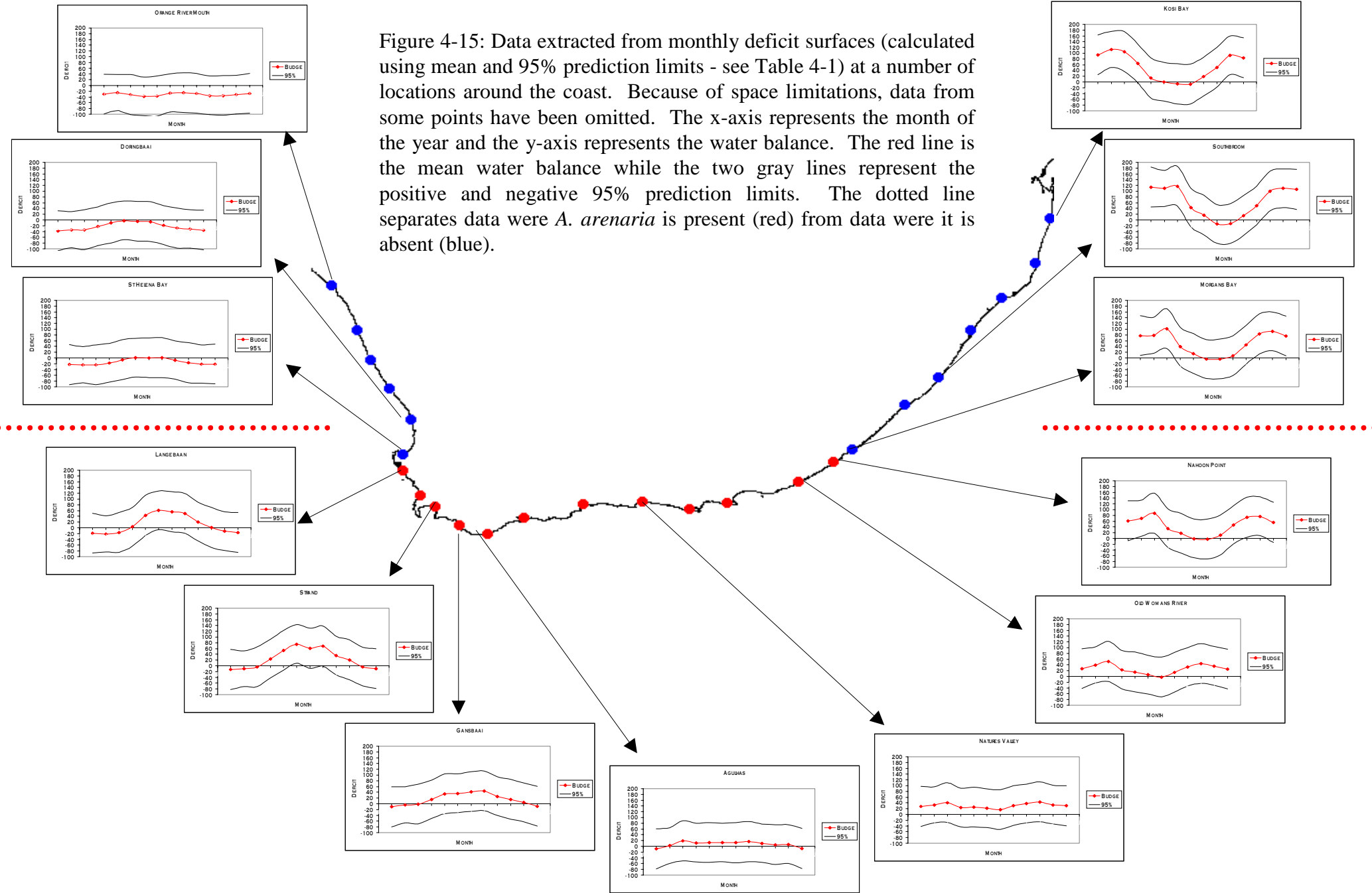


Figure 4-14: A) Annual average deficit for *A. arenaria* calculated from the mean regression of E to VPD (see Table 4-1). Inputs of temperature, and relative humidity were used to calculate E from this regression. E was subtracted from rainfall to give the water deficit on a 'litres per square metre of vegetated sand dune' basis. Data was then extracted from coastal pixels in Figure 4-8A, to show water surpluses and deficits graphically along the coast, x-axis: latitude, y-axis: longitude, z-axis: water balance (litres). Perspectives from the south-west (B) and from the north (C). Corresponding distribution of *A. arenaria* is plotted in blue.



Figure 4-15: Data extracted from monthly deficit surfaces (calculated using mean and 95% prediction limits - see Table 4-1) at a number of locations around the coast. Because of space limitations, data from some points have been omitted. The x-axis represents the month of the year and the y-axis represents the water balance. The red line is the mean water balance while the two gray lines represent the positive and negative 95% prediction limits. The dotted line separates data where *A. arenaria* is present (red) from data where it is absent (blue).



Potential water deficits in relation to distribution

The deficits presented include January (summer) and June (winter) as well as an annual deficit calculated from means of all twelve monthly deficits. As described above, the water deficit is the amount of water transpired by the plants subtracted from the rainfall received by one square metre of vegetated sand dune. They represent the balance between the transpirational extraction of water and rainfall input of water. Plots showing the changing deficit along the coast in three dimensions are included to help interpret the colours of the deficit surfaces. These three-dimension scatter plots are shown from the north and south so as to better illustrate the relationship of deficit to the observed distribution of the two species along different sections of the coast.

For both species there are similar trends with regard to the deficit surfaces produced. The lower transpiration rates of *A. arenaria* are balanced by the higher LAIs used in the calculation of deficits for this species which means that on the basis of a square metre of vegetated dune, there is more transpiring leaf area than in the case of *S. plumieri*.

In both cases there are water surpluses in summer (January, Figures 4-8 and 4-12), along the east coast and the eastern parts of the south coast. The western stretches of the coast have negative deficits. It is interesting that along the eastern parts of the country the water balance is close to zero in the region of Algoa Bay. In winter (June, Figures 4-9 and 4-13) the water surpluses shift to the winter rainfall region of the south-west Cape, from about Cape Agulhas to Cape Columbine. Much of the southern Cape also has surpluses, as does the bulge on the KwaZulu-Natal east coast between the Tugela river and Cape Vidal, centred on Cape St Lucia.

The surfaces of annual deficits (Figures 4-10 and 4-14) show that on a annual basis there are high water surpluses along the east coast and much of the southern and south-west coast (as far west as about Cape Columbine). The surpluses in the Algoa Bay and on the south coast from about Wilderness to Cape Agulhas are only slightly positive. On the west coast, north of Cape Columbine, low rainfall coupled with high temperatures and low relative humidities (high transpiration rates) result in permanently negative water deficits along this coast on a annual basis.

Regional water deficits of S. plumieri

The distribution of *S. plumieri* appears to be strongly correlated (visually) over much of its range with surpluses of rainfall in summer. The distribution only extends a short distance along the south-west coast (from about Wilderness to Cape Agulhas) where deficits are negative in summer (Figure 4-8).

In winter, water deficits along the east coast are substantial although around the ‘bulge’ at Cape St Lucia higher rainfall⁸ results in water surpluses developing. Along the southern coast there are surpluses of water but these are quite variable from one location to the next. It is only on the south-west coast (Cape Agulhas to Cape Columbine) where the potential⁹ water surpluses are high. This is a result of the very high winter rainfall in this region, which may be in excess of 100 mm a month around False Bay and the Cape Peninsula (Schulze *et al.* 1997). The distribution of *S. plumieri* does not extend into the regions of high winter rainfall surpluses of the south-west coast.

The annual deficit (average deficit from all twelve monthly deficits) shows that the distribution of *S. plumieri* corresponds with water surpluses on the east and southern coasts of the country. The plants are only absent from areas of the south-west coast where surpluses are high as a result of high winter rainfall.

Figure 4-11 shows the changing monthly deficit at a number of selected points (or ‘stations’) around the coasts where *S. plumieri* is present (red) and absent (blue). Along much of the east coast the deficit shows a seasonal change from water surpluses in the summer months to low surpluses or slight deficits in winter. Along the southern coasts the surpluses are low, and remain so throughout the year. At the extremities of the distribution of this species, water

⁸ In June 40 to 60 mm of rain falls around the ‘bulge’ as opposed to 10 to 20 mm for much of the rest of the east coast. On an annual basis this region has in excess of 1200 mm compared to 1000 to 1200 mm for the rest of the KwaZulu-Natal and former Transkei coasts (Schulze *et al.* 1997).

⁹ These deficits are termed ‘potential’ because extensive surveys have confirmed the absence of *S. plumieri* along this section of the coast.

deficits develop in summer when rainfall is low and transpiration rates high as a result of high temperature and humidity.

From Cape Agulhas (approximately the limit of *S. plumieri* distribution) to Cape Columbine there are surpluses of water in the cool winter months when rainfall is high (Figure 4-11). In these regions quite high deficits are attained in the warm, dry summer months. Along the west coast, north of Cape Columbine, deficits are consistent throughout the year, becoming more severe in the summer months.

S. plumieri is apparently limited to regions where water are adequate in summer and becomes less common along the southern coast where surpluses are low throughout the year. This species does not extend far into the region of the south-west Cape where deficits are negative in summer.

Regional water deficits of A. arenaria

Deficits calculated using *A. arenaria* transpiration rates are similar to those of *S. plumieri* as discussed above. Deficits calculated for January (summer) are not helpful in resolving what may limit the distribution of this species (Figure 4-12). The distribution straddles the positive water surpluses of the eastern parts of the coast and the negative deficits of the south-west Cape in summer. The species does not extend northwards into areas with water surpluses along the Transkei and KwaZulu-Natal coast.

Water surpluses calculated for June (winter) are substantially more visually correlated with distributions and show that the sampled distribution data correspond almost exclusively with areas of positive winter water balance along the south and south-west coast between Port Alfred and Cape Columbine (Figure 4-13).

The average annual deficits (Figure 4-14) suggest that negative deficits on a year round basis may play a role in limiting the distribution of this species in the north west of its range (Cape Columbine). However, the distribution in the east does not extend up into the region of water surplus along the Transkei and KwaZulu-Natal coasts, suggesting that the negative winter

deficits along the east coast may contribute to limiting this species distribution along the east coast.

For *A. arenaria* distribution is apparently strongly correlated with water surpluses in the winter months (June, Figure 4-13), while for *S. plumieri* distribution is well correlated with surpluses in the summer months (January, Figure 4-8). The correlation of distribution for each species in winter and summer for *A. arenaria* and *S. plumieri* respectively may correspond with the period of growth and reproduction in both species. This is discussed below.

Discriminant Function Analysis

It is not clear as to which climatic variables discriminate between presence and absence data of *S. plumieri* (Figure 4-16, Table 4-3). On root two, presence data and absence data on the west coast are distinct from absence sites on the south-west coast. On this root, maximum temperature discriminates in a positive direction while potential evaporation and the rainfall component one discriminates the absence points on the south-west coast in a negative direction. This suggests that on the south-west coast the potential evaporation environment and the absence of summer rainfall¹⁰ are important in limiting the distribution of *S. plumieri* despite water surpluses developing in winter and on an annual basis (Figures 4-9 and 4-10).

Root one discriminates absence data on both the west and south-west coasts in a positive direction (Figure 4-16) based primarily on potential evaporation but also solar radiation and the summer rainfall component (rainfall component one). Presence points are discriminated in a negative direction based on maximum temperature and minimum component one which is primarily summer minimum temperature (Appendix 5).

There is a slight overlap of presence and absence data on the south-west Cape coast. These points are marked with an asterisk and represent presence data at the extremity of the

¹⁰ The summer months contribute most strongly to the rainfall component one while the winter months contribute more to the second rainfall component. See appendix 4 for component loadings.

distribution of *S. plumieri* at Arniston and Witsands (Figure 4-7A), near Cape Agulhas. These sites may represent the edge of the climatic envelope which is acceptable to this species and are intermediate to the majority of the presence data and

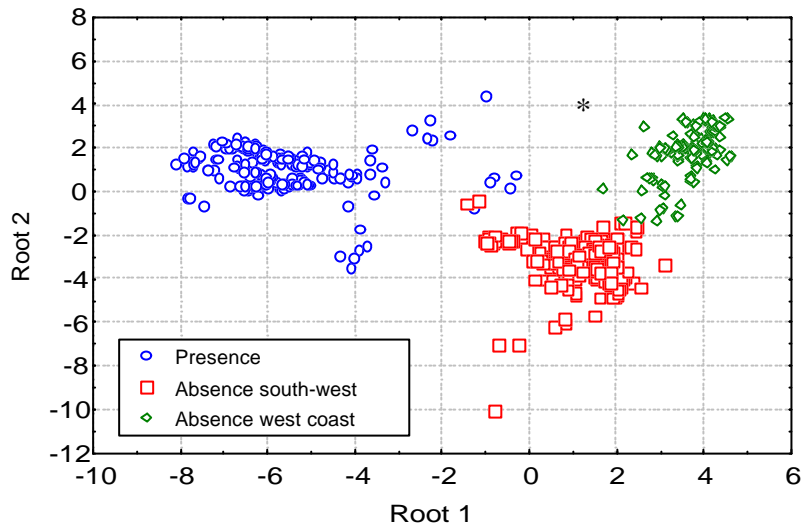


Figure 4-16: Discriminant function analysis of sites where *S. plumieri* is present along the southern coast as well as sites on the south-west and west coasts where this plant is absent. Coefficients defining root one and root two are listed in Table 4-3. Sites from the extreme west of the distribution of *S. plumieri* (at Arniston & Witsands), indicated with an asterisks, mark sites where the species is found but where climatic variables are intermediate to those of the south east coast and those of the south west coast.

Table 4-3: Standardized coefficients defining roots one and two in Figure 4-16 discriminating between presence and absence (on both the east and west coast) of *S. plumieri*. See Table 4-2 for an explanation of the abbreviations used. The component surfaces are ordered in terms of their coefficients from most positive to most negative. The most positive coefficients discriminate in a positive direction while highly negative coefficients discriminate in a negative direction for a particular root.

	Root 1		Root 2
ApanC1	1.529288	MaxC1	1.019969
SradC1	0.838927	MinC2	0.195529
RflC1	0.833209	SradC1	0.153753
MrhC1	0.265067	RflC1	-0.29129
RflC2	0.030922	MrhC1	-0.39376
MinC2	-0.40121	MinC1	-0.40337
MinC1	-0.71928	RflC2	-0.61933
MaxC1	-1.14855	ApanC1	-0.75923

the absence data of the south-west coast. The separation of absence data into two groups is artificial and is prompted by observations that the deficits presented above (Figure 4-10) show

that the west coast is quite distinct from the south-west sections. To a certain degree this separation is valid in that the majority of the points are separated into one of two groups. However, there is some communication between these two classes indicating that they may be extremes of gradually changing conditions.

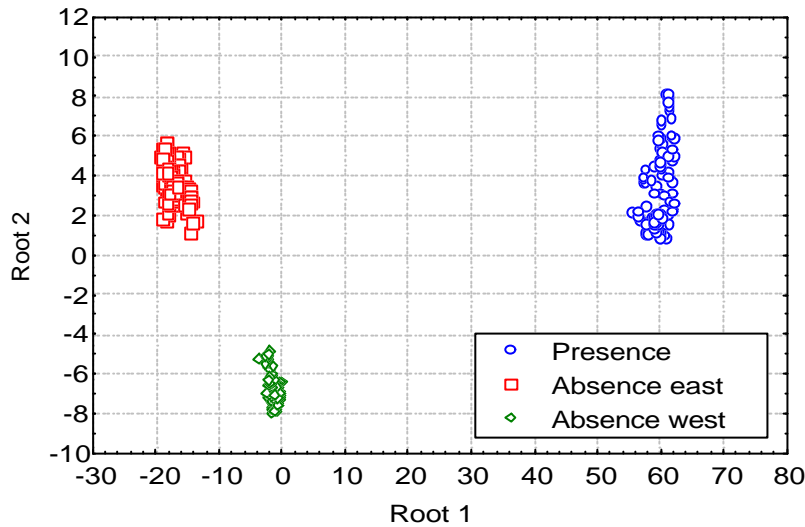


Figure 4-17: Discriminant function analysis of sites where *A. arenaria* is present along the southern coast as well as sites on the east and west coasts where this plant is absent. Coefficients defining roots one and two are listed in Table 4-4.

Table 4-4: Standardized coefficients defining roots one and two in Figure 4-17 discriminating between presence and absence (on both the east and west coast) of *A. arenaria*. See Table 4-2 for an explanation of the abbreviations used. The component surfaces are ordered in terms of their coefficients from most positive to most negative. The most positive coefficients discriminate in a positive direction while highly negative coefficients discriminate in a negative direction for a particular root.

	Root 1		Root 2
MaxC1	1.741958	MrhC1	1.514168
RflC2	0.766145	MaxC1	1.281423
MrhC1	0.729243	SradC1	0.609338
SradC1	0.354639	RflC1	0.145197
MinC2	0.30923	RflC2	-0.10474
ApanC1	0.213596	MinC2	-0.13692
RflC1	-0.21556	MinC1	-0.42564
MinC1	-2.31641	ApanC1	-0.63044

The results of the DFA for *A. arenaria* (Figure 4-17 and Table 4-4) suggest that temperature is important in separating sites where *A. arenaria* is known to occur from those where it is absent. Root one of Figure 4-17 effectively separates the southern parts of the coast where *A.*

arenaria occurs (see Figure 4-7B) from the more northerly sections of the coast where this species is absent (labelled 'absent east' and 'absent west' in Figure 4-17). As identified in Table 4-4, the main coefficients defining root one are minimum summer temperature component one (minC1, see loadings in Appendix 5) in a negative direction and maximum temperature component one in a positive direction.

On root two maximum temperature and mean relative humidity discriminate presence and absence on the east coast from absence points on the west coast (Figure 4-16 and Table 4-4). Potential evaporation and minimum summer temperature discriminate in a negative direction towards the absence point on the west coast. In terms of axis two, sites with *A. arenaria* present are similar to sites along the east coast where this species is absent on the basis of maximum temperature and mean relative humidity. These two sites are distinct from sites along the west coast.

Discussion

The modelling approach adopted here may be seen as a hybrid between conceptually simple correlative models and more complex mechanistic models. Knowledge of the two species ecophysiology is used to predict their water use, which is then subtracted from rainfall to provide information on the water deficits which might be experienced in different parts of the country and at different times of the year. These physiologically meaningful water deficits can then be compared to the observed distribution and investigated for correlations.

True, unambiguous mechanistic models predicting the distribution of individual species based on their physiology are rare. This is because of the difficulty in describing and defining the ecophysiological response of individual species to a variety of covarying climatic variables. Mechanistic models such as that proposed by Woodward (1987) predicting the distribution of different vegetation types draw on less specific physiological responses at the higher taxa or functional type level, and so are easier to implement and are in many cases more functional.

The deficit surfaces are probably useful summaries of many of the variables listed in Table 4-2. Transpiration is essentially driven by potential evaporation, which is in turn determined by temperature (maximum and minimum) and relative humidity, and less directly by solar

radiation. Transpiration rates are then subtracted from rainfall, thus incorporating this important variable into the deficit surfaces. This approach therefore integrates a number of different environmental variables which may play an important physiological role in limiting plant distribution. This is similar to the moisture index of Box (1981) which is calculated as mean annual precipitation divided by the estimated annual evapotranspiration¹¹ rate and “serves as the best single indicator of the dominant growth forms, general vegetation structure, and the degree of leaf xeromorphy” (Box 1981). Temperature and rainfall are considered by Woodward (1987) to be the most important of the above variables in defining distributions of vegetation types and play an important role in defining the deficits produced in this study.

As mentioned previously, the deficits produced for both species are similar, despite different transpiration rates (compare Figure 2-5 and 2-6), as a result of the different leaf area indices recorded for the two species (Chapter 3) and used in the calculation of these deficits. Examination of the deficit surfaces presented in this study suggest that the South African coastline can be divided into four sub-regions. These include the east coast, south to Algoa Bay with high water surpluses in summer and slightly negative winter deficits; the south coast (Algoa Bay to Cape Agulhas) with low surpluses present throughout much of the year; the south-west coast (Cape Agulhas to Cape Columbine) with negative summer deficits and winter water surpluses; and the west coast (north of Cape Columbine) with high negative deficits throughout the year.

It is clear that rainfall plays an important role in defining these deficits. Temperature may also be important in driving transpiration rates but this may be a more constant variable. For example, if water is not limiting, transpiration rates may be higher in canopies with low LAI due to these canopies being well ventilated as discussed in Chapter 2. Where canopies have a higher LAI, the increased boundary layers of such canopies reduce the effective transpiration rates. As a result, transpiration rates may be relatively constant while rainfall plays an important role in defining the water deficit. Deficits produced in this work show similar general trends in southern Africa to the moisture index presented by Box (1981)

¹¹ Box (1981) estimated evapotranspiration from monthly mean air temperature.

Distribution data for *A. arenaria* are comprehensive and show that this species has a relatively limited distribution in South Africa. For example, of the approximately 1600 pixels on the climatic surfaces that may be considered coastal, only 115 are pixels in which *A. arenaria* are confirmed to occur (less than seven percent of the coastline). Hertling (1997) suggests that *A. arenaria* is confined to the original planting sites and has not spread much since first planted in the 1870s (Hertling & Lubke 1999). Observations of the limited distribution of this plant, which in many cases is limited to the original stabilisation sites, suggests the climate may be partially unsuitable. Additional observations that this species grows well when irrigated (Hertling 1997, pers. obs.), for example at Bloubergstrand near Cape Town, suggest that water may be an important factor in limiting the distribution of *A. arenaria*, although experimental evidence is required in this regard.

Hertling & Lubke (1999) compare the climate (in terms of mean annual temperature and mean annual precipitation) at sites in South Africa where *A. arenaria* grows, as well as coastal centres in Europe near which *A. arenaria* grows. These authors suggest the European sites have colder, more humid climates than those in South Africa and this may explain the poor performance of *A. arenaria* in South Africa.

The situation is more complex than suggested by Hertling & Lubke (1999). The subspecies of *A. arenaria* growing in South Africa is *A. a. arundinacea* (pers. obs.), the distribution of which is restricted to the Spanish, Portuguese and Mediterranean coastlines (see Chapter 1). The climate along these coasts (from Table 2 of Hertling & Lubke 1999) is more comparable to those in South Africa, although there is a discrepancy in that temperatures are slightly lower and rainfall higher on average. While the climatic tolerances of these two subspecies are unknown, their distributions probably do correspond with two sets of climatic variables in their natural range. Subspecies *A.a. arenaria* can be considered to be the subspecies from cooler, wetter areas while *A.a arundinacea* occurs in the warmer, slightly drier areas of southern Europe and the Mediterranean (see Chapter 1 for a description of the subspecies distributions). These observations might explain early failure to introduce *A. arenaria* plants to South Africa from Britain. It was only with the collection of French seed, presumably from southern France, that plants (of *A.a arundinacea*) were successfully introduced to South Africa (Hertling 1997).

Much of this speculation remains unresolved and requires detailed investigation into the climatic tolerance of these two subspecies (descriptions of the climate of areas in which these two sub-species are found) as well as their phenology in relation to climate. It does however suggest that the climate in South Africa may be marginal for the growth of *A. arenaria*.

Shoot growth and flowering time for *A. arenaria* in Europe and North America is generally given as between April and September (Britton & Brown 1896, Huiskes 1979), corresponding with the boreal summer. No studies have been conducted in South Africa which document the growth and flowering times (Hertling 1997 does not provide timing of flowering and growth in South Africa) of *A. arenaria*. D. Van Eeden (pers. com.) uses this species for stabilisation purposes on the West Coast of South Africa in the vicinity of Langebaan. He has noted that the growth commences in May, depending on rainfall, while limited flowering occurs in early spring. This corresponds with September to November flowering times for plants growing on the south-east and south coasts (pers. obs.). Together this suggests that in South Africa the growing season and flowering occurs during the austral winter and spring months.

These growth and flowering times correspond with periods shown to have water surpluses, primarily in winter (Figure 4-13). This suggests that these plants may be limited to areas which have sufficient rainfall corresponding with relatively cool conditions which may approximate the natural range of these plants. The fact that this period of cool, wet conditions occurs in winter when, solar radiation is low and the days are relatively short may account for *A. arenaria* being relatively unsuccessful in South Africa.

Modelling the distribution of organisms correlatively relies on the assumption that the present distribution of the organism in question is in equilibrium with those environmental or climatic variables to which correlation has been demonstrated. This assumption may be violated by invasive organisms which are still expanding within the range of potential climate tolerance of the host area (Beerling *et al.* 1995). *A. arenaria* plants in South Africa have been artificially planted and, in a number of cases, are irrigated. This species may be considered to have been forced into marginal areas which may be climatically unsuitable to support it. These factors may also complicate distribution modelling of invasive (or exotic) species.

S. plumieri, on the other hand, has spread naturally to its current distribution along the east and south coasts of South Africa. This species may therefore be in equilibrium with its environment and, compared to *A. arenaria*, potentially provides a clearer picture of the relationship between distribution and climate at the species level.

The extensive distribution data collected in this study show that this species is abundant along the east and south-east coasts where it is perhaps the most important sand dune pioneer (pers. obs.). Along the southern coast of South Africa the distribution of this species becomes increasingly patchy moving from east to west, and species such as *Tetragonia decumbens* and *Thinopyrum distichum* become increasingly important pioneers along this coast. These observations point to an increasingly unsuitable climate for *S. plumieri* in the south-west of the country.

Evidence presented in Chapter 2 suggests that these plants are light-limited and might therefore be dependant on high summer solar radiation levels for maximum assimilation. During the winter solstice at the Old Woman's River study site the sun is only in the sky for 70% of the time that it is above the horizon at the summer solstice (data not shown). The intensity of the solar radiation is also lower (Schulze *et al.* 1997).

High assimilation rates may be required for growth and reproductive efforts during summer. Additional assimilates, for example, may be required to produce the numerous large drupes of these plant. As discussed in Chapter 2, this species has high transpiration rates which may be a result of maximising assimilation. For this reason, positive water deficits may be required during summer when these plants are reproducing and have maximum growth rates. If water is limiting during summer the plants may need to close their stomata so as to conserve water and, as a result, assimilation under such conditions might be reduced. In turn, growth and reproductive efforts might be reduced.

Steinke & Lambert (1983), working at Durban beaches, and Pammenter (1983), working on sand dunes at Mtunzini, show that leaf production is increased during the summer months. During the drier winter months, the rate of leaf abscission increases and in some months may

exceed leaf appearance. Leaf longevity is also considerably higher in winter compared to summer. Pammenter (1983) recorded leaf production of up to 6.4 leaves per month in summer, decreasing to 2.4 leaves per month in winter at Mtunzini. Further south at Durban, Steinke & Lambert (1983) recorded leaf production rates of 3.8 and 1.8 leaves per month in summer and winter respectively. At the Old Woman's River study site in the south-east, B.S. Ripley (unpublished data) recorded more or less constant leaf production of 2.1 leaves per month throughout the year. Steinke & Lambert (1983) recorded longevity of leaves in the region of 190 days in winter compared to 120 days in summer, while Harte and Pammenter (1985) noted values of 210 days and 140 days, suggesting that growth rates are depressed during winter periods and the plants retain their leaves for longer periods.

These monthly leaf production data were extracted from these three separate studies and compared to monthly water deficits as were produced in this work (Figure 4-18, see also the monthly deficit graphs for Mtunzini, Durban and Old Woman's River in Figure 4-11). This figure suggests that as water availability increases, there is a corresponding increase in leaf production. At Mtunzini, where water surpluses are the highest, leaf production rates are highest. Further south at Durban surpluses are slightly lower and corresponding to this is slightly lower leaf production rates. In winter at both sites the surpluses are much lower or even negative and concomitant production of leaves is much reduced. These lower winter leaf production rates in the north are within the range of leaf production throughout the year at Old Woman's River. At Old Woman's River year-round water surpluses are low, resulting in a more constant production of leaves by *S. plumieri* at this site.

It should be noted that these monthly leaf production measurements were collected in specific years by different researchers and are a result of the particular environmental 'regime' experienced in that year. The monthly deficit values, on the other hand, are calculated from long-term averages of temperature, relative humidity and rainfall and so are only approximates of the conditions experienced by the plants in a particular year. It is likely that this relationship would improve if deficits were calculated for the relevant year in which each of these leaf production data-sets were collected.

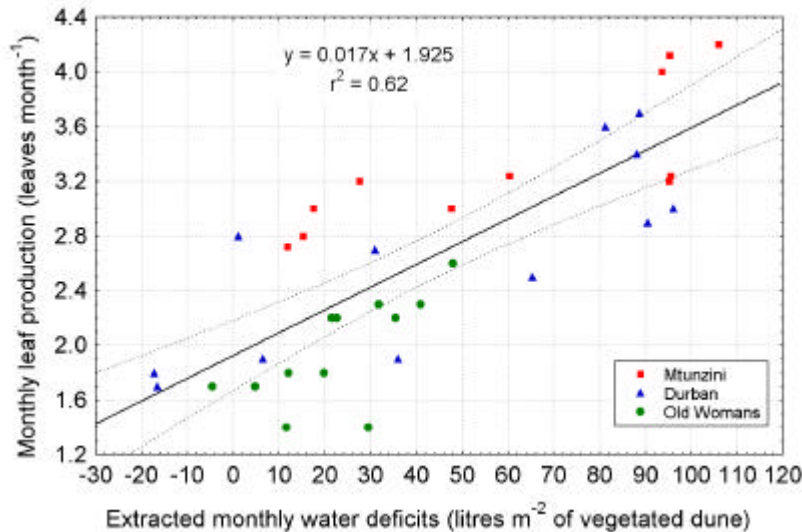


Figure 4-18: Monthly leaf production rates compared to monthly water deficits as determined at three separate sites along the east coast of South Africa. Monthly leaf production rates determined by Pammenter (1983) for plants growing at Mtunzini, by Steinke & Lambert (1983) for plants growing near Durban, and Ripley (unpublished data) for plants growing at Old Woman's River ($n=36$, $r^2=0.62$, $p=0.0000$)

Therefore, positive water balance in summer months which correspond to the active growing season might be important mechanistically in defining the distributions of *S. plumieri*. However, while light may be important in driving the mechanism proposed above, it is less important in defining the distribution of *S. plumieri* as is indicated by the relatively low importance of solar radiation in the discriminant function analysis.

For both species therefore, surpluses of water are most closely correlated with distributions in those months when the plants are thought to be more actively growing or reproducing, although phenological data of growth periods and flowering times for both species in South Africa are limited. In the case of *S. plumieri*, water surpluses correlate with the majority of the distribution points along the east and southern coasts of South Africa in the summer months. For *A. arenaria* the positive correlation of distribution to water surpluses is most distinct in the winter.

The nature of the coastline along the south-west sections of the coast also complicates interpretations of the relationship between distribution and climate as many stretches of this coast are steep and rocky. Sandy beaches are present along this coast (as evident by the

occurrence of *A. arenaria*), but these are more isolated and confined to bays and short sections of the coast.

Coastal pioneer plants are confined to the coastal belt by any one of a number of factors. This study therefore assumes that numerous factors such as the requirement for shifting sand, coarse well-drained substrate, reduced competition through tolerance to salt, and so forth, limit these two species to a narrow strip along the coast which is only a few hundred metres wide at most. Higher resolution studies will be required to elucidate the intricate relationships which confine obligate strand species to the young mobile sand dunes. Preliminary investigations by Lubke & Avis (1988) along the south-east coast, and Donnelly & Pammenter (1983) on the east coast of South Africa, describe the succession from pioneer dunes to climax vegetation in terms of the strong salinity gradient.

In terms of detailed physiological responses of strand plants to these various gradients, little is known about what limits species to the narrow band between the high water mark and the more stable vegetated dunes inland. It is likely that competition plays an important role in limiting different species to different zones in a succession sequence such as the zones proposed by Doing (1985).

Covarying climatic variables make it difficult to identify specific factors limiting the distribution of an organism in terms of correlative models (Beerling *et al.* 1995). These authors identified three climatic variables *a priori* for use in their study, whose mechanistic role in determining species distributions is physiologically understood, to an extent, after the work of Woodward (1987).

The explicit aim of the DFA in this study was to identify climatic variables which may be important in limiting the distribution of both species based on the difference of the climate at sites where the plants of one species are present and sites where the species is absent. As a result, no weighting of any variables was introduced for use in this study and the DFA was used to rank the variables according to their importance with regard to the role each variable plays in defining the distribution of the two species. While this may not resolve possible covarying

variables, it is probably more favourable to use all the variables available than to select a few which are perceived to be important for a particular organism.

As mentioned above, these variables, which are important in defining the distribution of the plants, are probably well summarised by the deficit surfaces. Based on the importance of rainfall in defining the deficit surfaces, this variable (rainfall) is perhaps important in defining the distribution of both species, particularly when considered in terms of growth and flowering seasons. The variables identified by the DFA as being important in limiting *S. plumieri*'s distribution include maximum temperature and potential evaporation (on both roots discriminating between presence and absence on the south-west and west coasts Figure 4-16), with rainfall and solar radiation contributing to a lesser extent. Temperature (minimum and maximum) contributes strongly in defining the areas where *A. arenaria* is present from those area where it is absent and supports the observations of Hertling & Lubke (1999) to some extent.

These results are preliminary and further ecophysiological work is required to better understand the potential role these variables may play in limiting the distribution of these two species.

Chapter 5

Conclusion and further studies

This work shows that at the leaf level, relatively accurate predictions of transpiration rates are possible for both *S. plumieri* and *A. arenaria*. These predictions are based on empirical relationships of transpiration rates to atmospheric vapour pressure deficits established independently for each species.

Transpiration rates were measured in the field using an LCA2 IRGA. This instrument uses dry air to calculate transpiration rates, which results in overestimates of these transpiration measurements. By comparing transpiration rates measured using the LCA2 with transpiration rates measured gravimetrically, it is possible to quantify the introduced error. This knowledge was used to recalibrate the data collected with LCA2 to provide more accurate measurements of transpiration rates.

Ambient temperature and relative humidity data were collected at the same time as specific transpiration measurements and used to calculate atmospheric VPD. Strong correlations of transpiration rates to atmospheric VPD in both species form the basis of correlation models for predicting the transpiration rates of individual leaves of both species from inputs of ambient temperature and relative humidity. As noted in Chapter 2, leaf-to-air VPD was not used to predict transpiration rates as there is no way to accurately estimate the leaf temperatures of these two species, therefore, predictions based on leaf-to-air VPD are not practical.

These predictive models are based on the understanding that the gradient of water vapour from the leaf airspaces to the bulk atmosphere drives transpiration. This approach may therefore be considered a phenomenological model as defined by Reynolds *et al.* (1993). Possible reasons for the strong correlation of E to VPD in both *S. plumieri* and *A. arenaria* are discussed:

The response of increased transpiration rates to increased VPD in *S. plumieri* is suggested to possibly be in response to light. Solar irradiance covaries with atmospheric VPD and in fact probably contributes significantly to determine VPD through its effects on both ambient temperature and humidity (Figure 2-8). In *S. plumieri*, assimilation is apparently unsaturated at midday solar irradiances, this has also been noted by Pammenter & Smith (unpublished manuscript). As assimilation increases with increased light, C_i concentrations are reduced. To avoid limiting assimilation through lack of substrate, the stomata open to restore C_i concentrations and, as a result, transpiration rates are increased with increased irradiance (Figure 2-12). If this speculation is accurate it suggests that water is readily available to these plants which can be considered quite wasteful in terms of their water use. This is supported by the fact that midday water potentials measured for this species are not particularly negative

In the case of *A. arenaria*, E responds linearly to increased atmospheric VPD at low VPDs. However, as VPD increases above 2.0 kPa, transpiration rates saturate and decline. This decline is linked to decreased leaf conductances at higher VPDs. This suggests that in the case of *A. arenaria* water becomes increasingly difficult to acquire as the day progresses. As noted by Huiskes (1979) this species has shallow adventitious root systems which may result in water acquisition being limited compared to the deep rooted *S. plumieri*. This speculation is supported by the compound sand water calculations (Chapter 3, Figure 3-8).

In Chapter 3, scaling of leaf level transpiration rates to the canopy leaf area is shown to be possible by direct extrapolation. This is more valid in the case of *S. plumieri* which has an open well-ventilated canopy. As a result, both the leaf and the canopy are probably coupled to the environment and transpiration is closely related to ambient 'evaporation environment.' In the case of *A. arenaria*, the large leaf and canopy boundary layer which are thought to be present, are likely to thwart the relatively simple extrapolation scaling approach presented here. However, no estimates of canopy or leaf boundary layers are available so this potential error is accepted. Future work which includes measures of either leaf or canopy boundary layers (or both) may improve the predictions of transpiration rates by incorporating inputs of wind speed for example.

Despite the potential error inherent in these calculations, they are probably more realistic than a number of other studies which have attempted to calculate the water requirements of sand

dune species (e.g. Salisbury 1952 & Pammenter 1983). This is because transpiration rates have been determined accurately, being hourly estimates and not averages or maximum values.

Water use by a square meter of sand dune covered with *S. plumieri* is likely to be less than is available through rainfall. However, the calculations presented in Chapter 3 (Figures 3-8 A and 3-8 B) are necessarily primitive as little information is available about the field capacity of dune sands, the movement of water through the sand column and interactions between water in the sand column and the 'store' of water in the dune aquifer. It is likely that excess water entering the sand column via rainfall seeps into the dune aquifer relatively quickly and therefore the rain may not elevate sand water concentration to the extent shown (Figure 3-8). These calculations also show the importance of an even temporal distribution of rainfall. Low, evenly spaced rainfall can perhaps support the plants better than high rainfall confined to a short period of the year. This is a result of the relatively low field capacity of beach sand. Also lacking is detailed information about the volume of sand the roots of these two species occupy which would allow for more accurate calculations than those presented in Chapter 3.

It would be ideal to investigate compound sand water at the regional scale using a GIS. However, such calculations take into account the detailed temporal distribution of rainfall and would require very large data sets which includes either daily or weekly surfaces of temperature, relative humidity and rainfall which would be specific to a particular year. The production of such surfaces is not feasible at this stage. While such high resolution investigations are not possible at a regional scale, it is possible to investigate the balance of water use and water availability on a monthly basis at the scale of the entire country (Chapter 4).

Using the leaf level models produced in Chapter 2 and validated at the larger canopy scale in Chapter 3, transpiration rates were calculated on a monthly basis from input surfaces of monthly mean temperature and relative humidity in a GIS. These transpiration surfaces express transpiration in terms of litres of water transpired per square metre of sand dune covered by either *S. plumieri* or *A. arenaria*. These transpiration rates were subtracted from surfaces of monthly median rainfall which is the input of water to the system. The result of these calculations are monthly surfaces of water deficit where transpirational water loss

exceeds water input on a square metre basis. Alternatively rainfall may exceed transpirational water use resulting in water surpluses.

Areas with water surpluses correlate well with the detailed distributions of both species, primarily in the months when the plants are most actively growing and reproducing. In the case of *S. plumieri*, correlations of distribution to positive water balance are strongest in summer when the plants are shown to be actively growing and reproducing. The importance of water surpluses in summer is explained in terms of the reliance of these plants on high light conditions to maximise assimilation rates (Chapter 2). In the case of *A. arenaria*, water surpluses correlate well with the distribution of this species in the winter month. This suggests that these plants are restricted to relatively cool and moist areas which may approximate the climate of the species natural range. The fact that *A. arenaria* grows and reproduces during the summer in its natural range, but shifts to a winter growth season in South Africa, also suggests that this climate may be marginal.

A number of problems were experienced while working with the GIS in Chapter 4. At the scale used in this study, the coastal sand dune ecosystem may be regarded as a discontinuous linear feature. These systems form a narrow band between the sea and the more diverse 'mature' vegetation inland. The reason for the sand dune species being restricted to such a narrow zone are complex and require studies of far higher resolution to help elucidate factors limiting the inland spread of the plants. A number of studies have investigated the zonation of dune plants and the role of various environmental variables in limiting dune plants to this narrow band. Lubke & Avis (1988) describe a successional sequence on Eastern Cape sand dunes. They suggest that moisture and salinity gradients interact in a complex manner with wind direction to drive succession. These factors may therefore contribute to the zonation of the dune plants. Donnelly & Pammenter (1983) show more directly that aerial salt spray and short term wind blown sand, both of which damage the plants mechanically, may be important in limiting the seaward spread of secondary dune plants. These authors speculate that pioneer species which can tolerate such conditions are out competed in the more sheltered parts of the dune systems where the secondary species are more prolific.

As noted in this chapter, the pixels of the various surfaces used in this study end short of the coastline thus complicating the investigation of these systems. Ideally these linear features

require a novel GIS analysis approach with variables that change continuously along the coastline being represented by a line in a vector system but with the analytical power of a raster system. Perhaps a short term solution would be to produce a high resolution raster representation of the coastline which can be analysed with a conventional raster GIS system.

High resolution, accurate distribution data are lacking for most species growing in this country. In this study, only very limited use could be made of the distribution data recorded on herbarium specimens at three of the more important national herbaria. Even economically important invasive alien plants have relatively poor distribution databases (M.P. Robertson pers. com.). The importance of locality data which include degrees, minutes and seconds should be stressed to all who collect specimens for herbaria, as this ensures the usefulness of these specimens in future mapping and modelling exercises at all resolutions.

Classification of the Southern African coastline

Lubke *et al.* (1997) classified the coast into a number of regions based on various criteria which may have included climate, attributes of the physical nature of the coast, the different biomes along the coastline, species distributions and political boundaries. The exact criteria and methods used by these authors are not explained but are related to Tinley (1985). Based on the deficits presented here, which help develop ideas about the general climate of coastal areas and how this may impact the biota of these regions, the scheme of Lubke *et al.* (1997) might be modified as follows:

Much of the east coast is homogeneous as far south as Algoa Bay (see Frontispiece Map 1), with water surpluses on a yearly basis (Figures 4-10 and 4-14) being a result of the warm, humid conditions and higher rainfall concentrated in summer. Parts of the southern region of this section of the coast are physically distinct, with small isolated sandy bays scattered along the predominantly rocky coast of the Transkei and southern KwaZulu-Natal (Tinley 1985, pers. obs.). This subsection of the east coast corresponds to a degree with the Transkei coast of Lubke *et al.* (1997), but is expanded here to include the steeply shelving coast of southern KwaZulu-Natal.

The south-east coast of Lubke *et al.* (1997) may be distinct as a transition zone between the subtropical, moist east coast and the warm, temperate south coast. However, in terms of the water balances presented here, as well as climate and possibly vegetation (pers. obs.), the majority of this section can be included in a larger east coast category. Algoa Bay has very low rainfall and, as a result, has mostly negative deficits. While this may not be an important barrier to the movement of species along the coast, it does provide a clear division between the warmer summer rainfall areas to the east and the cooler year-round rainfall areas of the southern coast.

The south coast can be defined as extending from Algoa Bay to between Cape Infanta and Cape Agulhas. This includes the regions of year-round rainfall along the southern parts of the country. This stretch can be further separated into two subsections, the wetter eastern section from Algoa bay to Wilderness, as well as the drier parts from Wilderness to Cape Infanta/Cape Agulhas. The boundary in the west is necessarily indistinct between Cape Infanta and Cape Agulhas as along this coast the climate changes from that with year-round rainfall to one with predominantly winter rainfall along the south-west.

The south-west coast then extends from this boundary (between Cape Infanta and Cape Agulhas) to Cape Columbine, north of the Langebaan Lagoon. This coast is characterised by high winter rainfall and has large water surpluses in winter as a result. Lubke *et al.* (1997) include areas as far north as the Olifants river. However, Cape Columbine is defined as the northern limit here, as the deficits in all cases (summer, winter and annual, Figures 4-8 to 4-15) show that deficits north of Cape Columbine become extremely negative. This relates to the high temperatures and solar radiation, low relative humidities and low rainfall that characterise the west coast (Schulze *et al.* 1997).

This scheme corresponds more closely with that of Tinley (1985) than of Lubke *et al.* (1997) and might be improved by considering additional factors such as the physical nature of the coastline as well as the nature of the coastal vegetation. Tinley (1985), for example, used physical and climatic factors to distinguish between different regions of the coast and such characteristics might contribute to 'fine-tuning' the scheme proposed here. Data presented here suggest that these categories may not be arbitrary and it will be interesting to investigate

how the strand vegetation changes around the coast in response to these different physical and climatic zones.

Further studies

- Quantifying the role of boundary layers in both species, particularly *A. arenaria* at both the leaf and canopy level, is desirable for more accurate predictions of transpiration. This is because boundary layers are perceived to be important in the dense canopy of *A. arenaria*. The incorporation of such terms may enable more accurate predictions of transpiration rates of this species to be made, by for example, adding input data of wind velocity.
- Little is known about our coastal dune aquifer system and the interaction between the water these aquifers contain and the biota that are thought to be dependant on this water source (Campbell *et al.*1992). The investigation of coastal aquifers has practical applications as this water is tapped by humans and also may support the vegetation that contributes to stabilising otherwise mobile dunes. Such baseline investigations may be essential for the wise and long-term use of this resource by humans if damage to the dune ecosystem is to be avoided.

There are also a number of theoretical questions which remain unanswered with regard to coastal aquifers. Importantly, there is little information about the interaction and transport of water from the dune aquifer to the sand column and vice versa. Such investigation may help resolve the question as to what is the source of the water in dune sands as investigated by other workers (Olsson-Seffer 1909a, Salisbury 1952, De Jong 1979).

- The compound sand water volumes presented in Chapter 3 are inaccurate due to limited knowledge about many aspects of the water within dune sands. Specifically, the field capacity of these sands and the mechanisms which operate to maintain relatively constant sand water percentages. In addition the volume of sand occupied by the roots of South African dune plants, and dune plants in general, is in most cases unknown.

- More detailed investigations into the relationship between growth and reproduction, and the water surpluses as identified in Chapter 4 may help explain the observed distribution of both species. Detailed information of the growth rates and phenology of *A. arenaria* in South Africa are lacking.
- This study suggests that the South African climate may be sub-optimal for *A. arenaria*. The entire southern coast of this country may be considered marginal based on the relatively poor performance of this species. However, it is not possible to resolve this question satisfactorily based on the available information. While Hertling & Lubke (1999) note that the South African climate is possibly warmer and drier than the climate of *A. arenaria*'s natural range, their investigation does not consider the complicating factors introduced when considering the two separate subspecies. Ideally the ecophysiological tolerances of the two subspecies need to be quantified, and this information coupled with investigations as to what subspecies is present may help resolve this question. Such detailed investigation will probably not be conducted soon. An alternative approach would be to document the bioclimatic envelope of both subspecies natural range and compare this bioclimatic envelope to the environmental variables of the present distribution of *A. arenaria* in South Africa.
- Useful insight is probably available from investigations into the bioclimatic tolerance of *A. arenaria* in north America where there is a large change in latitude along the coast. As a result, the climate along the coast is more variable, changing from the warm dry regions in the south which marks the southern limit of the plants to the cool moist northern parts of the coast where the plants grow very well.
- The investigation of broader species assemblages on fore-dunes along the coast and may provide more rigorous classifications of the different regions of the South African coast. Such a study will test the accuracy of the scheme purposed above to classify the South African coast in terms of biologically important climatic variables.

Appendices

Appendix 1: Abbreviations and Units

<i>a</i>	Leaf area or leaf areas of individual shoots	NU	Natal Herbarium
ADC	Analytical Development Corporation	OWR	Old Woman's River
C1	Component one	p	Statistical significance
C2	Component two	PAR	Photosynthetically Active Radiation
C ₃	Photosynthesis with an intermediate three carbon compound	PCA	Principle Component Analysis
C ₄	Photosynthesis with an intermediate four carbon compound	PRE	Pretoria Herbarium
CAM	Crassulacean Acid Metabolism	PLC	Parkinson's Leaf Chamber
C _i	Internal CO ₂ concentration	ppm	Parts per million
CO ₂	Carbon dioxide	r _a	Atmospheric resistance to water vapour conduction
cm	Centimetres	RH	Relative Humidity
DFA	Discriminant Function Analysis	RH _a	Ambient relative humidity
DL-2	Data logger for the LCA2	RH _{ave}	Average relative humidity
<i>e</i>	Vapour pressure at a particular temperature	r _l	Leaf resistance to water vapour conduction
E	Transpiration rate	r ²	The amount of variation common to two variables
g	Grams	<i>s</i>	Canopy leaf surface area
<i>G</i>	Ground area	s	Seconds
GIS	Geographical Information System	S	Standard deviation
GPS	Global Positioning System	SA	Selective Availability
GRA	Schönland Herbarium, Grahamstown	SAWB	South African Weather Bureau
IRGA	Infrared Gas Analyser	SSE	Sum of squares for error
kg	Kilograms	SVP	Saturation Vapour Pressure
km	Kilometres	<i>t</i>	Time
kPa	Kilopascals	T	Temperature
l	Litres	T _a	Ambient temperature
LAI	Leaf Area Index	T _{ave}	Average temperature
LCA2	Leaf Chamber Analyser 2	T _l	Leaf temperature
m	Metres	T _{max}	Maximum temperature
MFC	Mass Flow Controller	T _{min}	Minimum temperature
MJ	Megajoules	VPD	Vapour Pressure Deficit (primarily atmospheric VPD)
ml	Millilitres	W	Watts
mm	Millimetres	WGS84	World Geodetic System 84
mmol	Millimoles	\bar{x}	Mean
mol	Moles	μmol	Micromoles
MPa	Megapascals		
n	Number or sample size		

Appendix 2: Coastal sand dune species distributions

Table A-2A: List of species found in the pioneer strand zone (Zone 1 of Tinley 1985) around the South African coast as compiled by Tinley (1985). Names have been checked and modified according to Arnold & de Wet (1993). Distributions are those given by Tinley (1985): M = south Mozambique, T = Tongaland, N = Natal (and north Transkei), E = former east Cape (and southern Transkei), S = south coast, C = south west coast, W = west coast. Asterisks mark the most important pioneer species in the strand zone.

	←	M	T	N	E	S	C	W	→
<i>Aizoon rigidum</i> L. f.					6	6	6	6	6
* <i>Thinopyrum distichum</i> (Thunb.) Loeve					6	6	6	6	6
* <i>Arctotheca populifolia</i> (Berg.) T. Norl.			6	6	6	6	6	6	6
* <i>Canavalia maritima</i> (Aubl.) Thouars	6	6	6	6					
<i>Carpobrotus acinaciformis</i> (L.) L. Bol.						6	6	6	
<i>Carpobrotus dimidiatus</i> (Haw) L. Bol.	6	6	6	6	6				
<i>Carpobrotus edulis</i> (L.) L. Bol.						6	6	6	6
<i>Chenopodium</i> sp			6	6	6	6	6	6	6
* <i>Cyperus crassipes</i> Vahl	6	6	6	6	6	6	6		
<i>Dactyloctenium australe</i> Steud.	6	6	6	6					
* <i>Cladoraphis cyperoides</i> (thunb.) S.M. Phillips								6	6
<i>Eragrostis sabulosa</i> (Steud) Schweick.						6	6	6	6
<i>Gazania rigens</i> (L.) Gaertn.	6	6	6	6	6	6	6		
* <i>Halopyrum mucronatum</i>	6								
* <i>Hebenstretia cordata</i> L.						6	6	6	6
<i>Dasispermum suffruticosa</i> (Berg.) B.L. Burt			6	6	6	6	6	6	
* <i>Phylohydrax carnosa</i> (Hochst.) Puff		6	6	6	6	6	6		
* <i>Ipomea pes-caprae</i> (L.) R. Br.	6	6	6	6	6	6			
subsp <i>brasiliensis</i> (L.) Van Ooststr.									
<i>Ipomea stolonifera</i>	6								
* <i>Launaea surmentosa</i> (Wild.) Sch. Bip. Ex Kuntze	6	6	6	6					
Mesem creeper (AIZOACEAE)							6	6	6
<i>Osteospermum fruticosum</i> (L.) T. Norl.			6	6	6	6	6	6	6
<i>Paspalum vaginatum</i> Swartz.	6	6	6	6	6	6	6	6	
<i>Polygonum maritimum</i> L.				6	6	6	6	6	6
<i>Psoralea repens</i> L.					6	6	6		
<i>Pteronia onobromoides</i> DC.								6	6
<i>Salsola kali</i> L.				6	6	6	6	6	6
* <i>Scaevola plumieri</i> (L.) Vahl	6	6	6	6	6	6			
<i>Senecio elegans</i> L.				6	6	6	6	6	
* <i>Sporobolus virginicus</i> (L.) Kunth	6	6	6	6	6	6	6	6	6
<i>Stemotaphrum secundatum</i> (Walt.) Kuntze	6	6	6	6	6	6	6	6	
<i>Silene primuliflora</i> Eckl. & Zeyh.				6	6	6	6	6	6
<i>Tephrosia purpurea</i> (L.) Pers.	6	6	6						

* *Tetragonia decumbens* Mill.

6 6 6 6 6 6

Table A-2B: List of species found in the shrub zone (Zone 2 of Tinley 1985) around the South African coast as compiled by Tinley (1985). Names have been checked and modified according to Arnold & de Wet (1993). Distributions are those given by Tinley (1985): M = south Mozambique, T = Tongaland, N = Natal (and north Transkei), E = former east Cape (and southern Transkei), S = south coast, C = south west coast, W = west coast.

	←	M	T	N	E	S	C	W	→
<i>Ammophila arenaria</i> (L.) Link						6	6		
<i>Anthospermum littoreum</i> L. Bol.			6	6	6	6			
<i>Aster</i> sp.								6	6
<i>Asparagus capensis</i> (L.) Oberm.					6	6	6	6	
<i>Asystasia gangetica</i> (L.) T. Anders.	6	6	6	6					
<i>Spermacoce</i> sp.	6	6							
<i>Chironia loaccifera</i> L.			6	6	6	6	6		
<i>Chrysanthemoides monolifera</i> (L.) T. Norl.	6	6	6	6	6	6	6	6	
<i>Cleome stricta</i>	6	6							
<i>Cynanchum</i> sp.		6	6	6	6	6	6		
<i>Cynodon dactylon</i> (L.) Pers.		6	6	6	6	6	6	6	
<i>Didelta carnososa</i> (L.f.) Ait.								6	6
<i>Ehrharta villosa</i> Schult. f.					6	6	6		
<i>Felicia aphylla</i>						6	6		
<i>Felicia echinata</i> (Thunb.) Nees						6	6		
<i>Ficinia lateralis</i> (Vahl.) Kunth						6	6		
<i>Gloriosa superba</i> L.		6	6	6	6	6			
<i>Guettarda speciosa</i> L.	6	6							
<i>Helichrysum crispum</i> (L.) D. Don						6	6		
<i>Helichrysum asperum</i> (Thunb) Hilliard & Burtt			6	6	6	6	6		
<i>Helichrysum krausii</i> Sch. Bip.		6	6	6					
<i>Brachycloa shiemaniana</i> (Schweick) S.M. Phillips		6	6						
<i>Imperata cylindrica</i> (L.) Raeuschel		6	6	6	6	6	6		
<i>Indigofera kirkii</i>	6	6							
<i>Indigofera neglecta</i> N.E. Br.		6	6						
<i>Lbebckia cinerea</i> E. Mey.								6	6
<i>Limeum africanum</i> L.						6	6		
<i>Lycium</i> sp.					6	6	6	6	
<i>Mesema</i> (AIZOACEAE)							6	6	
<i>Metalasia muricata</i> (L.) D. Don					6	6	6		
<i>Myrica cordifolia</i> L.					6	6	6		
<i>Myrica guercifolia</i> L.						6	6		
<i>Nylandtia spinosa</i> (L.) Dumort.					6	6	6	6	
<i>Othonna floribunda</i> Schltr.								6	6
<i>Passerina falcifolia</i> C.H. Wr.						6	6		
<i>Passerina glomerata</i> Thunb.						6	6		
<i>Passerina paleacea</i> Wikstr						6	6		

Table A-2B

	←	M	T	N	E	S	C	W	→
<i>Passerina rigida</i> Wikstr			6	6	6	6	6		
<i>Passerina vulgaris</i> Thoday						6	6		
<i>Oncosiphon suffruticosum</i> (L.) Kallersjo								6	6
<i>Phyla nodiflora</i>			6	6	6	6	6		
<i>Phyllica ericoides</i> L.						6	6		
<i>Polygala myrtifolia</i> L.				6	6	6	6		
<i>Otholobium fruticans</i> (L.) C.H. Stirton						6	6		
<i>Ishyrolepis eleocharis</i> (Mast.) Linder						6	6		
<i>Ishyrolepis leptoclados</i> (Mast.) Linder						6	6		
<i>Rhoicissus</i> sp.		6	6	6	6	6			
<i>Salsola</i> sp.								6	6
<i>Scaevola sericea</i> Vahl.	6	6							
<i>Secamone alpini</i> Scultes		6	6	6	6	6			
<i>Senecio elegans</i> L.					6	6	6	6	
<i>Senecio halimifolius</i> L.							6		
<i>Senecio litorosus</i> Fourc.				6	6	6	6		
<i>Senecio maritimus</i> L.						6	6		
<i>Sesuvium portulacastrum</i> (L.) L.		6	6	6	6	6	6	6	
<i>Silene primuliflora</i> Eckl. & Zeyh.					6	6	6		
<i>Stipagrostis zeyheri</i> (Nees) De Winter			6	6	6	6	6		
<i>Stoebe plumosa</i> (L.) Thunb.					6	6	6		
<i>Tetragonia fruticosa</i> L.						6	6	6	
<i>Thesium</i> sp.						6	6		
<i>Trachyandra divaricata</i> (Jacq.) Kunth						6	6	6	
<i>Zygophyllum mogsana</i> L.						6	6	6	

Appendix 3: Macro for calculating water deficit surfaces

This appendix describes a 'macro' which was used in IDRISI for Windows version 2 (Eastman 1997c) to produce surfaces of monthly water deficit from input surfaces of mean monthly temperature, relative humidity and median monthly rainfall.

Only one step is included describing the actions taken to produce one monthly deficit surface. Additional steps for subsequent months are not included to avoid repetition. In this case the 01 used to name some of the surfaces indicates that this is the section of the macro which calculates the deficit for January. This section of the macro was written in Microsoft Excel and then copied so that it repeats twelve times, once for each of the months. Using the find and replace function in a spreadsheet, 01 was changed to 02 and so on for the various months. In addition, the time factor in line 22 (Table A-3) was altered to show the number of seconds in the different months.

SCALAR does scalar arithmetic on images by adding, subtracting, multiplying, dividing or exponentiating the pixels in the input image by a constant value. The scalar command line includes: input image, output image, operation number and scalar value. The operation numbers are: 1 add, 2 subtract, 3 multiply, 4 divide and 5 exponentiate (Eastman 1997a).

OVERLAY produces a new image from the data of two input images. New values result from applying one of the nine possible operations to the two input images, referred to as the first and second images during program operation. The overlay command line includes: operation number, first input image, second input image and output image. The operation numbers are: 1 add, 2 subtract, 3 multiply, 4 divide first image by the second image (Eastman 1997a).

Table A-3: Section of the macro used to produce monthly water deficit for the two species (*S. plumieri* in this case). Only one month is included here. In the full macro

this set of lines is repeated twelve times to produce twelve deficit surfaces for each species.

1	SCALAR	x	T01	ZTdiv1	4	254.4
2	SCALAR	x	blwt01	Z18x	3	18.564
3	OVERLAY	x	2	Z18x	ZTdiv1	Za
4	OVERLAY	x	3	T01	Za	Zta
5	SCALAR	x	T01	Zb	1	255.57
6	OVERLAY	x	4	Zta	Zb	Ztadivb
7	SCALAR	x	Ztadivb	Ztadvb10	4	10
8	SCALAR	x	blwt01	Z6x	3	6.13753
9	OVERLAY	x	6	Z6x	Ztadvb10	Zsvp
10	SCALAR	x	rh01	Zrhdv10 0	4	100
11	OVERLAY	x	3	Zsvp	Zrhdv100	Zsvprh
12	OVERLAY	x	2	Zsvp	Zsvprh	Zvpd
13	OVERLAY	x	3	Zvpd	Zvpd	Zvpdsqr e
14	SCALAR	x	Zvpdsqre	Zvpdsqr4	3	-0.0004
15	SCALAR	x	Zvpd	Zvpd36	3	0.0036
16	OVERLAY	x	1	Zvpdsqr4	Zvpd36	Zvpd1st 2
17	SCALAR	x	Zvpd1st2	Ze	2	0.0007
18	SCALAR	x	Ze	Zex95	3	0.95
19	SCALAR	x	Zex95	Ze9518	3	18
20	SCALAR	x	Ze9518	Ze95181	3	1.00294
21	SCALAR	x	Ze95181	Ze1000	4	1000
22	SCALAR	x	Ze1000	Zelitre1	3	267840 0
23	OVERLAY	x	2	mrfl01	Zelitre1	budg01

Lines 1 to 9 calculate SVP from temperature (T01).

Lines 10 to 12 calculate VPD from SVP and RH_{ave}.

Lines 13 to 17 calculate transpiration rate ($\text{mol m}^{-2} \text{s}^{-1}$) from VPD.

Lines 18 to 22 calculate transpiration in litres per month on a one square metre basis.

Line 23 subtracts transpiration (litre month^{-1}) from rainfall on a per square metre basis.

Intermediate surfaces produced are named descriptively, to represent briefly what each step calculates. The name given to each intermediate surface start with a 'Z' so as to make deletion of unwanted files easy.

Appendix 4: Macro for extracting surface data

The following is part of a macro used for extracting data from various surfaces in IDRISI for Windows version 2 (Eastman 1997c).

Table A-4: Section of a macro written to extract the values of a pixel which corresponds with a point.

1	INITIAL	x	XX01	1	1	0	1	Blwt01
2	POINTRAS	x	station	XX01	1			
3	Extract	x	XX01	YY01	1	1	ZZ01	

Line 1 creates a blank image with the same configuration as the image blwt01, a binary surface which has pixel values of one over the country, and zeros over the sea. Line 2 converts point vector data to a raster pixel. In this conversion an image file (XX01) is updated with vector point values in pixels where points overlap the corresponding pixel of the image. The pixels of this updated image (XX01) are used to extract data from the corresponding pixels of the deficit surface (YY01) to a value file (ZZ01) which is in a text format which can be readily imported to a spread sheet.

These three lines represent the section of the macro used for extracting data from the January deficit surface (01). Other months are appropriately numbered (except for blwt01) for later identification. The input/output images identified in bold are labelled XX, YY or ZZ, which can easily be found and replaced by specific names corresponding with the target surfaces in a spread sheet.

Appendix 5: Component loading of different principle components

The following loadings refer to the contribution each monthly surface makes to the final principle component summarising a particular set of variables. In cases where most of the variability of a set of monthly surfaces is summarised in a single component, all twelve contribute to the production of this single component. However, in the case of monthly minimum temperature and monthly median rainfall, two components are required to adequately summarise the original twelve surfaces. In these cases the first components are strongly defined by the summer surfaces, while the second components are more strongly defined by the winter surfaces.

Table A-5: Contribution of monthly surfaces to the loading of specific components used in the discriminant function analysis (DFA), see table 4-2.

Component:	Apan C1	Max C1	Min C1	Min C2	Mrfl C1	Mrfl C2	Mrh C1	Srad C1
January	0.993	0.996	0.962	-0.266	0.888	-0.430	0.998	0.993
February	0.986	0.996	0.965	-0.249	0.903	-0.400	0.998	0.995
March	0.989	0.998	0.978	-0.199	0.919	-0.314	0.999	0.999
April	0.997	0.999	0.997	-0.060	0.958	-0.078	1.000	0.999
May	0.996	0.998	0.975	0.202	0.724	0.664	0.999	0.995
June	0.987	0.993	0.835	0.539	0.420	0.896	0.996	0.990
July	0.988	0.994	0.812	0.578	0.431	0.893	0.997	0.991
August	0.988	0.996	0.944	0.306	0.522	0.846	0.998	0.995
September	0.992	0.997	0.989	-0.013	0.872	0.318	1.000	0.999
October	0.996	0.998	0.979	-0.179	0.966	-0.167	1.000	0.999
November	0.995	0.998	0.972	-0.229	0.918	-0.352	0.999	0.995
December	0.994	0.996	0.966	-0.254	0.893	-0.413	0.998	0.993

References

- ADC (1985) *Use of the LCA-2 analyser, air supply unit, leaf chamber and data processor for the measurement of CO₂ assimilation and transpiration of single leaves in the field*. The Analytical Development Company Ltd. Hoddeson, England.
- Alpha C.G., Drake D.R. & Goldstein G. (1996) Morphological and physiological responses of *Scaevola sericea* (Goodeniaceae) seedlings to salt spray and substrate salinity. *American Journal of Botany* **83**:86-92.
- Alves I., Perrier A. & Perrier L.S. (1998) Aerodynamic and surface resistances of complete cover crops: How good is the big "Big Leaf"? *Transactions of the American Society of Agricultural Engineers* **41**:345-351.
- Arnold T.H. & de Wet B.C. (1993) *Plants of southern Africa: names and distribution*. National Botanical Institute, Pretoria.
- Avis A.M. (1992) *Coastal dune ecology and management in the Eastern Cape*. Ph D Thesis, Grahamstown: Rhodes University.
- Baker W.L. & Weisberg P.J. (1997) Using GIS to model tree population parameters in the Rocky Mountain National Park forest-tundra ecotone. *Journal of Biogeography* **24**:513-526.
- Ball G.L. (1994) Ecosystem modelling with GIS. *Environmental Management* **18**:345-349.
- Barbour M.G. (1978) Salt spray as a microenvironmental factors in the distribution of beach plants at Point Reyes, California. *Oecologia* **32**:213-224.
- Barbour M.G. (1992) Life at the leading edge; the beach plant syndrome. In: *Coastal plant communities of Latin America* Seeliger U. (ed). Academic Press, London.
- Barbour M.G., De Jong T.M. & Pavlik B.M. (1985) Marine beach and dune plant communities. In: *Physiological Ecology of north American plant communities* Chabot B.F. & Mooney H.A. (eds). Chapman & Hall, London.
- Beadle C.L., Ludlow M.M. & Honeysett J.L. (1993) Water relations. In: *Photosynthesis and production in a changing environment*. Hall D.O., Scurlock J.M.O., Bolhar-Nordenkamp H.R., Leegood R.C. & Long S.P. (eds) Chapman and Hall, London.
- Berling D.J., Huntley B. & Bailey J.P. (1995) Climate and distribution of *Fallopia japonica*: use of an introduced species to test the predictive capacity of response surfaces. *Journal of Vegetation Science* **6**: 269-282.
- Berry J.A. & Raison J.K. (1982) Responses of macrophytes to temperature. In: *Physiological plant ecology I; Responses to the physical environment*. Lange O.L., Nobel P.S., Osmond C.B. & Ziegler H. (eds) **12a**:277-338.
- Bolhar-Nordenkamp H.R. & Draxler G. (1993) Functional leaf anatomy. In: *Photosynthesis and production in a changing environment*. Hall D.O., Scurlock J.M.O., Bolhar-Nordenkamp H.R., Leegood R.C. & Long S.P. (eds) Chapman and Hall, London.

- Box E.O. (1981) *Macroclimate and plant forms: an introduction to predictive modelling in phytogeography*. Tasks for Vegetation Science 1, Leith H. (ed). Dr. W. Junk Publishers, The Hague.
- Britton N.L. & Brown A. (1896) *Illustrated flora of the Northern States, Canada, Volume one*. Charles Scribner's Sons, New York.
- Bunce J.A. (1996) Does transpiration control stomatal responses to water vapour pressure deficit? *Plant, Cell and Environment* **19**:131-135.
- Busby J.R. (1991) BIOCLIM – a bioclimatic analysis and prediction system. *Plant Protection Quarterly* **6**:8-9.
- Caldwell M.M., White R.S., Moore R.T. & Camp L.B. (1977) Carbon balance, productivity and water use of cold-winter desert shrub communities dominated by C₃ and C₄ species. *Oecologia* **29**:275-300.
- Campbell E.E., Parker-Nance T. & Bate G.C. (1992) A compilation of information on the magnitude, nature and importance of coastal aquifers in Southern Africa. *Water Research Commission report no. 370/1/92*.
- Carpenter G., Gillison A.N. & Winter J. (1993) DOMAIN: a flexible modelling procedure for mapping potential distribution of plants and animals. *Biodiversity and Conservation* **2**:667-680.
- Claus S., Wernecke P., Pigla U. & Dubsy G. (1995) A dynamic model describing leaf temperature and transpiration of wheat plants. *Ecological Modelling* **81**:31-40.
- Davis Instruments Corporation (1994) *Weatherlink version 3.01*. Davis Instruments Corporation, Hayward, California.
- De Jong T.M. (1979) Water and salinity relations of Californian beach species. *Journal of Ecology* **67**:647-663.
- De Pury D.G.G. & Farquhar G.D. (1997) Simple scaling of photosynthesis from leaves to canopies without the error of big-leaf models. *Plant, Cell and Environment* **20**:537-557.
- Department of Water Affairs and Forestry - DWAF - (1997) *White Paper on a National Water Policy for South Africa*.
- Doing H. (1985) Coastal fore-dune zonation and succession in various parts of the world. *Vegetatio* **61**:65-75.
- Donnelly F.A. & Pammenter N.W. (1983) Vegetation zonation on a Natal coastal sand-dune system in relation to salt spray and soil salinity. *South African Journal of Botany* **2**:46-51.
- Drake B.G., Raschke K. & Salisbury F.B. (1970) Temperature and transpiration resistances of *Xanthium* leaves as affected by air temperature, humidity, and wind speed. *Plant Physiology* **46**:324-330.
- Dyer R.A. (1967) *The genera of Southern African flowering plants, volume 1, dicotyledons*. Department of Agriculture and Technical Services.
- Eastman J.R. (1997a) *IDRISI for Windows version 2; Users Guide*. Clark Labs, Clark University, Worcester. WEB: <http://www.clarklabs.org>
- Eastman J.R. (1997b) *IDRISI for Windows version 2; Tutorial exercises*. Clark Labs, Clark University, Worcester. WEB: <http://www.clarklabs.org>

- Eastman J.R. (1997c) *IDIRISI for Windows version 2*. Clark Labs, Clark University, Worcester. WEB: <http://www.clarklabs.org>
- Elston D.A. & Buckland S.T. (1993) Statistical modelling of regional GIS data: an overview. *Ecological Modelling* **67**:81-102.
- Esau K. (1977) *Anatomy of seed plants*. John Wiley and Sons, New York.
- Espejel I. (1987) A phytogeographical analysis of coastal vegetation in the Yucatan Peninsula. *Journal of Biogeography* **14**:499-519.
- Fink B.H. & Zedler J.B. (1990) Maritime stress tolerance studies of California dune perennials. *Madrono* **37**:200-213.
- Fitter A.H. & Hay R.K.M. (1995) *Environmental Physiology of Plants 2nd Edition*, Academic Press, London.
- Franks P.J., Cowan I.R. & Farquhar G.D. (1997) The apparent feedforward response of stomata to air vapour pressure deficit: information revealed by different experimental procedures with two rainforest trees. *Plant, Cell and Environment* **20**:142-145.
- Gadgil R.L. & Ede F.J. (1998) Application of scientific principles to sand dune stabilisation in New Zealand: Past progress and future needs. *Land Degradation and Development* **9**:131-142.
- Gates D.M. (1968) Transpiration and leaf temperature. *Annual Review of Plant Physiology* **19**:211-238.
- Gates D.M. (1976) Energy exchange and transpiration. In: *Water and Plant Life*. Lange O.L., Kappen L. & Schulze E-D. (eds) Ecological Studies (vol 19).
- Gibbs Russel G.E., Watson L., Koekemoer M., Smook L., Barker N.P. Anderson H.M. & Dallwitz M.J. (1990) Grasses of southern Africa. *Memoirs of the Botanical Survey of South Africa* No. **58**. National Botanical Institute, South Africa.
- Goff J.A. & Gatch S. (1946) *Trans. Amer. Soc. And Vent. Eng.* **52**:95.
- Guppy H.B. (1917) *Plants, seeds, and currents in the West Indies and Azores*. Williams and Norgate, London.
- Hall A.E. (1982) Mathematical models of plant water loss and plant water interactions. In: *Physiological plant ecology II; Water relations and carbon assimilation*. Lange O.L., Nobel P.S., Osmond C.B. & Ziegler H. (eds) **12b**:231-261.
- Hall D.O., Scurlock J.M.O., Bolhar-Nordenkamp H.R., Leegood R.C. & Long S.P. (1993) Photosynthesis & production in a changing environment; a field and laboratory manual. Chapman & Hall, London.
- Harley P.C. & Baldocchi D.D. (1995) Scaling carbon dioxide and water vapour exchange from leaf to canopy in a deciduous forest. I. Leaf model parameterisation. *Plant, Cell and Environment* **18**:1146-1156.
- Harte J.M. & Pammenter N.W. (1983) Leaf nutrient content in relation to senescence in the coastal sand dune pioneer *Scaevola thunbergii* Eckl. & Zeyh. *South African Journal of Science*. **79**:420-422.
- Herring T.A. (1996) The Global Positioning System. *Scientific American* (February 1996):32-38.

- Hertling U.M (1997) *Ammophila arenaria* (L.) Link (Marram Grass) in South Africa and its potential invasiveness. Ph.D, Thesis, Rhodes University, Grahamstown.
- Hertling U.M. & Lubke R.A. (1999) Use of *Ammophila arenaria* for dune stabilisation in South Africa and its current distribution – Perception and Problems. *Environmental Management* **24**:467-482.
- Hesp P.A. (1991) Ecological processes and plant adaptations on coastal dunes. *Journal of Arid Environments* **2**:165-192.
- Heyligers P.C. (1985) The impact of introduced plants on foredune formation in south-eastern Australia. *Proceedings of the Ecological Society of Australia* **14**: 23-41.
- Huiskies A.H.L. (1979) Biological flora of the British Isles, *Ammophila arenaria*. *Journal of Ecology* **67**:363-382.
- Huiskies A.H.L. (1980) The effects of habitat perturbation on leaf populations of *Ammophila arenaria* (L.) Link. *Acta. Bot. Neerl* **29**:443-450.
- Jarvis P.G. & Mansfield T.A. (1981) *Stomatal Physiology*. Society for experimental biology – Seminar Series; 8. Cambridge University Press, Cambridge.
- Jarvis P.G. & McNaughton G. (1986) Stomatal control of transpiration: Scaling up from leaf to region. *Advances in Ecological Research* **15**:1-49.
- Jarvis P.G. & Morison (1981) The control of transpiration and photosynthesis by the stomata. In: *Stomatal Physiology*. Jarvis P.G & Mansfield T.A. (eds). Society for experimental biology – Seminar Series; 8.
- Jeffrey C. (1979) On the nomenclature of the strand *Scaevola* species (Goodeniaceae). *Kew Bulletin* **34**(3):537-545.
- Jones H.G. (1998) Stomatal control of photosynthesis and transpiration. *Journal of Experimental Botany* **49** (Special issue):387-398.
- Kappen L. (1982) Ecological significance of resistance to high temperature. In: *Physiological plant ecology I; Responses to the physical environment*. Lange O.L., Nobel P.S., Osmond C.B. & Ziegler H. (eds) **12a**:439-474.
- Kramer P.J. (1983) *Water relations of plants*. Academic Press, London.
- Larcher W. & Bauer H. (1982) Ecological significance of resistance to low temperature. In: *Physiological plant ecology I; Responses to the physical environment*. Lange O.L., Nobel P.S., Osmond C.B. & Ziegler H. (eds) **12a**:403-438.
- Levin SA. (1993) Concepts of scale at the local level. In: *Scaling Physiological Processes: Leaf to Globe*. Ehleringer J.R. & Field C.B. (eds). Academic Press.
- Lindenmayer D.B., Nix H.A. McMahon J.P., Hutchinson M.F. & Tanton M.T. (1991) The conservation of Leadbeater's possum, *Gymnobelideus leadbeateri* (McCoy): a case study of the use of bioclimatic modelling. *Journal of Biogeography* **18**:371-383
- Loomis R.S., Rabbinge R. & Ng E. (1979) Explanatory models in crop physiology. *Annual Review of Plant Physiology* **30**:339-367.

- Lösch R. & Tenhunen J.D. (1981) Stomatal responses to humidity – phenomenon and mechanism. In: *Stomatal Physiology*. Jarvis P.G & Mansfield T.A. (eds). Society for experimental biology – Seminar Series; 8.
- Lubke R.A. & Avis A.M. (1988) Succession on the coastal dunes and dune slacks at Kleinemonde, Eastern Cape, South Africa. *Monograph of Systematic Botany, Missouri Botanical Gardens* **25**:599-622.
- Lubke R.A., Avis A.M., Steinke T.D. & Boucher C. (1997) Coastal vegetation. In: *Vegetation of Southern Africa*. Cowling R.A. (ed) Chapter **13**:300-321.
- Lubke R.A. & van Wijk Y. (1998) Terrestrial plants and coastal vegetation. In: *Field guide to the Eastern and Southern Cape coasts*. Lubke R.A. & de Moor I. (eds). University of Cape Town Press, Cape Town.
- Magellan (1998) *GPS 315/320 user manual*. Magellan Corporation San Dimas.
- Maguire D.J. (1991) An overview and definition of GIS. In: *GIS*. Maguire D.J., Goodchild M.F. & Rhind D.W. (eds). Longman, London.
- Manly B.F.J. (1994) *Multivariate statistical methods: A primer*. Chapman and Hall, London.
- Mansfield T.A., Travis A.J. & Jarvis R.G. (1981) Responses to light and carbon dioxide. In: *Stomatal physiology* Jarvis P.G. & Mansfield T.A. (eds) Cambridge University Press, Cambridge.
- Martinez M.L. & Moreno-Casasola P. (1996) Effect of burial by sand on seedling growth and survival in six tropical sand dune species from the Gulf of Mexico. *Journal of Coastal Research* **12**:406-419.
- Maun M.A. (1998) Adaptations of plants to burial in coastal sand dunes. *Canadian Journal of Botany* **76**:713-738.
- Maun M.A. & Baye P. (1989) The ecology of *Ammophila breviligulata* Fern. on coastal dune systems. *Critical Reviews in Aquatic Science* **1**:661-681.
- Moll E.J. (1972) A Preliminary account of the dune communities at Pennington Park, Mtunzini, Natal. *Bothalia* **10**:615-626.
- Monteith J.L. (1965) Evaporation and the environment. In: *The state and movement of water in living Organisms*. Fogg G.E. (ed), University press, Cambridge.
- Monteith J.L. (1995) A reinterpretation of stomatal responses to humidity. *Plant, Cell and Environment* **18**:357-364.
- Nix H.A. (1986) A Biogeographic analysis of Australian elapid snakes. In: *Atlas of elapid snakes* Longmore R. (ed), Australian Flora and Fauna series no. 7.
- Norman J.M. (1993) Scaling Processes between leaf and canopy levels. In: *Scaling Physiological Processes: Leaf to Globe*. Ehleringer J.R. & Field C.B. (eds). Academic Press.
- Olsson-Seffer P. (1909a) Hydrodynamic factors influencing plant life on sandy seashores. *New Phytologist* **8**:39-49.
- Olsson-Seffer P. (1909b) Relation of soil and vegetation on sandy sea shores. *Botanical Gazette* **47**:85-126.

- Oosting H.J. (1954) Ecological processes and vegetation of the maritime strand in the south-eastern United States. *Botanical Review* **20**:226-262.
- Pammenter N.W. (1983) Some aspects of the ecophysiology of *Scaevola thunbergii*, a subtropical coastal dune pioneer. in: *Sandy Beaches as Ecosystems* McLachlan A. & Erasmus T. (eds), W. Junk, the Hague, pp 675-685.
- Pammenter N.W. (1985) Photosynthesis and transpiration of the subtropical coastal sand dune pioneer *Scaevola plumieri* under controlled conditions. *South African Journal of Botany* **51**:421-424.
- Pammenter N.W. & Smith V.R. (unpublished manuscript) Carbon assimilation by a plant in the high-light coastal dune environment is apparently light limited.
- Panetta F.D. & Mitchell N.D. (1991) Homocline analysis and the prediction of weediness. *Weed Research* **31**:273-284.
- Passioura J.B. (1982) Water and the soil-plant-atmosphere continuum. In: *Physiological plant ecology II; Water relations and carbon assimilation*. Lange O.L., Nobel P.S., Osmond C.B. & Ziegler H. (eds) **12b**:5-33.
- Pavlik B.M. (1983a) Nutrient and productivity relations of the dune grasses *Ammophila arenaria* and *Elymus mollis* I. Blade photosynthesis and nitrogen use efficiency in the laboratory and field. *Oecologia* **57**:227-232.
- Pavlik B.M. (1983b) Nutrient and productivity relations of the dune grasses *Ammophila arenaria* and *Elymus mollis* II. Growth and patterns of dry matter and nitrogen allocation as influenced by nitrogen supply. *Oecologia* **57**:233-238.
- Pavlik B.M. (1983c) Nutrient and productivity relations of the dune grasses *Ammophila arenaria* and *Elymus mollis* III. Spatial aspects of clonal expansion with reference to rhizome growth and the dispersal of buds. *Bulletin of the Torrey Botanical Club* **110**:271-279.
- Pavlik B.M. (1984) Seasonal changes of osmotic pressure, symplastic water content and tissue elasticity in the blades of dune grasses growing *in situ* along the coast of Oregon. *Plant, Cell and Environment* **7**:531-539.
- Pavlik B.M. (1985) Water relations of the dune grasses *Ammophila arenaria* and *Elymus mollis* on the coast of Oregon, USA. *Oikos* **45**:197-205.
- Payn T.W., Hill, R.B., Hock B.K., Skinner M.F. Thorn A.J. and Rijkse W.C. (1999) Potential for the use of GIS and spatial analysis techniques as tools for monitoring changes in forest productivity and nutrition, a New Zealand example. *Forest Ecology and Management* **122**: 187-196.
- Peter C.I. & Ripley B.S. (in press) An empirical formula for estimating the water use of *Scaevola plumieri*. *South African Journal of Science*.
- Raschke K (1970) Temperature dependence of CO₂ assimilation and stomatal aperture in leaf sections of *Zea mays*. *Planta* **91**:336-363.
- Raschke K. (1975) Stomatal action. *Annual Review of Plant Physiology* **26**:309-340.
- Raschke K. (1979) Movements of stomata. In: *Encyclopædia of Plant Physiology* vol **7** Haupt W. & Feinleib M.E. (eds). Springer-Verlag, Berlin.

- Reynolds J.F., Hilbert D.W. & Kemp P.R. (1993) Scaling ecophysiology from the plant to the ecosystem: A conceptual framework. In: *Scaling Physiological Processes: Leaf to Globe*. Ehleringer J.R. & Field C.B. (eds). Academic Press.
- Richardson D.M. & McMahon J.P. (1992) A bioclimatic analysis of *Eucalyptus nitens* to identify potential planting regions in South Africa. *South African Journal of Science* **88**:380-387.
- Ridley H.N. (1930) *The dispersal of plants throughout the World*. L. Reeve & Co. Ltd. Kent.
- Ripley B.S., Pammenter N.W. & Smith V.R. (1999) Function of leaf hairs revisited: The hair layer on leaves *Arctotheca populifolia* reduces photoinhibition, but leads to higher leaf temperatures caused by lower transpiration rates. *Journal of Plant Physiology* **155**:78-85.
- Robertson M.P., Villet M.H. & Palmer A.R. (in prep) The Fuzzy Envelope Model: A correlative modelling technique for predicting potential distributions of organisms from presence locality records and environmental predictor variables using fuzzy classification.
- Rozema J., Bijl F., Dueck T. & Wesselman H. (1982) Salt-spray stimulated growth in strand-line species. *Physiologia Plantarum* **56**:204-210.
- Salisbury E. (1952) *Downs and Dunes. Their plant life and its environment*. G. Bell & Sons Ltd. London.
- Schelde K., Kelliher F.M., Massman W.J. & Jensen K.H. (1997) Estimating sensible and latent heat fluxes from a temperate broad-leaf forest using the Simple Biosphere (SiB) model. *Agricultural and Forest Meteorology* **84**:285-295.
- Schönherr J. (1982) Resistance of plant surfaces to water loss: Transport properties of cutin, suberin and associated lipids. In: *Physiological plant ecology II; Water relations and carbon assimilation*. Lange O.L., Nobel P.S., Osmond C.B. & Ziegler H. (eds) **12b**:135-153.
- Schulze E-D. (1982) Plant life forms and their carbon, water and nutrient relations. In: *Physiological plant ecology II; Water relations and carbon assimilation*. Lange O.L., Nobel P.S., Osmond C.B. & Ziegler H. (eds) **12b**:615-676.
- Schulze E-D. (1986) Carbon dioxide and water exchange in response to drought in the atmosphere and in the soil. *Annual Review of Plant Physiology* **37**:247-274.
- Schulze E-D. & Hall A.E. (1982) Stomatal responses, water loss and CO₂ assimilation rates of plants from contrasting environments. In: *Physiological plant ecology II; Water relations and carbon assimilation*. Lange O.L., Nobel P.S., Osmond C.B. & Ziegler H. (eds) **12b**:135-153.
- Schulze E-D, Lange O.L., Kappen L., Buschbom U. & Evenari M. (1973) Stomatal responses to changes in temperature at increasing water stress. *Planta* **110**:29-42
- Schulze R.E., Maharaj M., Lynch S.D., Howe B.J. & Melville-Thomas B. (1997) *South African atlas of agrohydrology and -climatology*. Water Research Commission report, TT82/96.
- Shillington F.A. (1986) Oceanography of the Southern African region. In: *Smiths' Sea Fishes*, Smith M.M. & Heemstra P.C. (eds) Southern Book Publishers, Johannesburg.
- Sphynx Ink. (1996) *Possim for Windows, Version 1.0*. Sphynx Ink.
- StatSoft, Inc. (1999a). *STATISTICA for Windows [Computer program manual]*. Tulsa, Oklahoma, USA. WEB: <http://www.statsoft.com>.

- StatSoft, Inc. (1999b). *Electronic Statistics Textbook*. Tulsa, Oklahoma, USA. StatSoft. WEB: <http://www.statsoft.com/textbook/stathome.html>.
- Steinke T.D. & Lambert G. (1986) A preliminary study of the phenology of *Scaevola plumieri*. *South African Journal of Botany* **52**:43-46.
- Stephenson N.L. (1998) Actual evapotranspiration and deficit: biological meaningful correlates of vegetation distribution across spatial scales. *Journal of Biogeography* **25**:855-870.
- Steponkus P.L. (1982) Responses to extreme temperatures. Cellular and sub-cellular bases. In: *Physiological plant ecology I; Responses to the physical environment* Lange O.L., Nobel P.S., Osmond C.B. & Ziegler H. (eds) **12a**:277-338.
- Stone A. W., Weaver A.vB. and West W.O. (1998) Climate and weather. In: Lubke R.A. and de Moor I. (eds) *Field guide to the Eastern and Southern Cape coasts*. University of Cape Town Press, Cape Town.
- Sykes M.T., Prentice I.C. & Cramer W. (1996) A bioclimatic model for the potential distributions of north European tree species under present and future climates. *Journal of Biogeography* **23**:203-233.
- Thornley J.H.M. (1996) Modelling water in crops and plant ecosystems. *Annals of Botany* **77**:261-275.
- Tinley K.L. (1985) Coastal dunes of South Africa. *South African National Scientific Programmes, Report No. 109*.
- Tutin T.G., Heywood V.H., Burges N.A., Moore D.M., Valentine D.H., Walkers S. M. & Webb D.A. (1980) *Flora Europaeae* vol 5. Cambridge University Press.
- van der Maarel E. & van der Maarel-Versluys M. (1996) Distribution and conservation status of littoral vascular plant species along the European coasts. *Journal of Coastal Conservation* **2**:73-92.
- van der Meulen F. & van der Maarel E. (1989) Coastal defence alternatives and nature development perspectives. In: *Perspectives in coastal dune management* van der Meulen F., Jungerius P.D. & Visser J. (eds). SPB Academic Publishing, The Hague.
- van der Putten W.H., van Dijk C. & Troelstra S.R. (1988) Biotic soil factors affecting the growth of *Ammophila arenaria*. *Oecologia* **76**:313-320.
- von Caemmerer S. & Farquhar C.D. (1981) Some relationships between the biochemistry of photosynthesis and the gas exchange of leaves. *Planta* **153**:376-387.
- Wackerly D.D., Mendehnhall (III) W. & Scheaffer R.L. (1996) *Mathematical statistics with applications*. Duxbury Press, London.
- Wiedemann A.M. & Pickart A. (1996) The *Ammophila* problem on the north-west coast of North America. *Landscape and Urban Planning* **34**:287-299.
- Weiss S.B. & Weiss A.D. (1998) Landscape-level phenology of a threatened butterfly: A GIS modelling approach. *Ecosystems* **1**:299-309.
- Weisser P.J., Garland I.F. & Drews B.K. (1982) Dune advancement 1937-1977 at the Mlalazi Nature Reserve, Mtunzini, Natal, South Africa, and a preliminary vegetation-succession chronology. *Bothalia* **14**:127-130.

Weyers J. & Meidner H. (1990) *Methods in Stomatal Research*. Longman Scientific and Technical, London.

Willis A.J. (1965) The influence of mineral nutrients on the growth of *Ammophila arenaria*. *Journal of Ecology* **53**:735-745.

Willmer C.M. (1983) *Stomata*. Longman, London.

Woodward F.I. (1987) *Climate and plant distribution*. Cambridge studies in ecology, Cambridge University Press, Cambridge.

Woodward F.I. & Williams (1987) Climate and plant distribution at global and local scales. *Vegetatio* **69**:189-197.

Web-sites

Web-site 1: <http://www.usf.edu/~isb/projects/atlas/maps/scaeplum.gif>

Web site 2: <http://linnaeus.nrm.se/flora/mono/poa/ammop/ammoare.html>